2-27-2013

# Covalent Protein Adduction by Drugs of Abuse

Kevin Schneider
*Florida International University*, kevinjschneider@gmail.com

**DOI:** 10.25148/etd.FI13040402

FLORIDA INTERNATIONAL UNIVERSITY

Miami, Florida

# COVALENT PROTEIN ADDUCTION BY DRUGS OF ABUSE

A dissertation submitted in partial fulfillment of

the requirements for the degree of

DOCTOR OF PHILOSOPHY

in

CHEMISTRY

by

Kevin J. Schneider

2013

To: Dean Kenneth G. Furton
College of Arts and Sciences

This dissertation, written by Kevin J. Schneider, and entitled Covalent Protein Adduction by Drugs of Abuse, having been approved in respect to style and intellectual content, is referred to you for judgment.

We have read this dissertation and recommend that it be approved.

_____
Kenneth Furton

_____
Bruce McCord

_____
Alexander Mebel

_____
Berrin Serdar

_____
Anthony DeCaprio, Major Professor

Date of Defense: February 27, 2013

The dissertation of Kevin J. Schneider is approved.

_____
Dean Kenneth G. Furton
College of Arts and Sciences

_____
Dean Lakshmi N. Reddi
University Graduate School

Florida International University, 2013

ABSTRACT OF THE DISSERTATION

COVALENT PROTEIN ADDUCTION BY DRUGS OF ABUSE

by

Kevin J. Schneider

Florida International University, 2013

Miami, Florida

Professor Anthony DeCaprio, Major Professor

Recreational abuse of the drugs cocaine, methamphetamine, and morphine continues to be prevalent in the United States of America and around the world. While numerous methods of detection exist for each drug, they are generally limited by the lifetime of the parent drug and its metabolites in the body. However, the covalent modification of endogenous proteins by these drugs of abuse may act as biomarkers of exposure and allow for extension of detection windows for these drugs beyond the lifetime of parent molecules or metabolites in the free fraction. Additionally, existence of covalently bound molecules arising from drug ingestion can offer insight into downstream toxicities associated with each of these drugs.

This research investigated the metabolism of cocaine, methamphetamine, and morphine in common *in vitro* assay systems, specifically focusing on the generation of reactive intermediates and metabolites that have the potential to form covalent protein adducts. Results demonstrated the formation of covalent adduction products between biological cysteine thiols and reactive moieties on cocaine and morphine metabolites. Rigorous mass spectrometric analysis in conjunction with *in vitro* metabolic activation, pharmacogenetic reaction phenotyping, and computational modeling were utilized to characterize structures and mechanisms of formation for each resultant thiol adduction product. For cocaine, data collected demonstrated the formation of adduction products from a reactive arene epoxide intermediate, designating a novel metabolic pathway for cocaine. In the case of morphine, data expanded on known adduct-forming pathways using sensitive and selective analysis techniques, following the known reactive metabolite, morphinone, and a proposed novel metabolite, morphine quinone methide. Data collected in this study describe novel metabolic events for multiple important drugs of abuse, culminating

in detection methods and mechanistic descriptors useful to both medical and forensic investigators when examining the toxicology associated with cocaine, methamphetamine, and morphine.

TABLE OF CONTENTS

LIST OF TABLES

LIST OF FIGURES

FIGURE PAGE

ABBREVIATIONS AND ACRONYMS

| | |
|---|---|
| γ-GT | γ-glutamyltransferase |
| AcCoA | acetyl coenzyme A |
| AcPAACAA | acetyl-Pro-Ala-Ala-Cys-Ala-Ala-OH |
| AcPAAHAA | acetyl-Pro-Ala-Ala-His-Ala-Ala-OH |
| AcPAAKAA | acetyl-Pro-Ala-Ala-Lys-Ala-Ala-OH |
| ADME | absorption, distribution, metabolism, and elimination |
| AEME | anhydroecgonine methyl ester |
| Alm | alamethicin |
| AMP | amphetamine |
| BE | benzoylecgonine |
| BNE | benzoylnorecgonine |
| cDNA | complimentary DNA |
| CNS | central nervous system |
| CYP | cytochrome P450 |
| CYT | human liver cytosol |
| DFT | density functional theory |
| DMSO | dimethyl sulfoxide |
| EGC | ecgonine |
| $E_{HOMO}$ | HOMO energy |
| $E_{LUMO}$ | LUMO energy |
| EME | ecgonine methyl ester |
| ER | endoplasmic reticulum |
| ESI | electrospray ionization |
| FAES | fatty acid ethyl synthase |
| FMO | flavin monooxygenase |
| FOT | frontier orbital theory |

| | |
|---|---|
| FWHM | full width at half max |
| GSH | glutathione |
| GST | glutathione-*S*-transferase |
| hCE-1 | human liver carboxylesterase 1 |
| hCE-2 | human liver carboxylesterase 2 |
| HLM | human liver microsomes |
| HOMO | highest occupied molecular orbital |
| HRP | horseradish peroxidase |
| HSAB | hard and soft acid and base |
| LC | liquid chromatography |
| LUMO | lowest unoccupied molecular orbital |
| M3G | morphine-3-glucuronide |
| M6G | morphine-6-glucuronide |
| MDMA | 3,4-methylenedioxymethamphetamine |
| MOPAC | molecular orbital package |
| MRM | multiple reaction monitoring |
| MS | mass spectrometry |
| MS/MS | tandem mass spectrometry |
| MW | molecular weight |
| NADPH | nicotinamide adenine dinucleotide phosphate |
| NAC | *N*-acetylcysteine |
| NAH | *N*-acetylhistidine |
| NAK | *N*-aceyllysine |
| NAT | *N*-acetyltransferase |
| NC | norcocaine |
| NM | normorphine |
| OH-BE | hydroxybenzoylecgonine |

| | |
|---|---|
| OH-COC | hydroxycocaine |
| OH-MET | hydroxymethamphetamine |
| OH-NC | hydroxynorcocaine |
| PAPS | phosphoadenosine phosphosulfate |
| PCP | phencyclidine |
| QQQ | triple quadrupole |
| QTOF | quadrupole time-of-flight |
| rhCYP | recombinant human CYP |
| RT | retention time |
| S9 | human liver S9 fraction |
| SAM | *S*-adenosylmethionine |
| SULT | sulfotransferase |
| UDP-GlcUA | uridine diphosphoglucuronic acid |
| UGT | uridine diphosphoglucuronosyltransferase |
| UHPLC | ultra-high performance liquid chromatography |

## 1. INTRODUCTION

The toxicological fate of ingested xenobiotics, while extremely complex, is vital to understanding the downstream impact a drug will impart. Covalent adducts formed between products of drug metabolism and endogenous biomolecules (including proteins and DNA) represent a largely unexamined branch of toxicology that is a key factor mediating the overall toxicokinetic and toxicodynamic properties of a drug. While playing a diverse role in the apparent pharmacology of a substance, these permanent modifications to existing biomolecules act as biomarkers of exposure and, in certain cases, are unequivocal evidence of xenobiotic intake that persist even after the free fraction is cleared from the body. Mechanistic and analytical designation of covalent biomolecular adduction is of particular interest to forensic and medical specialists, granting insight into toxicity mechanisms (for acute, chronic, and idiosyncratic toxicities), carcinogenicity, teratogenicity, bioaccumulation, bioavailability, addiction pathology, and exposure assessment. While these properties are examined by myriad assays and models during clinical development of pharmaceuticals, illicit substances lack the rigorous testing milieu afforded to regulated drugs. This research examined the metabolic fate of three commonly abused drugs (cocaine, methamphetamine, and morphine), specifically illustrating structures and mechanisms associated with the formation of currently uncharacterized irreversible protein modifications.

Distinct protein adducts described by this research were generated using various metabolic model systems employed by pharmaceutical companies and characterized using liquid chromatography tandem mass spectrometry (LC-MS/MS) for structural designation. In conjunction with experimental design, these structural analyses were the basis for mechanistic description of the adduction process and were used as physiochemical estimators of *in vivo* environments. This research provides a more complete depiction of the metabolic fate of cocaine, methamphetamine, and morphine in the human body in addition to forming the foundation for the future development of assays to designate past drug use based on detection of covalent protein adducts.

## 2. LITERATURE REVIEW

### 2.1. **Xenobiotic Biotransformation**

Pharmacokinetically, the lifetime of a xenobiotic *in vivo* can be characterized by the absorption, distribution, metabolism, and elimination (ADME) scheme. While each of these four stages is imperative in considering the fate of a drug *in vivo*, perhaps the most complex is the metabolism phase. Involving the synchronization of numerous enzymes, cofactors, and other biochemical processes, xenobiotic transformation significantly influences the potency, activity, and lifetime of drugs and other exogenous chemicals in the body. While the process of metabolism is unique to each individual because of biological and physiochemical factors, general trends in biotransformation are able to be characterized.

The process of xenobiotic metabolism in the body is a complex system of modification and conjugation in order to produce a product that is readily eliminated from the body (*i.e.*, a polar, water-soluble product). The extent of xenobiotic metabolism is dependent on numerous factors, including innate hydrophilicity, the number of functional groups amenable to biotransformation, and half-life. In addition to conventional Phase I and Phase II biotransformation processes, subsequent interaction with endogenous biomolecules or other xenobiotics shape the metabolic and elimination schemes for certain compounds. These events include protein binding (reversible and irreversible), pooling of drugs or metabolites in specific tissues, multiple drug interactions, and co-metabolic production of unique metabolites.

Within the category of biotransformation are two major subdividing classifications: Phase I and Phase II metabolism. Phase I metabolism pertains to several "functionalizing" reactions including oxidation, reduction, and hydrolysis.[1] While Phase I metabolism is pervasive throughout cellular tissues including brain and kidney and has also been detected in extracellular environments, the epicenter of Phase I biotransformation in the human body is within liver tissue.[2,3] The workhorses behind "non-synthetic" Phase I reactions in the liver are various mixed function oxidases, primarily cytochrome P450 (CYP) and flavin monooxygenase (FMO) families.[4]

Among the numerous enzymes responsible for xenobiotic modification, the CYP enzymes are capable of catalyzing myriad oxidative biotransformation reactions on a multitude of compounds with

diverse chemical structures and physiological actions. The membrane-bound CYP superfamily of enzymes is characterized by incorporation of an iron-containing heme cofactor (Figure 1).

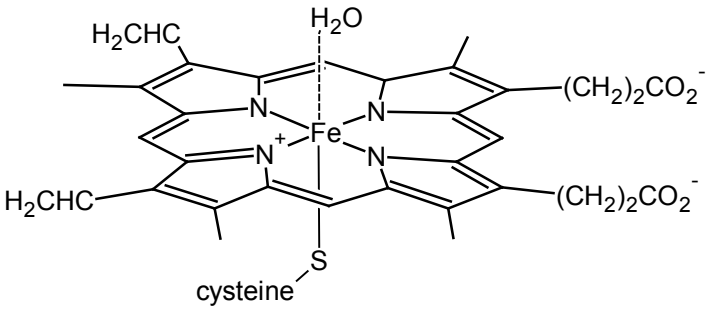


**Figure 1: Iron-containing heme cofactor in CYP enzymes**

When these hemoproteins are reduced and a complex is formed between heme iron and carbon monoxide, the resultant structure absorbs light at 450 nm, justifying their classification as "P450" enzymes. While the CYP superfamily of enzymes shares commonality in the iron-containing heme group, there are numerous CYP isoforms that differ in enzymatic structure, substrate specificity, efficiency, and tissue localization (more detail on CYP isozymes is reported in Section 2.2). Cytochrome P450-catalyzed oxidation is uncharacteristic of typical oxidative processes because these enzymes succeed in facilitating reactions that are energetically unfavorable at ambient temperatures (*e.g.*, hydroxylation of non-functionalized alkyl groups).

Cytochrome P450 enzymes are able to oxidatively modify xenobiotics by generating highly reactive intermediates through cycling the oxidative state of the iron heme group and introducing molecular oxygen.[5] While the exact mechanics behind CYP-catalyzed oxidations are still being researched, a brief outline is presented in Figure 2.[6-8] In the substrate-free form, most CYP hemes exist in a hexa-ligated low-spin state via $H_2O$ coordination (Figure 2a). Introduction of substrate into the catalytic site of the enzyme displaces the coordinated water molecule, resulting in a modified geometry for the penta-ligated high-spin iron complex (Figure 2b). Acceptance of an electron from the cofactor flavoprotein NADPH cytochrome P450 reductase reduces the iron to the reactive $Fe^{II}$ species (Figure 2c), which is able to bind molecular oxygen (Figure 2d). A second reduction step by a cofactor flavoprotein (NADPH cytochrome P450 reductase or cytochrome $b_5$) (Figure 2e) and input of protons (Figure 2f) results in the heterolytic cleavage of the O-O bond, loss of $H_2O$, and production of the reactive "oxenoid" species (Figure 2g). Substrate

oxidation (Figure 2h) and release followed by water coordination regenerates the substrate-free hexa-ligated low-spin iron ensemble. Dashed arrows in Figure 2 represent "leaky" reactive oxygen species-producing branches of the CYP catalytic cycle (including the "peroxide shunt" (b)↔(f) pathway).

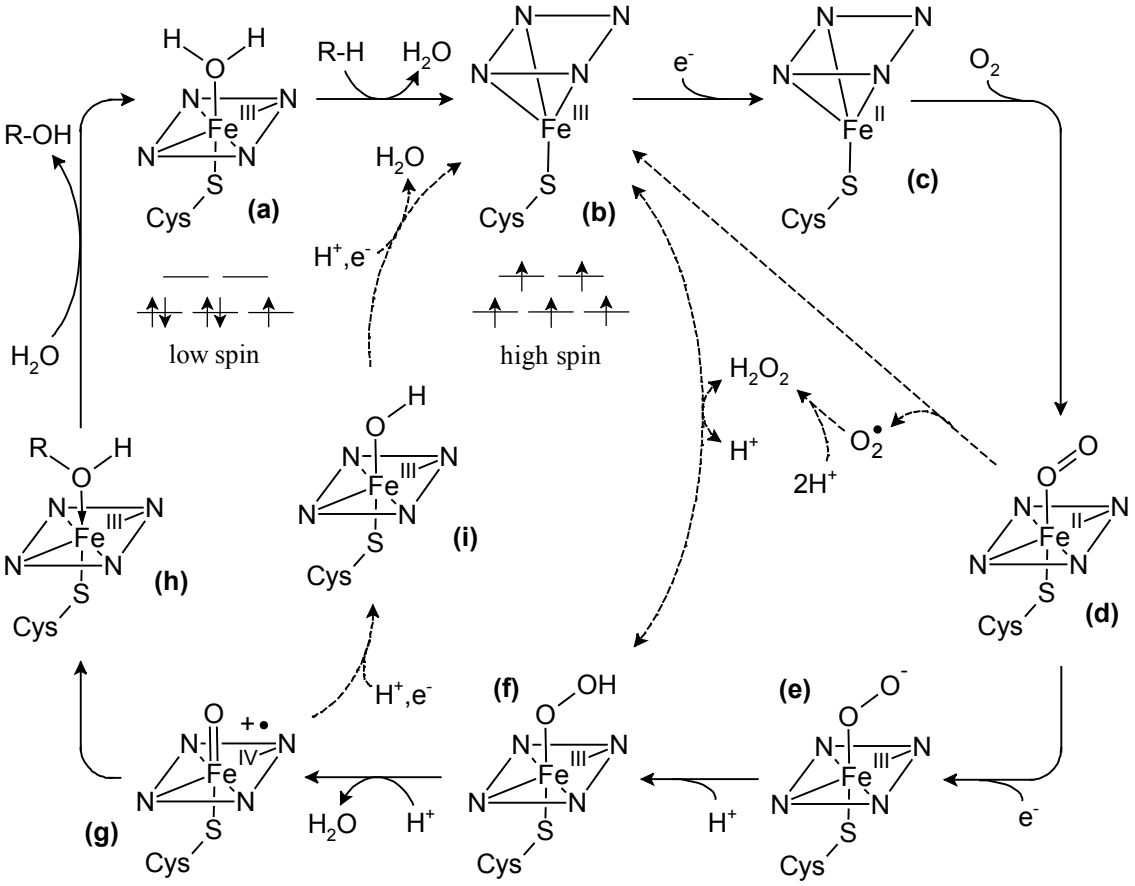


**Figure 2: Cytochrome P450 catalytic cycle**
**(a) $H_2O$ coordinated hexa-ligated low-spin heme, (b) penta-ligated high-spin iron complex, (c) reduced $Fe^{II}$ species, (d) $Fe^{II}$ heme with bound molecular oxygen, (e) peroxy ion heme complex, (f) hydroperoxo iron heme complex, (g) $Fe^{IV}$ reactive oxenoid, (h) coordinated oxidized substrate, (i) hydroxyl iron heme complex. Dashed arrows represent "leaky" reactive oxygen species-producing branches.**

While there are many considerations in assigning mechanisms to CYP oxidation reactions, a system in which there are two electrophilic oxidants and a reactive two-state ensemble for the oxo-iron intermediate seems to explain many inconsistencies that have been observed between previous theories and empirical data.[5] In this model, the early oxidants (*i.e.*, hydroperoxo-iron (Figure 2f), iron-complexed hydrogen peroxide) react via the insertion of $OH^+$ to produce protonated alcohols, which are the species responsible for cationic rearrangement products (Figure 3, Scheme 1). On the other hand, a two-state

reaction model for the action of the oxo-iron reactive species divides the mechanism of this intermediate between the low-spin and high-spin ensembles capable of abstracting hydrogen from the substrate followed by oxygen-rebound (Figure 3, Scheme 2). Previously considered a mechanism for CYP oxidation, concerted oxene insertion (Figure 3, Scheme 3) has since been dismissed on the basis of empirical data demonstrating large intramolecular kinetic isotope effects, loss of stereochemistry, and substrate rearrangements inconsistent with this mechanism.[8]

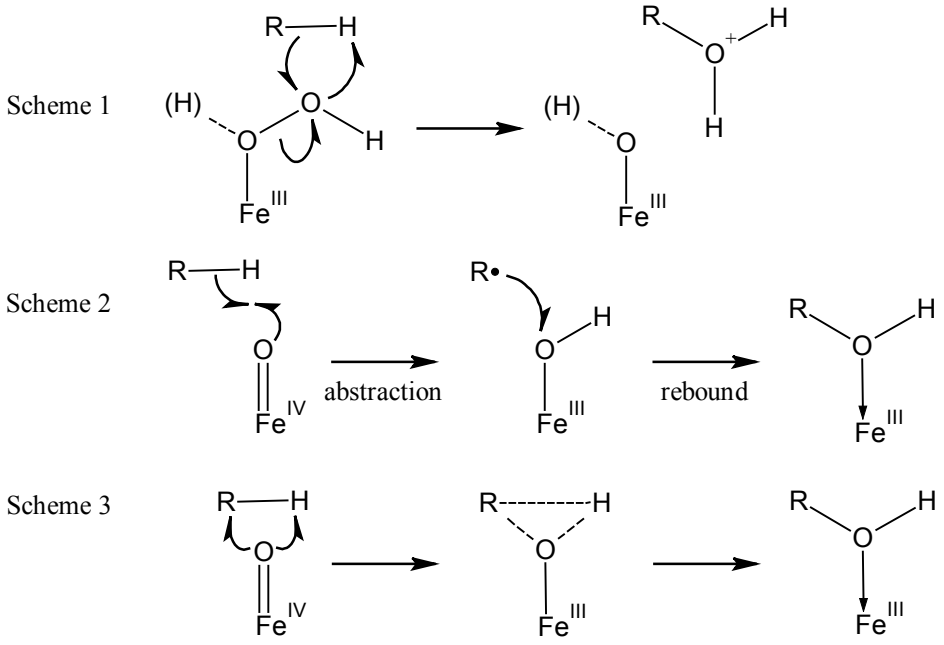


**Figure 3: CYP oxidation schemes.**
**Scheme 1: Insertion of $OH^+$ by hydroperoxo-iron or iron-complexed hydrogen peroxide.**
**Scheme 2: Iron-oxo hydrogen atom abstraction and oxygen-rebound.**
**Scheme 3: Oxene insertion.**

In addition to CYP biotransformation, the FMO enzyme family plays a diverse role in xenobiotic biotransformation. Membrane-bound, FMOs utilize an oxidized flavin moiety to elicit oxidation of xenobiotics from molecular oxygen (Figure 4).[6] Primary action of FMOs includes the oxidation of nucleophilic nitrogen, sulfur, and phosphorus heteroatoms, generating many biotransformation products analogous to CYP activity. While similar in substrate and action, FMOs account for only a small percentage of overall xenobiotic metabolic activity (<5%) compared to CYP isoforms (~75%).[9] Aside from the CYP and FMO families, there are various additional oxidases, peroxidases, dehydrogenases,

esterases, reductases, and hydrolases that contribute to the complex web of Phase I metabolic processes in the human body.[10]

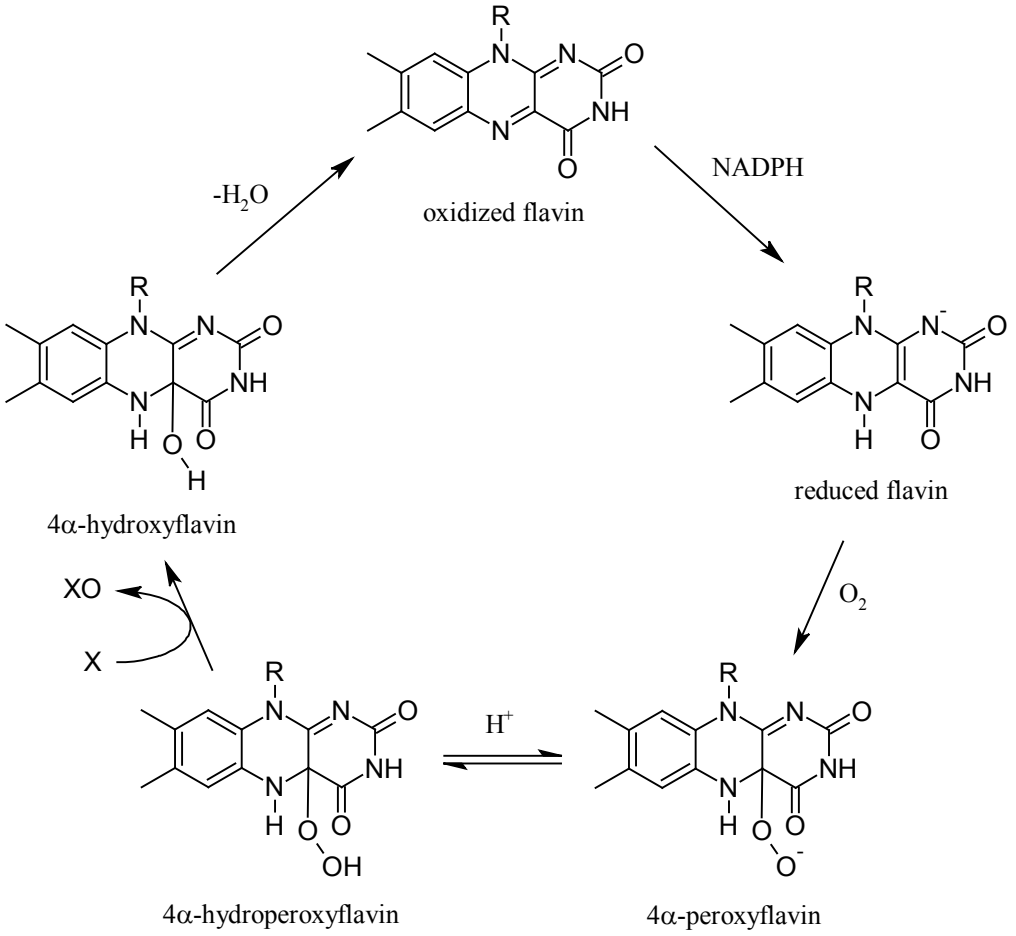


**Figure 4: Flavin monooxygenase oxidation mechanism**

Acting concurrently with Phase I functionalization reactions, conjugative Phase II metabolic events contribute to the biotransformation of many drugs *in vivo*. Phase II conjugation reactions involve the addition of an endogenous moiety to existing or induced/exposed functional groups on xenobiotics, encompassing glucuronidation, sulfonation (sulfation), acetylation, methylation, and conjugation to glutathione or amino acids (*e.g.*, glycine, taurine, glutamic acid).[11] With the notable exception of methylation, Phase II conjugative activities increase the overall polarity of target molecules, facilitating elimination in one or more biological excretions (*e.g.*, urine, bile, sweat, feces). Biochemical pathways will often favor the removal of certain Phase II conjugates via a preferred matrix. For example, it has been

demonstrated in rats that glucuronides formed with aglycones (parent molecules or unconjugated metabolites) of molecular weight (MW) <250 Da are preferentially excreted via urine while aglycones >350 Da are primarily excreted in bile, making the biliary excretion MW cutoff in rats ~325 Da.[12,13] While similar patterns in high MW glucuronide biliary excretion are documented across species, MW cutoffs for excretion matrix preference vary among mammalian species (*e.g.*, ~400 Da in guinea pigs, ~500 Da in rabbits).

Several classes of Phase II conjugative enzymes exist in humans, each facilitating a single conjugative activity and requiring distinct cofactors as summarized in Table 1.[6,11,14] Similar to CYP enzymes, many Phase II enzyme families contain several isoforms, each with distinct substrate selectivity/specificity.

**Table 1: Phase II enzyme class information**

| Conjugative Process | Enzyme Family | Cofactor(s) |
|---|---|---|
| **Glucuronidation** | Uridine diphosphoglucuronosyltransferase (UGT) | Uridine diphosphoglucuronic acid (UDP-GlcUA) |
| **Sulfation** | Sulfotransferase (SULT) | Phosphoadenosine-phosphosulfate (PAPS) |
| **Acetylation** | *N*-acetyltransferase (NAT) | Acetyl-coenzyme A (AcCoA) |
| **Methylation** | Various | *S*-adenosylmethionine (SAM) |
| **Glutathione Conjugation** | Glutathione-*S*-transferase (GST) | Glutathione (GSH) |
| **Amino Acid Conjugation** | Various | Gly, Glu, Tau |

While some Phase II biotransformation products do not undergo further metabolism, certain classes of conjugates are further modified to aid in elimination. Some conjugative products can undergo subsequent Phase I or Phase II processes depending on substrate structure and enzyme selectivity. Successive modifications to the conjugated moiety are also a viable pathway with other conjugated products. This process is sometimes termed "Phase III" metabolism.[15] The most pervasive of Phase III metabolic events in humans is the continued metabolism of GSH-bound xenobiotics to form *N*-

acetylcysteine (mercapturic acid) conjugates, which are excreted in the urine. Subsequent to GSH conjugation by GST or non-enzymatic reaction, a cascade of additional enzymatic processes is necessary to biosynthesize mercapturates (Figure 5).[16] Removal of glutamate and glycine by γ-glutamyltransferase (γ-GT) and dipetidases, respectively, leaves the cysteine-bound electrophile available for *N*-acetylation via typical NAT/AcCoA activity.

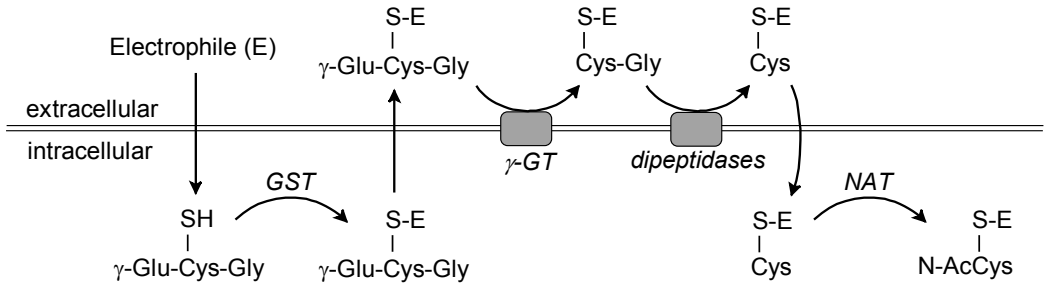


**Figure 5: Biodegradation of glutathione conjugates to mercapturic acids**

The extent of xenobiotic metabolism within an individual relies on a series of factors associated with that individual. While the metabolic events described above are generally conserved among individuals within a species, there are myriad factors that impact the biochemical processes associated with enzymatic xenobiotic metabolism. Genetic factors, epigenetics, sex, age, biological rhythms, pregnancy, stress, nutritional factors, enzyme induction and inhibition, and disease state are all mediating factors in enzyme expression, function, and efficiency.[3]

### 2.2. **Cytochrome P450 Isozymes**

While oxidative mechanisms are maintained across the CYP superfamily, there are myriad subclasses, each with preferential substrate, activity, and body tissue distribution. Fifty-seven of these distinct enzymes (known as isoforms) have been classified by the human genome project and the general substrate activity for major enzymes has been cataloged; however, individual reaction phenotyping is required to designate isoform action on a specific substrate.[10] Reaction phenotyping is of great importance for both medical and forensic analyses involving a given xenobiotic. Specific metabolism by a given isoform can influence a substance's toxicology in combination with other xenobiotics or modify pharmacokinetics based on genetic factors.

Induction or inhibition of a specific isoform by a secondary xenobiotic can drastically modify the pharmacokinetic (and therefore pharmacodynamic) properties of a drug. For example, the antibiotic ciprofloxacin is a potent inhibitor of isoform CYP1A2, the enzyme responsible for metabolism of imipramine (an anti-depressant).[17,18] Co-administration of ciprofloxacin with imipramine would disrupt conventional imipramine therapeutics and could potentially lead to toxicity. Specific knowledge of enzymes responsible for a drug's metabolism (or even those responsible for an individual biotransformation pathway) may grant insight into an individual's reaction to a specific dose of the drug. Stimulation of a metabolic pathway that produces a toxic metabolite can account for individual toxicities not normally encountered with a given dose (*i.e.*, idiosyncratic toxicities). Synergistic effects caused by co-administration can be better understood with knowledge of reaction phenotyping.

Similarly, genetically determined expression of CYP enzymes can also mediate toxicokinetic and toxicodynamic parameters. Aside from inter-individual differences in base enzyme expression, the existence of numerous polymorphisms among the CYP isoforms (*i.e.*, CYPs 1A1, 1A2, 2C19, 2D6, and 2E1) can significantly impact xenobiotic metabolite profiles. For example, CYP2D6 has multiple known variant alleles leading to polymorphic enzyme expression. Each allelic variation influences enzymatic function, leading to phenotypes characterized by increased enzyme activity (CYP2D6 × 2 × n), inactive enzyme (CYP2D6 × 4), absent enzyme (CYP2D6 × 5), unstable enzyme (CYP2D6 × 10), and reduced enzyme activity (CYP2D6 × 17).[2] Genetic influences on drug biotransformation via modifications of enzymatic expression represent a subset of a group known as "biomarkers of susceptibility." Biomarkers of susceptibility represent conditions that modify an organism's response to molecular exposure.[19] Marked shifts in the qualitative or quantitative response to chemical exposure can account for genotype-specific toxicities.

Each of the 57 CYP isoforms designated by the human genome project maintains individual substrate specificities and expression in various tissues and matrices throughout the human body. Responsible for myriad synthetic, metabolic, and catabolic events for both endogenous and exogenous agents, only a subset of the know CYP enzymes are relevant to drug metabolism in humans. Even within this subset of CYP isoforms, factors such as protein concentration, tissue distribution, enzyme kinetics,

substrate specificity, and substrate affinity mediate the ultimate impact of each isoform. The most influential among these enzymes are presented in Figure 6 according to their concentration within liver tissue and relevance to xenobiotic metabolism (the latter is estimated as a factor of cataloged substrates for each isoform).[6]

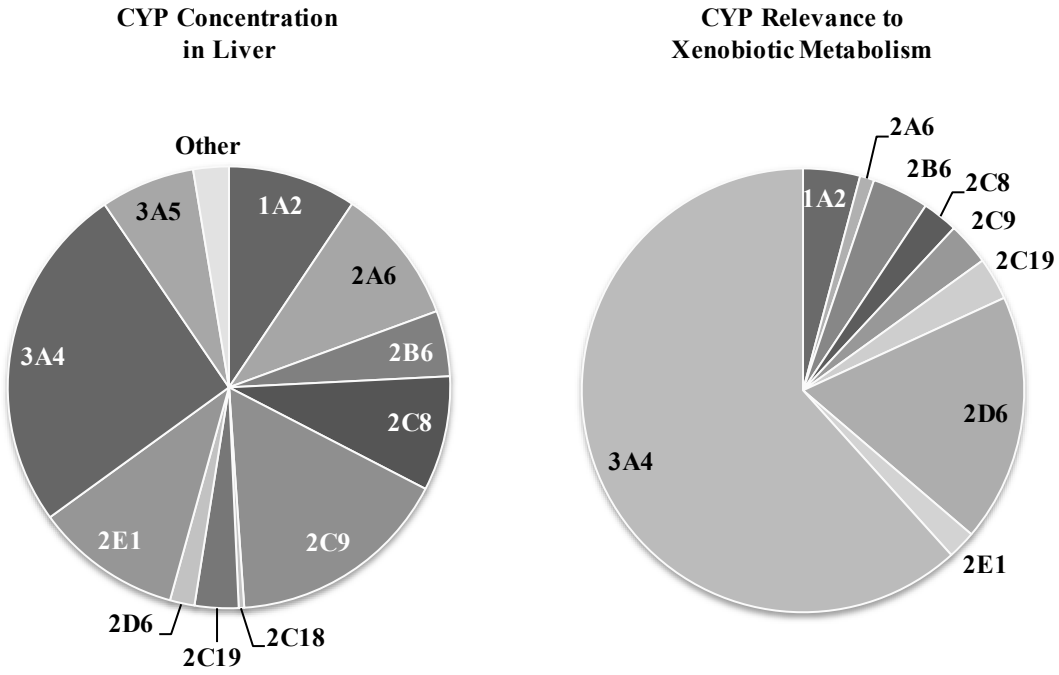


**Figure 6: Distribution of cytochrome P450 enzymes and relevance to xenobiotic metabolism (from reference 6)**

### 2.3. **Drug of Abuse Metabolism: Cocaine, Methamphetamine, and Morphine**

While most drugs of abuse undergo a degree of metabolism, the three examined in this study (cocaine, methamphetamine, and morphine) are modified in very different ways by metabolic enzymes and processes. In addition to their distinct metabolism, each drug possesses unique clinical manifestations resultant from the drug's pharmacology.

Cocaine (Figure 7, **1**) is a psychotropic stimulant extracted from the plant *Erythroxylon coca* that has been used for over 2000 years.[20] Pharmacological activity of cocaine is induced via blockage of dopamine, norepinephrine, and serotonin reuptake in the central nervous system (CNS) while simultaneously stimulating release of dopamine from storage vesicles.[21] Flooding of synapses with

neurotransmitters results in extreme stimulation of CNS pathways, generating feelings of euphoria, psychic energy, and self-confidence. Pharmacokinetic data for cocaine have demonstrated a very short plasma half-life of 0.7-1.5 h with a low volume of distribution (1-3 L/kg), demonstrating little cocaine sequestering by tissues.[22]

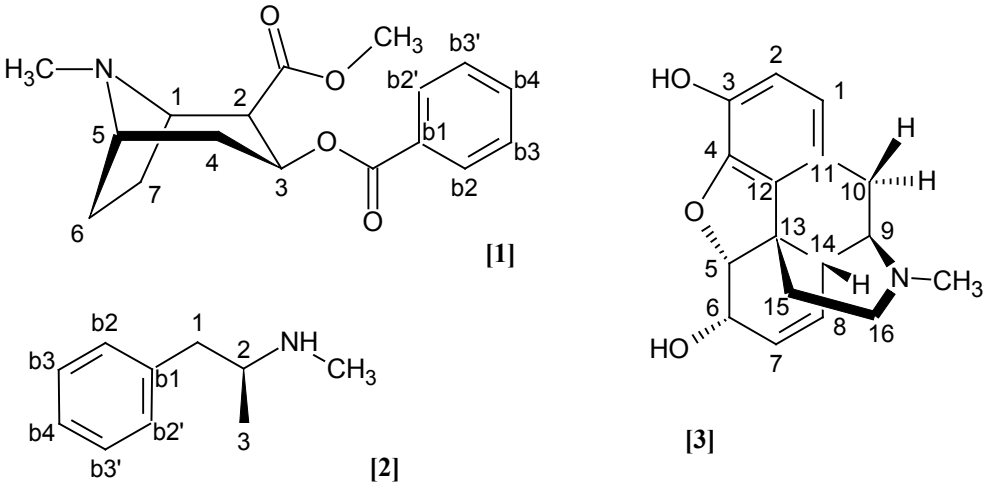


**Figure 7: Chemical structures of cocaine [1], methamphetamine [2], and morphine [3]**

Once ingested, cocaine undergoes extensive Phase I biotransformation *in vivo* (Appendix 1). The majority of these metabolic steps involve aromatic oxidation, *N*-dealkylation, *N*-oxidation, and ester hydrolysis. The hydrolysis of the methyl ester to yield benzoylecgonine is the predominant pathway for *ex vivo* degradation of cocaine (however, human liver carboxylesterase 1 (hCE-1) promotes the hydrolytic cleavage *in vivo*).[23,24] In the body, enzymatic cleavage of the benzoyl ester to form ecgonine methyl ester is catalyzed by plasma pseudocholinesterase and human liver carboxylesterase 2 (hCE-2).[20,23,24] Co-administration of cocaine with ethanol results in the production of cocaethylene via transesterification by hCE-1 and fatty acid ethyl synthase (FAES).[20,24] If cocaine is smoked, the pyrolysis products of cocaine, anhydroecgonine methyl ester and associated metabolites (*e.g.*, anhydroecgonine), can be detected in the blood.[20] In addition to Phase I metabolism, research has suggested that products of cocaine biotransformation are amenable to Phase II modification (*e.g.*, methylation, sulfation, glucuronidation) at the sites of Phase I hydroxylation (*i.e.*, aromatic hydroxyl(s), *N*-hydroxyl), although identification of such conjugation products has yet to be reported in the literature.[23,25] While the majority of these metabolites are

pharmacologically deactivated by Phase I and II biotransformation, the transesterification product cocaethylene has been shown to maintain similar physiochemical properties to cocaine.[20]

Methamphetamine (Figure 7, **2**) is a sympathomimetic amine with CNS stimulant properties whose pharmacological action is a result of dopamine release from storage vesicles. Methamphetamine itself is also an agonist for neurotransmitter transporters, causing serotonin, norepinephrine, and dopamine release.[26] Similar to cocaine pharmacology, release of neurotransmitters causes a general feeling of euphoria. However, the long half-life of methamphetamine (~9 h) leads to lengthened clinical experience of symptoms compared to cocaine and other designer sympathomimetic amines with shorter *in vivo* half-lives.[22] The lipid solubility of methamphetamine can cause minor sequestering in fatty tissues, leading to a volume of distribution of 3-7 L/kg.[26]

Methamphetamine biotransformation involves Phase I processes (Appendix 2); however, the metabolic steps involved are slightly different from those seen in cocaine metabolism. Phase I metabolism of methamphetamine is a result of aromatic oxidation, *N*-dealkylation, *N*-oxidation, and aliphatic oxidation with the primary route of biotransformation being *N*-demethylation to amphetamine and aromatic oxidation to the hydroxymethamphetamine isomers. Unlike cocaine, the metabolism of methamphetamine is relatively slow, with the majority of the elimination product being the parent compound (40-50% of ingested dose).[26] The numerous hydroxylated products produced allow for subsequent conjugation of methamphetamine metabolic products via Phase II conjugation to glucuronide or sulfate moieties.[27] As a result of the chemical nature of sympathomimetic amines, the metabolism of methamphetamine produces numerous pharmacologically active metabolites such as amphetamine.

Morphine (Figure 7, **3**) is a naturally occurring opiate narcotic analgesic extracted from the opium poppy, *Papaver somniferum*.[28] Pharmacological properties of morphine and its congeners are mediated by the μ, κ, and δ opioid receptors. Morphine is a strong agonist of μ opioid receptors, which are responsible for CNS depression clinically manifested as analgesia, miosis, euphoria, and hypothermia. Conversely, morphine only acts as a weak agonist of κ and δ receptors, which mediate analgesia, sedation, diuresis, delusions, and hallucinations.[28] While possessing a relatively short half-life (2-3 h) and a volume of

distribution of 3-5 L/kg, morphine is known to bind to proteins (20-35% plasma protein binding), complicating pharmacokinetic estimations.[22]

Unlike cocaine and methamphetamine, morphine's primary biotransformation pathway involves the Phase II glucuronidation and sulfation of the parent drug (Appendix 3). While a minor amount of Phase I metabolism can occur (by means of *N*-dealkylation, dehydrogenation, and reduction), the free hydroxyl groups at the 3- and 6- positions are the primary active sites for conjugation. The pharmacological activity of morphine is reliant on the free hydroxyl group at the 3-position; consequently morphine-6-glucuronide maintains opioid receptor agonist properties while morphine-3-glucuronide is not active as an opioid agonist. Therefore, even with a relatively short half-life, morphine is able to maintain its pharmacological effects through the continued action of pharmacologically active metabolites. It is noteworthy in consideration of total biotransformation that complete mass balance of morphine metabolism has not yet been achieved, suggesting the existence of unidentified morphine metabolites.[29]

### 2.4. ***In Vitro*** **Metabolic Assays**

*In vitro* metabolic assays are typically employed by the pharmaceutical industry to assess the extent and rate of xenobiotic metabolism and examine the formation of active or toxic products.[30] Other researchers have employed metabolic assays in pharmaceutical protein binding studies.[31] While the assays used for these purposes are numerous and varied, toxicologists must balance the effectiveness, applicability, ease of use, and overall cost of each assay to determine the optimal system for their individual aims. The most common *in vitro* model metabolic systems utilize one of the following as the primary contributor of Phase I and Phase II metabolic activity: hepatocyte cultures, liver homogenate fractions (including microsomes, cytosol, and S9 fraction), horseradish peroxidase, and individual heterologously expressed enzymes. While the addition of cofactors and trapping agents may impact the effectiveness of each assay, the base activity and fundamental enzymatic ability of each metabolic model is mediated by the selection of one of the systems above.

Hepatocyte-based assays (*e.g.,* cultured hepatocytes, liver slices) are the most biologically relevant of the *in vitro* assays because of their innate representation of the hepatic microenvironment. However, the

need for fresh harvesting of live hepatocytes and the risk of decreased viability arising from cryopreservation processes limits the use of hepatocyte-based assays. Non-human peroxidase substitutes (*e.g.*, horseradish peroxidase) are sometimes used as models for non-P450 mediated oxidative activity by various endogenous peroxidases.[10] Recently, recombinant complimentary DNA (cDNA) technology has allowed for the insertion of genetic material coding for individual enzymes into simple organisms (*e.g.*, bacteria, insects), facilitating single enzyme/isoform assay systems. The cDNA-based assays have found particular use in CYP isoform reaction phenotyping, allowing researchers the ability to assign individual enzymatic contribution to metabolic events and calculation of specific enzyme-substrate kinetics. However, these assays only offer a unilateral view of a xenobiotic's metabolism, limiting their effectiveness as comprehensive metabolic model systems. The advantages and disadvantages of the above-mentioned assay systems have been reviewed by Brandon *et al.*[32]

By far, the sub-cellular fractions of liver homogenate are the most commonly utilized metabolic model systems. Of the fractions that can be obtained by differential centrifugation, the three most common utilized for *in vitro* assay protocols are the S9, cytosol, and microsome fractions. After homogenizing liver tissue, centrifugation at 9,000 × *g* removes intact cells, nuclei, and large organelles such as mitochondria. The remaining supernatant, known as the "S9" fraction, is a suspension of soluble proteins and remnants of organelles such as endoplasmic reticulum (ER) and Golgi. The S9 fraction contains many of the enzymes responsible for the Phase I and Phase II biotransformation of xenobiotics including the CYP isoforms, FMOs, and UGTs. Further centrifugation of the S9 fraction at 100,000 × *g* produces a pellet containing microsomes (vesicle-like artifacts formed from the ER when eukaryotic cells undergo homogenization procedures in the laboratory). Microsomal fractions contain a concentrated suspension of membrane-associated enzymes including the CYP isoforms, FMOs, and UGTs. The S9 fraction has only 20-25% of the ER-bound enzymatic activity as microsomal fractions because the microsomes make up approximately one-fifth of the S9 fraction.[33] The supernatant remaining after removal of the microsomes is the cytosolic fraction, which contains soluble proteins and enzymes. Table 2 lists the enzymatic components found in each differential centrifugation fraction.[33]

**Table 2: Enzymatic components of microsomal, cytosolic, and S9 liver fractions**

| Metabolic Enzymes | Microsomes | Cytosol | S9 |
|---|---|---|---|
| Alcohol dehydrogenase | | × | × |
| Aldehyde dehydrogenase | | × | × |
| Amino acid conjugations | × | | × |
| CYP | × | | × |
| Esterases | × | × | × |
| FMO | × | | × |
| GST | × | × | × |
| Methyltransferases | × | × | × |
| NAT | | × | × |
| Reductases | × | × | × |
| SULT | | × | × |
| UGT | × | | × |

Unlike the self-sustained system present in cultured hepatocytes, assays utilizing microsomal, cytosolic, and S9 fractions require the addition of various cofactors to facilitate enzyme function or provide precursor molecules necessary for certain metabolic processes (*e.g.*, glucuronidation, sulfation, glutathione conjugation). Typical cofactors introduced include nicotinamide dinucleotide phosphate (NADPH), $MgCl_2$, NADPH regeneration systems, alamethicin, and Phase II conjugate donor molecules. NADPH is required for the function of many enzymes responsible for Phase I metabolism, including CYPs and FMOs. The addition of a divalent metal ion (*e.g.*, $Mg^{+2}$, $Ca^{+2}$, $Sr^{+2}$) has been found to increase the activity of systems containing CYP enzymes by stimulating the electron transfer from NADPH cytochrome P450 reductase to cytochrome $b_5$ and CYP enzymes.[34] The addition of a NADPH regeneration system allows for the cyclic regeneration of the activating cofactor NADPH. Typical regeneration systems include an enzymatic component capable of reducing $NADP^+$ back to NADPH by oxidizing a substrate additive. Common NADPH regeneration systems are glucose-6-phosphate/glucose-6-phosphate dehydrogenase and isocitrate/isocitrate dehydrogenase.

Phase II conjugation can be performed using *in vitro* systems by supplementation with additives containing conjugate moieties (see Table 1 for cofactors corresponding to Phase II processes). Typically,

no additional cofactors beyond those listed in Table 1 are necessary to facilitate conjugation; however, glucuronidation processes are enhanced by the addition of alamethicin (Alm) as a cofactor. UGTs are membrane-bound proteins with active sites localized inside the lumen of the ER.[35,36] To facilitate substrate access to UGT binding sites for glucuronidation, Alm is added to the reaction mixture. Alm is a 20-residue antibiotic fungal peptide that forms multiconductance channels across lipid bilayers. The well-defined pores are formed by the introduction of a hexameric bundle of the largely α-helical Alm across the lipid bilayer of the ER, thereby decreasing the observed enzymatic latency arising from the ER membrane acting as a diffusional barrier for substrates, cofactors, and products.[35-38]

While the above describes a complete *in vitro* metabolic system capable of producing Phase I and Phase II biotransformation products, further supplementation with additional nucleophilic "trapping molecules" expands the breadth of data obtained from *in vitro* metabolic assays. A large subset of these trapping agents are biomolecules of varying complexity employed to approximate interactions between substrates and endogenous biomolecules *in vivo*. Such trapping agents include single nucleophilic amino acids, synthetic and natural peptides, purified proteins, GSH, cyanide, semicarbazide, methoxylamine, and 2'-deoxyguanosine.[31,39-49]

### 2.5. **Biomarkers of Exposure, Protein Adduction, and Adduction Mechanisms**

The term "biomarker of exposure" refers to a group of molecules that provide physiochemical evidence of exposure to a xenobiotic.[19] Often, these biomarkers are generated by the modification of an endogenous biomolecule such as DNA or protein. There are two classes of biomarkers of exposure. The first is a biomarker that is indicative of, but not unique to, exposure to a given molecule. For example, the addition of methyl groups to DNA bases can arise from exposure to methylmethane sulfonate (a cancer treatment agent); however, dimethylsulfate (a chemical warfare agent) is also a potent methylating agent of DNA bases (Figure 8a).[50,51] While useful as corroborating evidence of exposure, these non-unique entities are not unequivocal proof of exposure on their own. The second type of exposure biomarker is one that contains a moiety unique to the analyte of interest (typically a portion of the analyte molecule itself). These biomarkers provide unequivocal evidence of exposure, as their mechanism of formation precludes

generation by any other analyte. Both clozapine and diclofenac are examples of xenobiotics that form unique adducts with cysteine thiols on proteins (Figure 8b).[43]

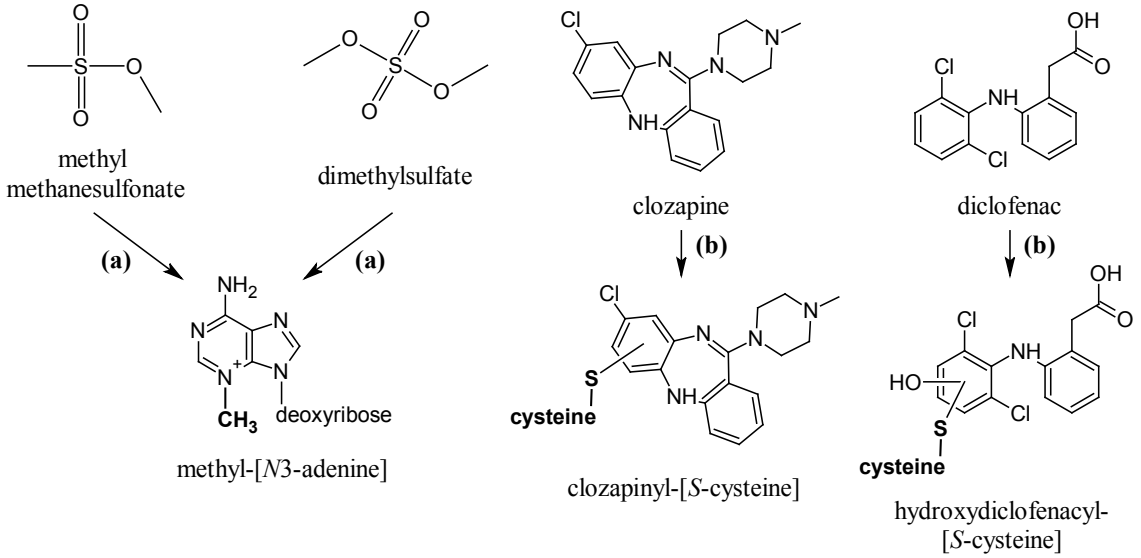


**Figure 8: Examples of (a) non-unique and (b) unique biomarkers of exposure**

Unique biomarkers of exposure are commonly the result of xenobiotic adduction to endogenous biomolecules. Adduction refers to the irreversible covalent modification of reactive nucleophilic sites on biomolecules by inherently reactive electrophilic xenobiotics or metabolically activated moieties (either reactive metabolites or short-lived intermediates). Biomolecular adduction typically occurs on reactive nucleophilic functional groups within DNA or protein structure. The reactivity of individual biological nucleophiles is attributed to a combination of physiochemical factors including electron density, polarizability, the nature of the interacting xenobiotic species (electrophile), and steric factors that influence reactive site availability. In recent years, great progress has been made in modeling these interactions, with the goal of predicting the nature and extent of reaction of electrophilic xenobiotics with biological nucleophiles. These concepts are discussed below.

The hard and soft acid and base (HSAB) theory is a compendium of calculations, estimators, and chemical properties that characterize the thermodynamic and physical interactions between electrophilic and nucleophilic entities that can bring about the formation of adducts. In 1963, Pearson first described HSAB theory, stating that hard (*i.e.*, nonpolarizable) acids preferentially bind to hard bases while soft (*i.e.*, polarizable) acids prefer to bind to soft bases, in consideration of both thermodynamic and kinetic

properties.[52] "Hardness" is a measure of resistance to change of an electron cloud, either by means of gain or loss of electrons or by polarization.[53] While the hardness (and by association, softness) of a species mediates its reactivity (both global and localized), the property itself cannot be directly measured quantitatively. In a simplified form, chemical hardness (η) can be related to electronegativity (χ) (described in Equation (1)) by expressing it as a function of ionization energy (*I*) and electron affinity (*EA*), as in Equation (2).

Equation (1) $$\chi = \frac{I + EA}{2}$$

Equation (2) $$\eta = I - EA$$

Chemical softness (σ) can, therefore, be described as the inverse of hardness, as shown in Equation (3).

Equation (3) $$\sigma = \frac{1}{\eta} = \frac{1}{I - EA}$$

However, these equations represent only the surface of the complex calculations that are used by chemists to theoretically estimate the quantitative role of such parameters in reaction thermodynamics.

Additional advances have been made in recent years with the application of density functional theory (DFT) calculations to estimations of chemical hardness. Frontier orbital theory (FOT) is an approximation of chemical exchange which asserts that interactions between frontier molecular orbitals (and the valence electrons they hold) are the primary contributors to inter-molecular interactions. FOT maintains the basic principles of HSAB theory, purporting that adduct formation occurs when a soft nucleophile donates its highest energy electron to the lowest unoccupied molecular orbital (LUMO) of a soft electrophile. In consideration of FOT, useful descriptor calculations regarding reactivity of electrophile-nucleophile interactions only require the estimation of LUMO energy ($E_{\mathrm{LUMO}}$) and highest occupied molecular orbital (HOMO) energy ($E_{\mathrm{HOMO}}$), which can be performed by commercially available computational programs (*e.g.*, Spartan and Gaussian). From these values, basic parameters including hardness (η), softness (σ), and chemical potential (μ) can be calculated as follows:

Equation (4) $$\eta = \frac{E_{\mathrm{LUMO}} - E_{\mathrm{HOMO}}}{2}$$

Equation (5) $$\sigma = \frac{1}{\eta} = \frac{2}{E_{\text{LUMO}} - E_{\text{HOMO}}}$$

Equation (6) $$\mu = \frac{E_{\text{LUMO}} + E_{\text{HOMO}}}{2}$$

FOT also facilitates the calculation of higher order descriptors that combine the above lower order parameters to deliver multifaceted summaries of chemical reactivity. Sensitive measures of electrophilic ($\omega$) and nucleophilic ($\varphi$) reactivity involve mathematical combinations of chemical hardness ($\eta$) and chemical potential ($\mu$):

Equation (7) $$\omega = \frac{\mu^2}{2\eta}$$

Equation (8) $$\varphi = \frac{1}{\omega} = \frac{2\eta}{\mu^2}$$

While the above parameters are useful in examining the relative reactivity of substances within a class, they are not sufficient to examine the interaction that occurs between a nucleophile and an electrophile during the adduction process. In contrast, the reaction index ($\omega^-$) summarizes the reactivity of two species as a function of their respective hardness and chemical potential as shown in Equation (9) ("A" refers to the nucleophile, "B" refers to the electrophile).

Equation (9) $$\omega^- = \frac{\eta_A(\mu_A - \mu_B)^2}{2(\eta_A - \eta_B)^2}$$

When comparing reactivities between electrophile-nucleophile pairs, the higher the $\omega^-$ value, the more favorable adduct formation is within the system on the basis of electronic factors.

Qualitatively, HSAB theory is a lens through which the covalent adduction of xenobiotics to biomolecules can be viewed. Two common targets of biomolecular adduction are DNA and proteins. DNA is composed of four subunit bases (adenine, cytosine, guanine, and thymine) held together via hydrogen bonding and linked in strands by a phosphate-deoxyribose backbone. Covalent adduction to nucleophilic sites on the subunit bases or the phosphate moiety of the backbone chain has been characterized for numerous reactive xenobiotics. Generally, reactive sites on DNA are hard nucleophiles,

making DNA a reservoir for the preferential adduction by hard electrophilic species (see Table 3).[44,54] Clear implications exist for the downstream impact of covalent DNA modifications, especially concerning epigenetic and carcinogenic factors. Disruption of any pathway vital to transcription or DNA replication can generate a cascade of ill effects at cellular (*e.g.*, mutation, apoptosis) or tissue (*e.g.*, carcinoma formation, necrosis, teratogenesis) levels.

**Table 3: Examples of hard and soft electrophilic and nucleophilic functional groups**

| Type | Electrophiles | Nucleophiles |
|---|---|---|
| **Hard** | alkyl carbonium ions | oxygen atoms of DNA bases |
| | benzylic carbonium ions | endocyclic nitrogens of bases in DNA |
| | iminium ions | oxygen atoms of serine and threonine |
| | aldehydes | |
| **Soft** | epoxides | thiol group of cysteine |
| | enones | thiol group of glutathione |
| | quinone imides | amine groups of lysine and histidine |
| | quinone methides | |
| | imine methides | |
| | isocyanates | |
| | isothiocyanates | |
| | aziridinium ions | |
| | episulfonium ions | |

Unlike DNA, proteins are polymeric chains of amino acids connected by peptide amide linkages. While cofactors including heme groups and functional metal ions can be incorporated into protein structure, higher order structural characteristics of proteins are typically associated with amino acid sequence and structure. Each of the 20 naturally occurring amino acids has a distinct side-chain structure, imparting physiochemical properties to the parent protein and immediate microenvironment. Among these amino acids are nucleophilic residues that have the potential to form covalent adducts with electrophiles depending on individual electronic and steric factors. Among the nucleophilic amino acids, some of the most reactive are the harder nucleophiles serine and threonine as well as the softer nucleophiles lysine and histidine, with cysteine being the softest and generally most reactive biological nucleophile. Additionally,

the free amino terminus is a highly reactive nucleophile in proteins (although it is often blocked in cellular proteins).

Reactivity of amino acid residues within proteins is a product not only of innate reactivity arising from structure, but is also a function of positioning within a protein and electronic influences resulting from adjacent residues.[55,56] Variability in amino acid reactivity can be exemplified by nucleophilic lysine and cysteine residues. Nucleophilic reactivity of both residues is mediated by their ionization state. Maximal reactivity of lysine residues requires the ε-amino group to be in the unprotonated state, while the anionic thiolate form of the sulfhydryl is the more reactive form for cysteine. Both residues rely on their respective $pK_a$ values to determine ionization state. Even though lysine has a base $pK_a$ of ~10.4, it has been demonstrated that apparent lysine $pK_a$ values can vary greatly within a single protein.[55] At physiological pH (7.4), lysine residues with low apparent $pK_a$ values are largely in the reactive nucleophilic unionized state.

Cysteine has a base $pK_a$ of ~8.3; therefore, at physiological pH, deprotonation of the sulfhydryl to form the thiolate is not favored. However, the occurrence of catalytic diads can significantly modify cysteine $pK_a$ values, promoting thiolate formation.[56] Catalytic diads are cysteine residues adjacent to basic residues (*i.e.*, lysine, histidine, arginine) that facilitate in the formation of thiolates from cysteine sulfhydryls. Figure 9 shows the influence of adjacent basic residues in forming thiolate ions from cysteine sulfhydryl moieties.[56] An example of one such catalytic diad is Cys-25 in the proteinase ficin.[57] Cys-25 interacts with a basic histidine moiety (His-159), imbuing Cys-25 with a depressed $pK_a$ of 2.5, creating a hyper-reactive nucleophilic center, likely prone to adduction by soft electrophiles.

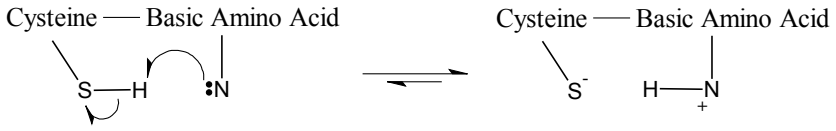


**Figure 9: Mechanism of cysteine thiolate formation in catalytic diad configurations**

As functional biomolecules, proteins experience a series of consequences arising from covalent modification by reactive electrophiles. The site of covalent modification on a protein can be a factor mediating downstream impact. Binding to non-essential domains within a protein's structure may leave the

protein fully functional and unaffected. However, it is more likely that structural deformation resultant from adduction or binding at an enzymatic active site can decrease or completely inhibit protein function. Well-characterized acetaldehyde adducts arising from ethanol metabolism have been shown to detrimentally impact the function of numerous proteins, particularly those containing critical reactive lysine residues.[58-60] There are even documented cases where covalent protein binding has elicited immunological responses in humans, causing accelerated catabolism of adducted (often functionally inhibited) proteins. Consumption of alcohol has been found to cause the generation of antibodies with acetaldehyde adduct specificity, with the highest titer of such antibodies found in patients with alcoholic liver disease.[61-63]

It is noteworthy that unlike DNA adducts, there is not a mechanism in place for the repair of adducted proteins.[64] Consequently, protein adducts are persistent until the protein itself is degraded or replaced, which makes them excellent long-term exposure markers. While the length of time a protein adduct can be detected is strictly dependent on the lifetime of the target protein *in vivo*, certain proteins are particularly advantageous to act as molecular dosimeters of xenobiotic exposure. For example, hemoglobin is removed from circulation with erythrocytes after approximately 120 days in humans, allowing it to act as a cumulative dosimeter for xenobiotic exposure.[65] While other protein targets may have shorter lifetimes in the body, they may find utility on the basis of other considerations. Serum albumin has a relatively shorter *in vivo* half-life of ~20 days, but is biosynthesized in hepatocytes, making it an ideal target for short-lived reactive metabolites produced in the liver.[65,66] Utilizing a battery of exposure indicators can allow for estimation of retrospective dose reconstruction, differentiating complex scenarios such as chronic vs. single dose exposure.[67]

While numerous hypotheses exist regarding relative toxicity of covalently bound protein adducts, effective methods for determination of protein adduct mediated toxicity do not yet exist.[54] However, even though specific mechanisms of toxicity cannot always be established, evidence and characterization of covalent protein adduction can give insight into downstream xenobiotic pathology including occurrences of idiosyncratic toxicity and target organ system toxicities.[61,63,68,69]

From the standpoint of both the forensic and medical disciplines, unique biomarkers of exposure are preferred because of their inherent ability to confirm exposure to specific xenobiotics. Development of

analytical assays to detect unique biomarkers could assist in designating exposure beyond the lifetime of the parent drug or metabolites in common matrices (*e.g.*, blood, urine). Biomarkers could also be of potential use in examining multiple-drug interactions and to give insight into toxicity and adverse interactions arising from drug exposure. Furthermore, biomarkers of exposure specific to illicit drugs could benefit law enforcement officials by extending detection timelines, a tool that can be useful when exposure determination is critical (*e.g.*, in parole monitoring). Methods developed for adduct analysis may range from more complex direct analysis of modified endogenous proteins to simpler, less invasive measures such as examination of mercapturates in urine or GSH conjugates in blood. Laying the groundwork for such assays requires the complete characterization of protein adducts formed by the analyte of interest and includes studies into their mechanism of formation.

### 2.6. **Protein Adduction by Drugs of Abuse**

While licit pharmaceuticals undergo protein binding studies amidst the rigorous milieu of safety testing required prior to approval within the USA, similar studies are not afforded to illicit drugs. Consequently, few investigations into protein adduction by drugs of abuse, either to identify potential biomarkers or possible mediators of drug toxicity, have been reported in the literature. For the latter, even minor biotransformation pathways leading to irreversible protein adduction may have severe consequences for drug abusers because of the tendency to co-abuse multiple drugs simultaneously and to use higher doses that result in depletion of cellular defense against reactive electrophilic species (*i.e.*, GSH), as chronic abusers develop tolerance to their habitual drug(s) of choice.

One of the most investigated drugs of abuse (although licit for recreational use) has been ethanol, or more specifically, ethanol's reactive metabolite, acetaldehyde.[70] Acetaldehyde has been found to form numerous adduction products with endogenous biomolecules with severe implications into the resultant toxicity experienced by alcohol abusers. Acetaldehyde is known to form Schiff base adduction products with Lys residues in proteins[71], functionally inhibiting proteins reliant on Lys residues at the catalytic site.[60] In conjunction with protein inactivation, these adducts have also been linked to downstream immunogenic and histopathological detriments impacting chronic alcoholics.[61,63,72] Supplemental to toxicological

implications, acetaldehyde adducts are also biomarkers of ethanol exposure. Detection of known Schiff base adduction products on Lys residues is indicative of ethanol exposure. While some of the acetaldehyde adducts are unstable *in vivo*, others are stable and are useful in retrospective exposure assessment.[73,74]

Among illicit drugs, phencyclidine (PCP) is one of the most studied for its protein binding properties. Protein adduction resultant from PCP exposure is the result of several reactive metabolites including a cyclic iminium ion as well as epoxide and quinone methide intermediates.[75-77] Research has demonstrated the direct impact of these reactive compounds via the adduct-induced inactivation of human CYP enzymes (specifically CYPs 2B6 and 2C19) as a direct result of PCP exposure.[78,79]

Protein binding elicited by morphine metabolism has also been examined to a limited extent. Oxidation of morphine by morphine-6-dehydrogenase or free hydroxyl radicals to yield the reactive α,β-unsaturated carbonyl, morphinone, has been shown to lead to binding with biomolecular thiols, including GSH and 2-mercaptoethanol via covalent attachment at the 8-C of morphinone in numerous species including humans (Pathway (a), Figure 10).[80-84] Specific structural examination by Ishida *et al.* determined the formation of the distinct 8α- stereospecific product.[85] Further *in vivo* and *in vitro* studies with mice and rats by Nagamatsu and colleagues have demonstrated that macromolecular binding of morphinone directly correlated with hepatotoxicity.[86,87] Indeed, previous research has shown that total morphinone produced (measured as the sum of GSH-bound and free fraction) exceeded that of normorphine in both the rat and guinea pig, suggesting morphinone production as the secondary major biotransformation route of morphine metabolism after Phase II conjugative events.[80,81]

A second set of morphine-based adduction products relies on the formation of an unknown electrophilic metabolite that binds to protein thiol models (*i.e.*, *N*-acetylcysteine, GSH) at the 10-C position in rats and humans (Pathway (b), Figure 10).[88-90] Correia and colleagues have specifically designated the formation of a CYP-mediated oxidative product that is an electrophilic species capable of reacting with nucleophilic thiols, forming the distinct 10α- stereospecific product. While these results are encouraging in accounting for incongruence in the mass balance of morphine metabolism, further investigations into the identity and mechanism of formation for the responsible unknown metabolite have not been pursued to date (since 1986).

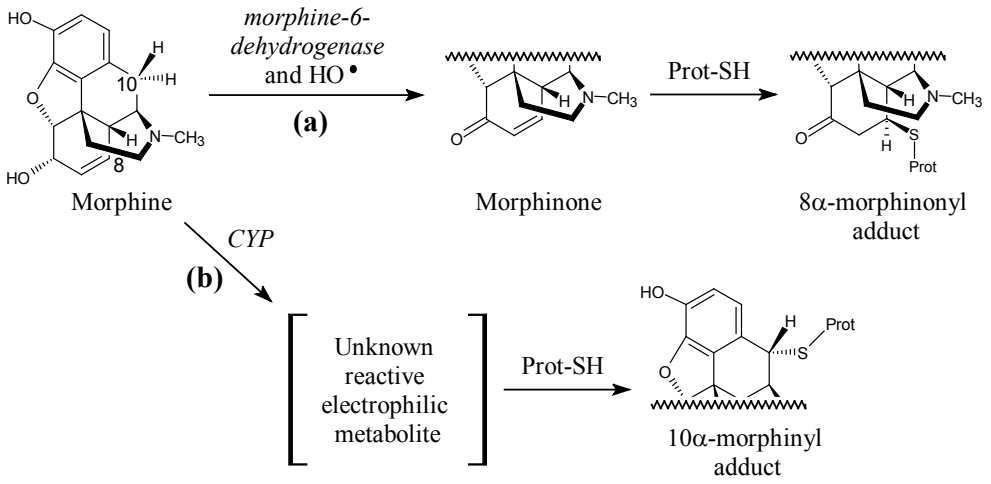


**Figure 10: Mechanisms for irreversible protein adduction by morphine**

As with morphine, cocaine ingestion is known to result in measurable levels of irreversible protein binding, as demonstrated by numerous histopathological studies, investigations utilizing radiolabeled drug, and analysis of immunogenic antibodies present in the blood of cocaine abusers.[91-96] While these studies demonstrate the existence of cocaine protein adducts and correlate their formation with cocaine toxicity, little conclusive data exists for the direct analysis of cocaine-derived adduction products. Numerous hypotheses have been proposed as to the reactive species responsible for cocaine-derived irreversible protein binding, including nitrosonium ions resultant from tropane oxidation (Pathway (a), Figure 11)[23,95-97] and intramolecular acid-catalyzed activation of the methyl ester with subsequent adduction to ε-amine groups on Lys residues (Pathway (b), Figure 11)[98]. A third pathway for cocaine protein adduction was more recently investigated, involving the adduction potential the of pyrolysis product anhydroecgonine methyl ester (AEME) with biological thiol models (Pathway (c), Figure 11)[99]. Work performed by Myers and colleagues demonstrated the production and toxicity of thiol conjugates arising from AEME, suggesting a potential role of such metabolic pathways in the sequelae of abused cocaine related toxicities. However, as with research into the pathways responsible for protein binding in morphine, investigations into mechanisms responsible for irreversible cocaine protein binding have remained dormant since the mid 2000s.

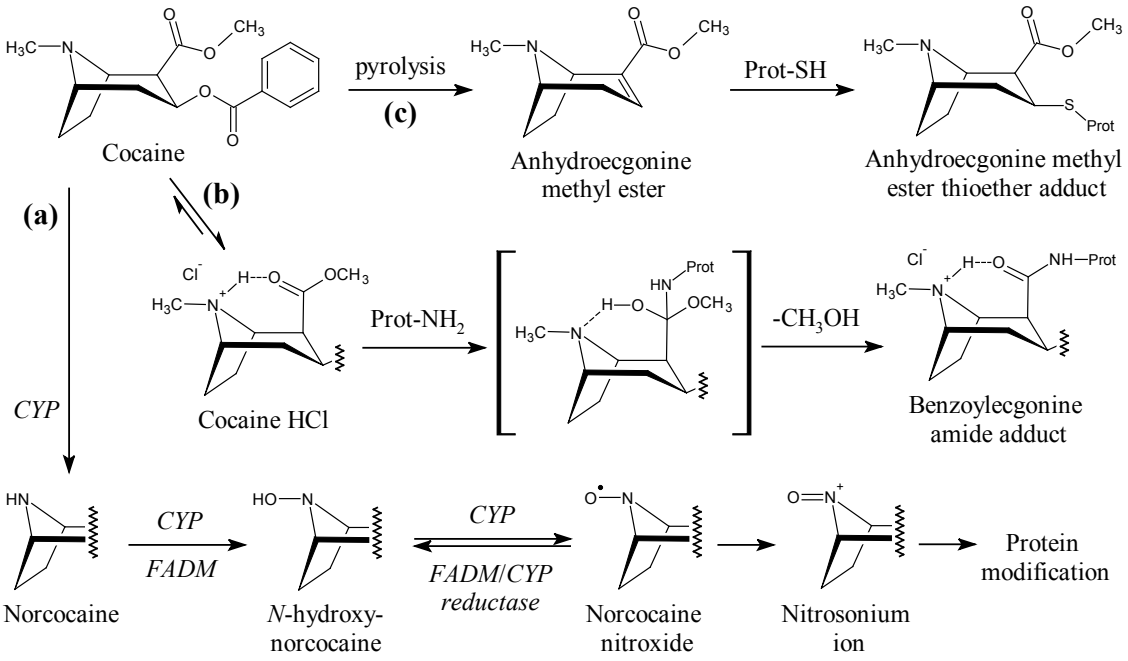


**Figure 11: Hypothesized mechanisms of irreversible protein modification by cocaine**

Aside from those drugs listed above, there have been few data collected on protein adduction by drugs of abuse. Formation of melanin-amphetamine irreversible adducts generated during the enzymatic production of melanin in hair has been examined.[100] Unlike the typical formation of irreversible covalent adduction products, melanin-amphetamine adduction requires the enzymatic activation of melanin prototype molecules in order to generate an electrophile capable of reacting with amphetamine molecules. Examinations into another phenethylamine, 3,4-methylenedioxymethamphetamine (MDMA), have demonstrated the formation of covalent adduction products resultant from catechol metabolite conversion to an *ortho*-quinone and subsequent reaction with biological thiols (*i.e.*, GSH and *N*-acetylcysteine).[101] Such MDMA-adducted thiols are suspected of playing a mechanistic role in observed MDMA-induced neurotoxicity.[102] While phenethylamines and other nascent designer drug classes are currently receiving great attention from the toxicology community, the majority of research is focused on parent drug and metabolite detection while virtually no data are available on the protein binding potential of these and other drugs of abuse.

## 2.7. **Research Objectives**

This research was conducted to test three main hypotheses:

*Hypothesis I:* In vitro *assay systems can be used as effective models of* in vivo *human hepatic metabolism for drugs of abuse.*

*Hypothesis II: Specific enzymes in the human body are responsible for biotransformation pathways that result in the formation of reactive metabolites and unstable intermediates.*

*Hypothesis III: Drugs of abuse form irreversible covalent adduction products with endogenous proteins and biomolecules.*

The primary objective of this research was to employ sensitive and specific scientific methods to examine the fate of cocaine, methamphetamine, and morphine during and after biotransformation in the human body. The content of this report presents data obtained via instrumental evaluation of *in vitro* assay samples modeling the metabolism of each important drug of abuse. The different tasks addressed are listed below:

a. Optimization of methods for the comprehensive analysis of cocaine, methamphetamine, and morphine metabolic products by LC-MS/MS separation and identification using multiple reaction monitoring, including:
    i. Absolute quantification performed where possible.
    ii. Individual optimization of ionization and MS/MS parameters for each analyte where possible.
    iii. Synthesis of metabolic products for parameter optimization purposes where synthetic methods were available and procedures were feasible within the scope of the project.
b. Optimization of *in vitro* metabolic assay parameters for the rapid generation of major metabolic products from xenobiotics:
    i. Assay system additives
    ii. Incubation time

iii. Component concentrations

c. Evaluation of metabolic profiles of drugs of abuse across different *in vitro* assay systems.

d. Optimization of bactosome-based *in vitro* assays for single-isozyme metabolism of xenobiotics.

e. Determination of specific cytochrome P450 isoforms responsible for production of primary metabolic products of cocaine, methamphetamine, and morphine using data from bactosome-based assays.

f. Screening of assays containing nucleophilic trapping agents in the presence of active metabolism mechanisms for hypothesized adduction products arising from cocaine, methamphetamine, morphine, or their metabolites:

   i. Trapping agents: *N*-acetylcysteine, *N*-acetylhistidine, *N*-acetyllysine.

   ii. Product confirmation via MS/MS product ion scans of suspected adduction products.

g. Optimization of LC-MS/MS separation and identification methods for confirmed adduction products.

h. Characterization of metabolic processes associated with adduction products:

   i. Enzyme class determination.

   ii. Cytochrome P450 isoform designation.

   iii. Mechanism of electrophile/nucleophile interaction.

   iv. Binding potential with complex biomolecules.

i. Correlation of *in vitro* generated adduction products with *in silico* predictions of electrophile/nucleophile reactivity.

## 3. METHODOLOGY

### 3.1. **Instrumentation**

Analysis of samples by LC-QQQ-MS was performed on an Agilent 6460 triple quadrupole mass spectrometer while samples analyzed by LC-QTOF-MS employed an Agilent 6530 quadrupole time-of-flight system. Both mass spectrometers were coupled to an Agilent 1290 Infinity ultra-high performance liquid chromatography (UHPLC) system using Jet Streaming electrospray ionization (ESI) technology. All chromatographic separations were elicited using an Agilent ZORBAX Rapid Resolution HD Eclipse Plus $C_{18}$ column (50 mm × 2.1 mm, 1.8 μm particle size) maintained at 40°C. Data acquisition and analysis were performed using the Agilent MassHunter software package for both systems.

### 3.2. **Synthesis of Monohydroxylated Cocaine Metabolite Isomers**

Chromatographic peak assignments as well as ionization and fragmentation parameters for select aromatic oxidation isomers were determined by in-house synthesis and analysis of nine metabolic products of cocaine containing monohydroxylated arene moieties (2-, 3-, and 4-hydroxybenzoylecgonine; 2-, 3-, and 4-hydroxycocaine; and 2-, 3-, and 4-hydroxycocaethylene), using the previously reported Steglich esterification method (see Appendix 4 for reaction mechanism).[103,104] Briefly, 0.1 mg of drug precursor, 0.5 mg of hydroxybenzoic acid, 1 mg of 1,3-dicyclohexylcarbodiimide, and 2 drops of pyridine in 1 mL of methylene chloride were added to a 5 mL reaction vial. The solution was stirred at 50°C for 2 h. After cooling to room temperature, the reaction mixture was washed with 2 mL of water and extracted with 2 mL of 2 M HCl. The acidic solution was washed with 2 mL of methylene chloride to remove non-basic components. The aqueous solution was adjusted to pH 8.5 using 1 M $NH_4OH$ and extracted with two 2 mL volumes of chloroform/2-propanol (3:1), and the combined organic extracts were evaporated to dryness using vacuum centrifugation and reconstituted in 100 μL of dimethyl sulfoxide (DMSO). The drug precursors utilized for synthesis were as follows: ecgonine for hydroxybenzoylecgonine isomers, ecgonine methyl ester for hydroxycocaine isomers, and ecgonine ethyl ester for hydroxycocaethylene isomers. 2-, 3-, and 4-hydroxybenzoic acids were utilized to generate isomers substituted at the 2-, 3-, and 4- positions, respectively.

Thorough characterization of individual isomers utilized MS/MS examination on the LC-QQQ-MS system. In order to better understand the structural characteristics of some MS/MS fragment ions, pseudo-$MS^3$ was performed via an in-source decay method. In-source decay of hydroxycocaine isomers was elicited by increase of optimized fragmentor voltage from 135 to 200 V. Quadrupole filtering for MS/MS fragments of interest followed by subsequent fragmentation in the collision cell yielded pseudo-$MS^3$ spectra allowing for in-depth structural analyses.

### 3.3. **Comprehensive Drug Metabolite Analysis**

Targeted metabolites for cocaine, methamphetamine, and morphine were identified by an examination of the literature for metabolites reported in authentic human samples and biotransformation products that were hypothesized in published literature based on postulated metabolic pathways. Comprehensive tables of the metabolites examined for cocaine, methamphetamine, and morphine are found in Appendices 5, 6, and 7, respectively. Gradient elution of drug metabolites and standards of cocaine, methamphetamine, and morphine utilized a biphasic system of eluents according to the parameters described in Appendix 8. When possible, ionization and MS/MS fragmentation parameters were individually optimized for parent drugs and metabolites using the Agilent Optimizer software. For instances where reference standards were unavailable and optimization could not be performed, the ionization and fragmentation parameters of a structurally similar metabolite were applied (*e.g.*, conditions optimized for benzoylnorecgonine were applied to *N*-hydroxybenzoylnorecgonine because no reference standard for *N*-hydroxybenzoylnorecgonine was available).

Individual analytes were monitored by LC-QQQ-MS using two multiple reaction monitoring (MRM) transitions (one primary quantifier and one secondary qualifier). MRM transitions as well as ionization and fragmentation parameters for each metabolic analyte are summarized in Appendix 5 (cocaine), Appendix 6 (methamphetamine), and Appendix 7 (morphine). When possible, absolute quantification of metabolite formation was performed by generating calibration curves using reference standards. A series of calibrators (5000, 4000, 2000, 1000, 500, 100, 10 and 1 ng/mL in DMSO for cocaine; 5000, 2000, 1000, 500, 100, 10, 1, and 0.1 ng/mL in water for methamphetamine and morphine)

was utilized to generate each standard curve and individual sample quantification was performed utilizing Agilent MassHunter Quantitative Analysis software (Table 4 lists analytes for which absolute quantification was performed). For instances where calibrated reference standards were not available, data analysis was performed by converting raw peak areas into ratios relative to the internal standard in order to account for instrumental variation. While no absolute quantitative assessment could be determined for these compounds, inter-assay comparisons revealed the ability of individual systems to mediate specific biotransformation pathways.

**Table 4: Analytes quantified using standard calibration curves**

| Cocaine | Methamphetamine | Morphine |
|---|---|---|
| benzoylecgonine | amphetamine | hydromorphone |
| cocaethylene | ephedrine | morphine-3-glucuronide |
| ecgonine | norephedrine | normorphine |
| ecgonine ethyl ester | | |
| ecgonine methyl ester | | |
| norcocaine | | |

DMSO (a polar aprotic substance) was utilized as a solvent for cocaine samples in order to avoid the passive hydrolysis of cocaine and certain metabolites. It was experimentally determined that 1 μL injections of DMSO did not significantly impact analyte retention or peak shape. In order to compensate for decreased method sensitivity brought on by injection volume reduction, sample and calibration concentrations were increased for cocaine analysis. Methamphetamine and morphine were not observed to undergo analogous passive hydrolytic events; therefore water was utilized as a solvent for methamphetamine and morphine metabolism samples.

### 3.4. **Metabolic Assays**

In order to examine the ability of *in vitro* assays to produce metabolites for cocaine, methamphetamine, and morphine, various systems modeled after those employed in pharmaceutical evaluations were compared.[31] These assays contained a mixture of biotransformation enzymes, cofactors,

and test compound according to the specifications detailed in Table 5. The system containing no metabolic enzymes or cofactors was utilized to examine the passive biotransformation of each drug (*e.g.*, non-enzymatic hydrolysis). Human liver microsomes (HLM), human liver cytosol (CYT), and human liver S9 fraction (S9) assays examined the Phase I biotransformation and Phase II conjugative activity of each compound. Horseradish peroxidase (HRP) provided a system to model non-CYP mediated oxidative metabolism. Positive controls for Phase I and Phase II metabolism were performed by incubating zolpidem and nicotine, respectively, according to identical procedures as drug substrates.

**Table 5: Summary of sample preparation for metabolic assay incubations**

| **Component** | **Metabolic System** | | | | | | |
|---|---|---|---|---|---|---|---|
| | **No Enzyme** | **HLM, CYT, or S9** | | | | **HRP** | |
| | | **+1** | **+2** | **+1/2** | **-** | **+** | **-** |
| **Activating cofactors** | N/A | 2.0 mM NADPH | 2.0 mM UDP-GlcUA | 2.0 mM NADPH<br>2.0 mM UDP-GlcUA | N/A | 500 µM $H_2O_2$ | N/A |
| **Buffer** | 10 mM pH 7.4 sodium phosphate buffer | | | | | | |
| **Substrate** | 200 µM cocaine, methamphetamine, morphine, or positive control | | | | | | |
| **Enzyme** | N/A | 2.0 mg/mL HLM, CYT, or S9 | | | | 0.1 µg/mL HRP | |
| **Non-activating cofactors** | N/A | 50 µg/mL alamethicin<br>3.0 mM $MgCl_2$ | | | | N/A | |
| **Regeneration system** | N/A | 0.4 U/mL glucose-6-phosphate dehydrogenase<br>3.0 mM glucose-6-phosphate | | | | N/A | |

All *in vitro* incubations were performed in 10 mM sodium phosphate buffer (pH 7.4) at 37°C to model physiological conditions. All components except the activating cofactor(s) were added to an Eppendorf tube and pre-incubated for 5 min to bring the system to appropriate temperature. The activating cofactor(s) were then added to each reaction vessel (50 µL final sample volume), which was then mixed and incubated for up to 24 h. At 0.5 and 24 h, 25 µL aliquots of each sample were withdrawn and processed for LC-QQQ-MS analysis. To each 25 µL aliquot, 25 µL of ice-cold acetonitrile were added to precipitate proteins and cease metabolism. Samples were centrifuged at 15,000 at 4°C for 30 min to pellet protein. The supernatant was recovered, evaporated to dryness, and reconstituted in the appropriate

solvent with added internal standard (DMSO with benzoylecgonine-$D_3$ for cocaine, water with methamphetamine-$D_5$ for methamphetamine, water with morphine-$D_3$ for morphine) for subsequent LC-QQQ-MS analysis.

Determination of assay enzymatic activity was performed by subtracting analyte concentrations found in control samples from active systems. For example, the analyte concentration determined in HLM preparations without added NADPH or UDP-GlcUA (*i.e.*, HLM-) was subtracted from that in HLM with added NADPH (*i.e.*, HLM+1), HLM with added UDP-GlcUA (*i.e.*, HLM+2), or HLM with both cofactors added (*i.e.*, HLM+1/2) (see Table 5). When absolute concentrations were not determined due to lack of calibrated standards, analogous corrections were performed by subtracting ratios relative to internal standard. Consequently, all comparative data are presented as "deviation from control" in either ng/mL (where calibrated standards were available) or relative ratio to internal standard (where calibrated standards were not available).

### 3.5. **Cytochrome P450 Isoform Metabolic Assays for Reaction Phenotyping**

Designation of individual CYP isoform contributions to specific biotransformation pathways was performed with the aid of bactosomes (microsomes harvested from *Escherichia coli* heterologously expressing human genes that code for CYP isoform production co-expressed with human NADPH-cytochrome P450 reductase). The individual isoforms examined included CYPs 1A2, 2B6, 2C8, 2C9, 2C19, 2D6, and 3A4. Samples were created according to the specifications given in Table 6 and following the same procedures for preparation as detailed in Section 3.4. Final sample volumes were 50 µL each and were incubated at 37ºC for 30 min. Metabolism was ceased by addition of 50 µL of ice-cold acetonitrile followed by centrifugation at 15,000 × *g* for 30 min at 4°C to pellet proteins. Supernatants were evaporated to dryness, reconstituted in solvent, and subjected to LC-QQQ-MS analysis by the appropriate "Drug Metabolite Analysis" method (see Appendix 8).

**Table 6: Summary of sample components for metabolic reaction phenotyping assays**

| Component | rhCYP System | |
|---|---|---|
| | **Control (-)** | **Positive (+)** |
| **Activating cofactor** | N/A | 2.0 mM NADPH |
| **Buffer** | 10 mM sodium phosphate buffer (pH 7.4) | |
| **Substrate** | 200 μM cocaine, methamphetamine, or morphine | |
| **Enzyme** | 2.0 mg/mL rhCYP bactosome | |
| **Non-activating cofactors** | 5.0 mM $MgCl_2$ | |
| **Regeneration system** | 0.4 U/mL glucose-6-phosphate dehydrogenase<br>3.0 mM glucose-6-phosphate | |

The viability of each isoform was evaluated using a modified cocktail assay containing six probes incubated according to the sample preparation procedures outlined above.[105] Metabolic probe concentrations within each positive control sample were as follows: 4 μg/mL melatonin, 2 μg/mL bupropion, 2 μg/mL amodiaquine, 6 μg/mL tolbutamide, 20 μg/mL omeprazole, and 2 μg/mL dextromethorphan. Chromatographic separation of positive control probe compounds and metabolites monitored as evidence of isoform activity was elicited by a biphasic system according to the gradient described in Appendix 8. Optimized MS/MS parameters were determined using Agilent MassHunter Optimizer software and one MRM transition was selected to monitor the presence of positive control compounds and resultant metabolites (optimized MS/MS parameters and retention times listed in Table 7).

**Table 7: Summary of positive control probe information and LC-MS/MS parameters for CYP isoform viability assay**

| Probe/Monitored Metabolite | Ion Transition | Fragmentor | Collision Energy | Retention Time |
|---|---|---|---|---|
| **CYP1A2** | | | | |
| **melatonin**[a] | 233 → 174 | 100 V | 8 V | 2.37 min |
| 6-hydroxymelatonin | 249 → 190 | 100 V | 8 V | 1.64 min |
| **CYP2B6** | | | | |
| **bupropion** | 240 → 184 | 100 V | 8 V | 2.34 min |
| hydroxybupropion | 256 → 238 | 100 V | 8 V | 1.93 min |
| **CYP2C8** | | | | |
| **amodiaquine** | 356 → 283 | 110 V | 12 V | 1.33 min |
| desethylamodiaquine | 328 → 283 | 110 V | 12 V | 1.21 min |
| **CYP2C9** | | | | |
| **tolbutamide** | 271 → 91 | 100 V | 32 V | 3.90 min |
| hydroxytolbutamide | 287 → 171 | 100 V | 12 V | 2.59 min |
| **CYP2C19** | | | | |
| **omeprazole** | 346 → 198 | 100 V | 4 V | 2.37 min |
| desmethylomeprazole | 332 → 198 | 100 V | 4 V | 2.19 min |
| **CYP2D6** | | | | |
| **dextromethorphan** | 272 → 171 | 130 V | 40 V | 2.74 min |
| dextorphan | 258 → 199 | 130 V | 28 V | 1.84 min |
| **CYP3A4** | | | | |
| **omeprazole** | 346 → 198 | 100 V | 4 V | 2.37 min |
| omeprazole sulfone | 362 → 150 | 100 V | 36 V | 2.19 min |

[a] Positive control probes are listed in bold; metabolic products characteristic of isoform activity are listed in plain text

As heterologously expressed recombinant enzymes, recombinant human CYP (rhCYP) bactosomes do not maintain the same relative isoform concentration distribution as human liver tissue. However, rhCYP bactosomes purchased for this study ("EasyCYP" bactosomes, Cypex) are standardized to contain specific CYP content at 100 pmol/mg total protein. Assuming that CYP activity within bactosomes is analogous to the human hepatic microenvironment in conjunction with standardized "EasyCYP" bactosome preparations from Cypex, only basic data transformation is necessary to approximate the influence of relative isoform concentrations within human liver tissue.[106] Raw data were

multiplied by literature values for relative isoform concentrations in human liver samples[6,38,106] (Table 8) and normalized to the highest contributing isoform (*i.e.*, highest contributing isoform was set to 100%). Relative assignments of isoform contributions to individual biotransformation events were ranked according to the following criteria: major contribution, 60-100%; moderate contribution, 20-60%; minor contribution, 10-20%; any contribution below 10% was not considered significant and was not reported as a mediating isoform in that oxidative pathway.

**Table 8: CYP isoform distribution in human liver tissue**

| Isoform | Percent of Total CYP Content in Liver |
|---|---|
| **CYP1A2** | 9.8% |
| **CYP2B6** | 4.6% |
| **CYP2C8** | 8.3% |
| **CYP2C9** | 17.7% |
| **CYP2C19** | 3.3% |
| **CYP2D6** | 2.0% |
| **CYP3A4** | 21.5% |

### 3.6. **Reactive Metabolite Trapping and Protein Adduction Model Systems**

Reactive metabolites were generated using *in vitro* assay incubations for cocaine, methamphetamine, and morphine supplemented with a biomolecular model trapping agent. While reaction systems were similar to those employed for metabolite analysis, total protein content (*i.e.*, HLM concentration and NADPH regeneration system) was decreased in order to minimize protein nucleophile reservoirs within the assay system to ensure maximal adduction to trapping molecules.

Preliminary screenings were performed for each drug– trapping agent combination on the basis of expected adduct structures formed between the trapping molecules and predicted reactive functional groups within each parent drug and/or major metabolites (Table 9).[107] Trapping molecules examined for screening purposes included *N*-acetylcysteine (NAC), *N*-acetyllysine (NAK), and *N*-acetylhistidine (NAH). Analytes detected via LC-MS screening and suspected of being the result of covalent adduction between drugs and trapping agents were subjected to MS/MS analysis for structural clarification. Positive control incubations

using the known reactive drugs clozapine and benzyl bromide as substrates were performed to confirm active mechanisms for reactive metabolite production and subsequent trapping by biomolecular models.

**Table 9: Theoretical adduction products for preliminary screening methods**

| | Metabolite | Base MW (as $[M+H]^+$) | NAC Adduct +161 (+163)[a] | NAK Adduct +186 (+188) | NAH Adduct +195 (+197) |
|---|---|---|---|---|---|
| COC | P[b] | 304 | 465 (467) | 490 (492) | 499 (501) |
| | P+O | 320 | 481 (483) | 506 (508) | 515 (517) |
| | P-$CH_2$ | 290 | 451 (453) | 476 (478) | 485 (487) |
| | P-$COC_6H_4$ | 200 | 361 (363) | 386 (388) | 395 (397) |
| | P+2O | 336 | 497 (499) | 522 (524) | 531 (533) |
| | P-2$CH_2$ | 276 | 437 (439) | 462 (464) | 471 (473) |
| | P-$CH_2$+O | 306 | 467 (469) | 492 (494) | 501 (503) |
| | P-$CH_2$+2O | 322 | 483 (485) | 508 (510) | 517 (519) |
| | P+O-H | 319 | 480 (482) | 505 (507) | 514 (516) |
| | P-O-$CH_3$[c] | 273 | N/A | 460 | N/A |
| MET | P | 150 | 311 (313) | 336 (338) | 345 (347) |
| | P-$CH_2$ | 136 | 297 (299) | 322 (324) | 331 (333) |
| | P+O | 166 | 327 (329) | 352 (354) | 361 (363) |
| | P+2O | 182 | 343 (345) | 368 (370) | 377 (379) |
| | P-$CH_2$+O | 152 | 313 (315) | 338 (340) | 347 (349) |
| | P-$CH_2$+2O | 168 | 329 (331) | 354 (356) | 363 (365) |
| MOR | P | 286 | 447 (449) | 472 (474) | 481 (483) |
| | P-$CH_2$ | 272 | 433 (435) | 458 (460) | 467 (469) |
| | P-2H | 284 | 445 (447) | 470 (472) | 479 (481) |
| | P-$CH_2$-2H | 270 | 431 (433) | 456 (458) | 465 (467) |

[a] Addition of nucleophile mass factoring in loss of 2H; Parentheses present addition of nucleophile mass without the loss of 2H
[b] "P" refers to parent compound
[c] Adducting species proposed by Deng *et al.*[98]; known to only form adduction products with Lys residues

Screening samples were created according to the "Active Trapping Sample" specifications in Table 10. Buffer, microsomes, substrate (cocaine, methamphetamine, morphine, or positive control), and trapping agent were added to an Eppendorf tube and pre-incubated at 37°C for 5 min followed by addition of NADPH and $MgCl_2$, gentle mixing, and incubation for 1.5 h at 37°C (final sample volume 125 μL). Metabolism was ceased by addition of ice-cold acidified acetonitrile (5% v/v acetic acid) and proteins pelleted by centrifugation at 15,000 × *g* for 30 min at 4°C. Supernatants were directly analyzed by LC-

MS/MS. Chromatographic separations were elicited by a biphasic system of eluents according to the "General adduct screening" gradient listed in Appendix 8.

**Table 10: Reactive metabolite trapping and control incubation specifications**

| Component | Reactive Metabolite Trapping and Control Incubations | | | |
|---|---|---|---|---|
| | **Active Trapping Sample** | **Control 1** (no NADPH) | **Control 2** (no drug) | **Control 3** (no trapping agent) |
| **Activating cofactor** | 2.0 mM NADPH | N/A | 2.0 mM NADPH | 2.0 mM NADPH |
| **Substrate** | 100 μM drug | 100 μM drug | N/A | 100 μM drug |
| **Trapping system** | 20 mM trapping agent | 20 mM trapping agent | 20 mM trapping agent | N/A |
| **Buffer** | 50 mM pH 7.4 potassium phosphate buffer | | | |
| **Enzyme** | 1.0 mg/mL human liver microsomes | | | |
| **Non-activating cofactors** | 3.0 mM $MgCl_2$ | | | |

Samples in which MS/MS investigations provided evidence for the covalent adduction of drug to trapping agent underwent more thorough and rigorous investigations. First, gradient elutions for chromatographic separation were optimized for individual substrate-trapping agent pairs (see Appendix 8 for parameters corresponding to individually optimized methods). Once optimized, control incubations were run in parallel to examine NADPH-dependence and reliance on the presence of drug and trapping molecule to clarify mechanism of formation ("Controls 1-3," Table 10).

Studies examining the influence of increasing incubation time and secondary supplementation with additional NADPH were performed to elicit maximal adduct formation for downstream analysis. Data were collected for incubation times of 1.5, 3.0, 4.5, and 6.0 h, as well as an additional data point for 6.0 h incubation with an additional supplementation of 2.0 mM NADPH at t = 3.0 h (4.0 mM total NADPH).

When irreversible adduction was determined to occur with one of the simple biomolecule model systems (*i.e.*, NAC, NAK, or NAH), further probing of more complex trapping agents was performed to confirm analogous adduct structure across various nucleophilic protein models. Substrates demonstrating adduction products resultant from binding to NAC were incubated with reactive metabolite trapping system containing the biological tripeptide, GSH, and a separate incubation containing a synthetic hexapeptide,

acetyl-Pro-Ala-Ala-Cys-Ala-Ala-OH (AcPAACAA). Similarly, substrates demonstrating adduction potential with NAK or NAH were incubated with the synthetic hexapeptides, acetyl-Pro-Ala-Ala-Lys-Ala-Ala-OH (AcPAAKAA) or acetyl-Pro-Ala-Ala-His-Ala-Ala-OH (AcPAAHAA), respectively. LC-MS/MS methods for the analysis of resultant products are detailed in Appendix 8.

### 3.7. **Protein Adduct rhCYP Isoform Assays**

Determination of CYP isoform contributions to reactive metabolite/adduct formation were designated by *in vitro* incubation using heterologously expressed rhCYP bactosomes in place of human liver microsomes at 1.0 mg/mL rhCYP total protein (100 pmol/mL specific CYP isoform) concentration. All other parameters for incubations were analogous to the "Active Trapping Sample" in Table 10, with isoform assignments determined for all screening samples testing positive for covalent adduction (*i.e.*, cocaine−NAC and morphine−NAC). Samples were incubated for 1.5 h at 37°C, quenched by addition of ice-cold acidified acetonitrile (5% v/v acetic acid), centrifuged at 15,000 × *g* for 30 min at 4°C, and supernatants were directly analyzed via the LC-MS/MS analysis methods reported in Appendix 8.

Isoform designation panels are presented both as raw data and also as data adjusted by multiplying by literature values for relative isoform concentrations in human liver samples and normalized to highest contributing isoform (similar to data transformation described in Section 3.5).

### 3.8. **Quantum Mechanical Calculations for Reactivity and Adduction Potential**

Calculations to approximate the properties of chemical potential (μ), chemical hardness (η), chemical softness (σ), electrophilicity index (ω), nucleophilicity index (φ), and reactivity index ($\omega^-$) were performed by determining the $E_{HOMO}$ and $E_{LUMO}$ for reactive electrophilic metabolites and nucleophilic structures modeling reactive sites within proteins. The menu of compounds examined for their electrophilic/nucleophilic potential included cocaine; 2-, 3-, and 4-hydroxycocaine; cocaine-3,4-epoxide; morphine; morphinone; morphine quinone methide; Cys; His; Lys; NAC; NAH; NAK; and GSH. Initial structure geometries were generated via molecular orbital package (MOPAC) optimization using Chem3D Ultra software (Version 8, CambridgeSoft Corporation) and were exported to Gaussian 03 software

(Gaussian, Inc.)[108]. Iterative structural geometry optimization was carried out, and $E_{HOMO}$ and $E_{LUMO}$ were calculated at the density functional level using a B3LYP functional with 6-31G* basis set within Gaussian 03. Individual properties were calculated according to equations consistent with FOT and HSAB theory using $E_{HOMO}$ and $E_{LUMO}$ as presented in Section 2.5 (Equations 4-9).

## 4. RESULTS AND DISCUSSION

### 4.1. Cocaine Metabolite Synthesis and Analytical Characterization

The modified Steglich esterification procedure employed to synthesize nine monohydroxylated cocaine metabolites was found to be a fast, cost-effective method to assign chromatographic peaks, determine optimal ionization and fragmentation parameters, and obtain characteristic MS/MS spectra for comparison to *in vitro* assay-generated metabolic profiles. As a result of the synthetic mechanism (involving activation of carboxylic acids by 1,3-dicyclohexylcarbodiimide followed by reaction with free alcohol groups; see Appendix 4 for mechanism), numerous side products were expected to be present in the final synthetic preparations. Evidence of side product formation was seen in the low relative yields for those preparations containing multiple carboxylic acid and alcohol groups (*i.e.*, hydroxybenzoylecgonine isomers). However, even with sub-milligram quantities of desired product yield, complete MS/MS spectra that matched theory and literature were obtained for 2-, 3-, and 4-hydroxycocaine; 2-, 3-, and 4-hydroxybenzoylecgonine; and 2-, 3-, and 4-hydroxycocaethylene. These are presented in Figure 12, Figure 13, and Figure 14, respectively.

Chromatographic separation according to the gradient elution used for cocaine metabolites (see Appendix 8) was able to achieve baseline separation of each set of structural isomers (Figure 15). Elution order on the reversed-phase LC system was also consistent within each set of isomers examined.[109] The 4-hydroxy isomers eluted first, followed by the 3-hydroxy and the 2-hydroxy isomers.

MS/MS analysis revealed high similarity among isomeric structures. The fragment at *m/z* 182 for hydroxycocaine is representative of the $[M\text{-}OC(O)C_6H_4OH]^+$ ion and is a common ion monitored for MRM-based cocaine analysis methods.[110,111] Structural identity of fragment ion *m/z* 200 for hydroxycocaine was investigated via pseudo-$MS^3$ by means of in-source decay. Figure 16a shows a representative spectrum of $MS^2$ fragmentation obtained by inducing in-source decay of 4-hydroxycocaine. Fragment ions observed were comparable to authentic $MS^2$ spectra for 4-hydroxycocaine (Figure 12c). Figure 16b and 16c are 4-hydroxycocaine pseudo-$MS^3$ spectra of *m/z* 182 and 200, respectively, under in-source decay conditions. On the basis of qualitative similarity of pseudo-$MS^3$ fragmentation, fragment ion *m/z* 200 is likely derived from the addition of water to the *m/z* 182 ion $[M\text{-}OC(O)C_6H_4OH+H_2O]^+$. The

presence of ions from *m/z* 200 fragmentation maintaining a +18 mass shift concordant with water addition (designated by "*" in Figure 16c) provides further evidence supporting the chemical species identity as *m/z* 182+$H_2O$. Analogous results were obtained for 2-hydroxycocaine, demonstrating conserved mechanisms of *m/*z 200 fragment ion formation regardless of hydroxylation position.

However, under identical fragmentation conditions, characteristic differences between MS/MS spectra were noted for each isomer, allowing for unequivocal structural designation based on fragment ion peak ratios. Figure 17 contains the MS/MS spectra of 2-, 3-, and 4-hydroxycocaine obtained under identical fragmentation parameters. When fragmented at CE = 18 V, the ratios of *m/z* 182 to *m/z* 200 were dependent on the position of aromatic hydroxylation. The ratios of these ions were 1:3 for 2-hydroxycocaine, 1:0 (*i.e.*, no *m/z* 200 peak) for 3-hydroxycocaine, and 1:0.2 for 4-hydroxycocaine. Similar fragmentation patterns and ion ratios were observed for the ring-hydroxylated isomers of benzoylecgonine and cocaethylene. The characteristic elution order, fragmentation patterns, and specific retention times allowed for definitive assignments of individual hydroxylated isomers.

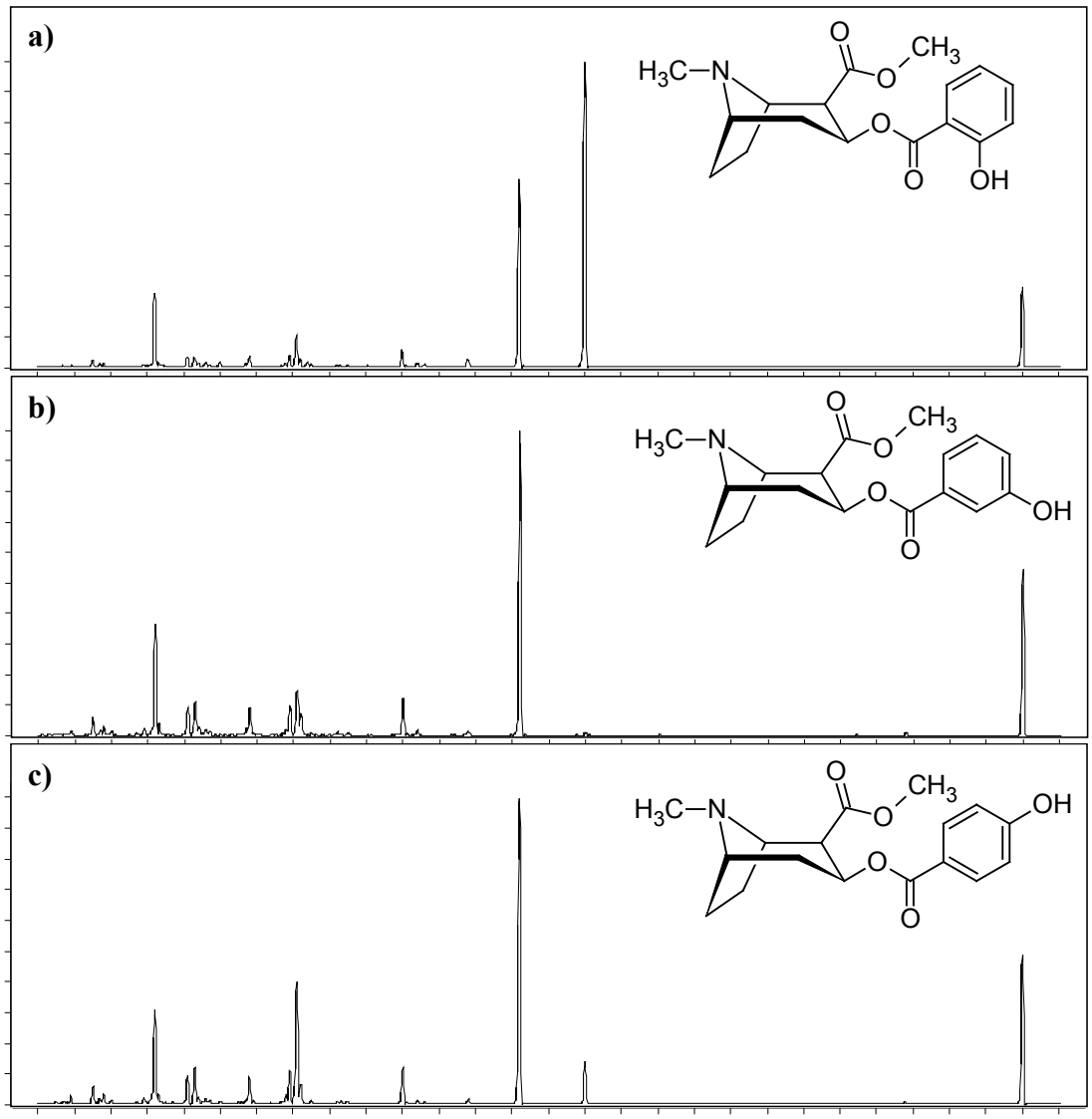


**Figure 12: MS/MS spectra of (a) 2-hydroxycocaine, (b) 3-hydroxycocaine, and (c) 4-hydroxycocaine**

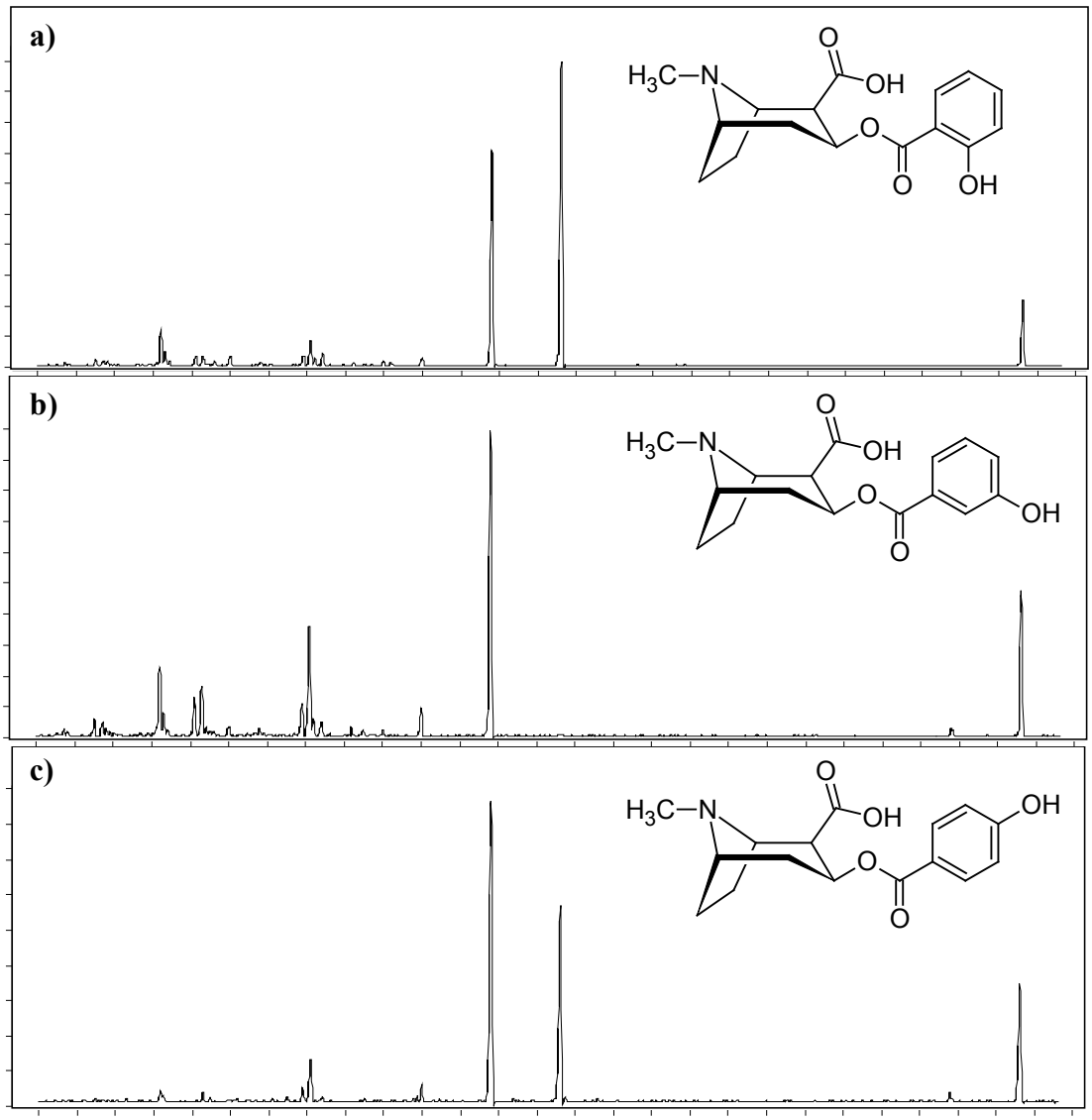


**Figure 13: MS/MS spectra of (a) 2-hydroxybenzoylecgonine, (b) 3-hydroxybenzoylecgonine, and (c) 4-hydroxybenzoylecgonine**

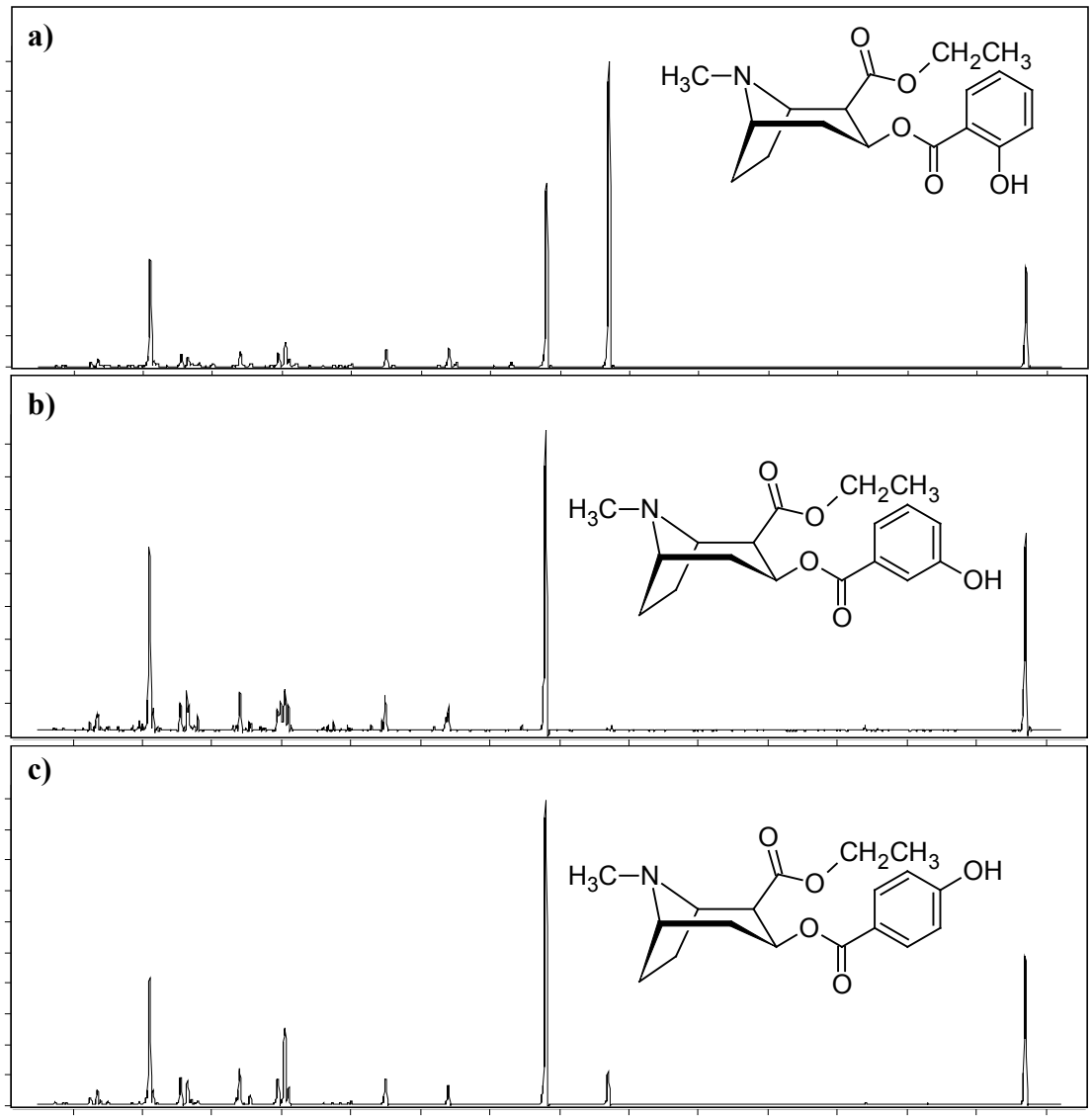


**Figure 14: MS/MS spectra of (a) 2-hydroxycocaethylene, (b) 3-hydroxycocaethylene, and (c) 4-hydroxycocaethylene**

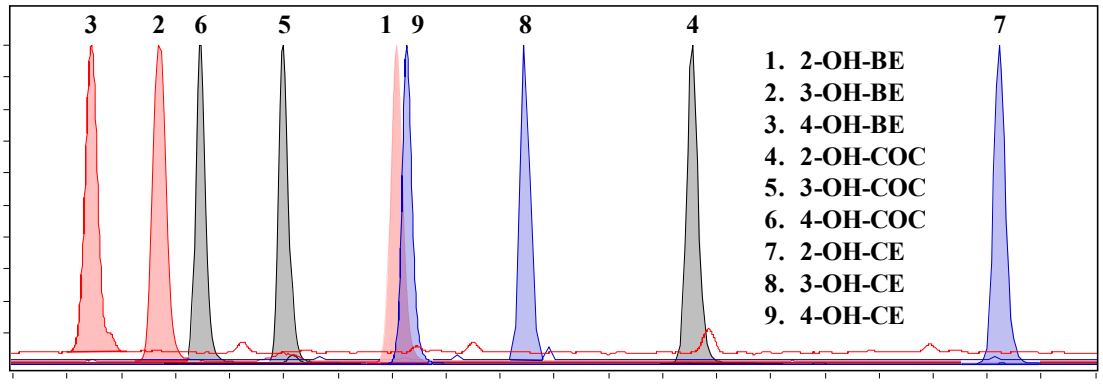


**Figure 15: Chromatographic separation of nine synthesized monohydroxylated cocaine metabolites Abbreviations: OH-BE, hydroxybenzoylecgonine; OH-CE, hydroxycocaethylene; OH-COC, hydroxycocaine**

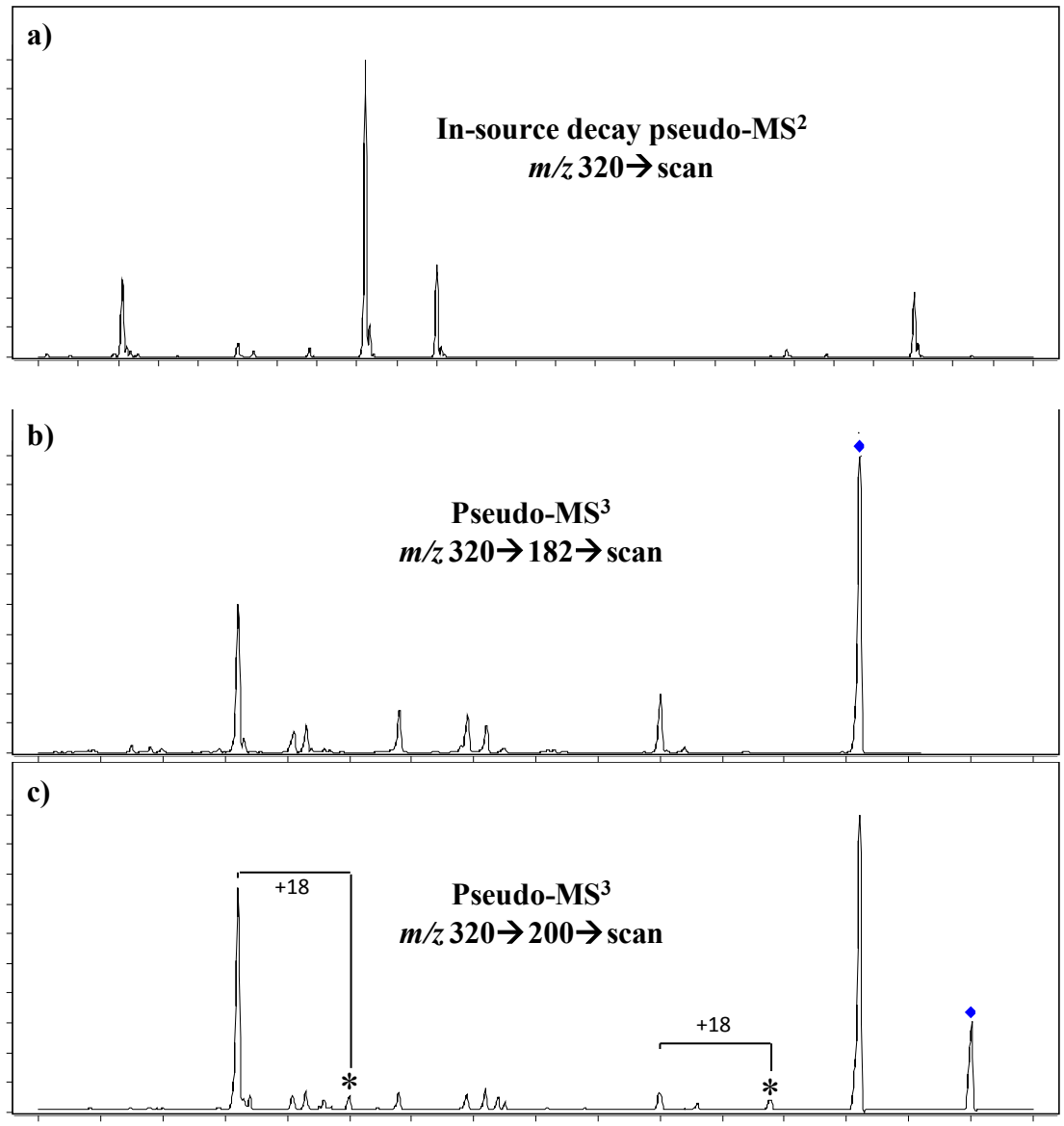


* Designates fragment ions maintaining +18 mass unit addition

**Figure 16: Psuedo-MS$^3$ analysis of 4-hydroxycocaine fragment ions**

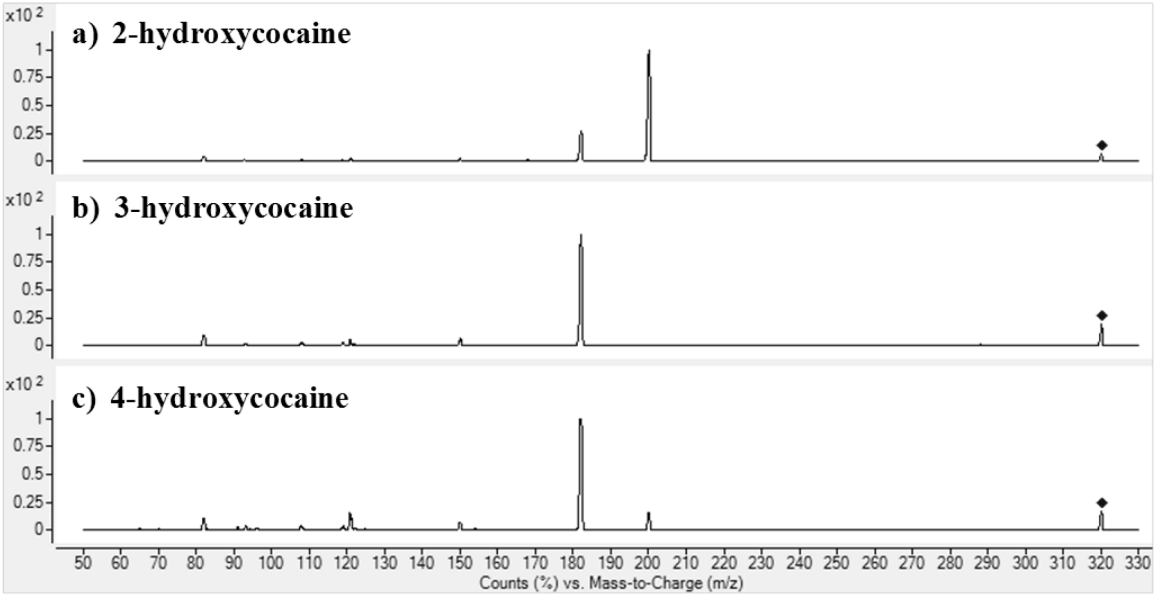


**Figure 17: Comparison of positional hydroxycocaine isomers under identical MS/MS conditions**

4.2. **Metabolic Assays**

After processing, cocaine metabolism samples were reconstituted in DMSO in order to prevent nonenzymatic hydrolytic cleavage of labile ester bonds in cocaine and metabolites. Other solvents were examined (acetonitrile and methanol), but were found to negatively impact retention time and peak shape on the chromatographic system. Table 11 displays data showing the impact of solvent selection on analyte retention time, peak shape (evaluated by full width at half max peak height (FWHM) comparison), and any additional detriment imparted on the data collected using cocaine as a model for comparison. Statistical comparisons of cocaine retention time among the solvent systems demonstrated that retention times were significantly different from that of cocaine in water when acetonitrile, methanol, and DMSO were employed as solvents for reconstitution (using 5 µL injections). Injections of DMSO samples at 1 µL maintained chromatographic retention times statistically indistinguishable from cocaine in water. Likewise, 1 µL injection of DMSO was the only solvent system to not detrimentally affect FWHM (and therefore peak shape). Reduction of injection volume for acetonitrile and methanol systems was discounted because of additional solvent system issues (*i.e.*, contamination peaks with acetonitrile and split analyte peaks with methanol). Cocaine metabolism samples dissolved in DMSO at 1 µL injection volumes were

therefore selected for future analysis. While the decrease in injection volume did somewhat limit the sensitivity of this method, it was deemed necessary to maintain the integrity of metabolic profiles for each sample during time in the autosampler prior to analysis.

**Table 11: Comparison of solvents for cocaine analysis**

| Solvent | Cocaine Retention Time (min) | FWHM (min) | Note |
|---|---|---|---|
| **Water** | 4.116 ± 0.003[a] | 0.073 | N/A |
| **Acetonitrile** | 4.002[b] | 0.162 | Contamination Peaks |
| **Methanol** | 4.091[b] | 0.135 | Split Peak |
| **5 µL DMSO** | 4.081[b] | 0.122 | N/A |
| **1 µL DMSO** | 4.113 | 0.061 | N/A |

[a] n=10
[b] Denotes statistically significant difference from cocaine retention time using water solvent system

Control incubations of methamphetamine and morphine in sodium phosphate buffer (pH 7.4) without addition of cofactors or enzymes did not produce any metabolic product within the anticipated profile for either drug. Lack of passively generated metabolic products demonstrated the stability of both methamphetamine and morphine throughout the course of the assay procedure and, therefore, did not necessitate examination of substitute solvent systems to replace water during post-dry-down reconstitution to ensure metabolic profile integrity while in the autosampler.

Activity of Phase I metabolic enzymes was confirmed via hydroxyzolpidem isomer production from control incubations containing zolpidem as target substrate (Figure 18).[112] Similarly, Phase II glucuronidation pathway activity was determined by conjugation of nicotine to form nicotine-*N*-glucuronide (Figure 19).[113]

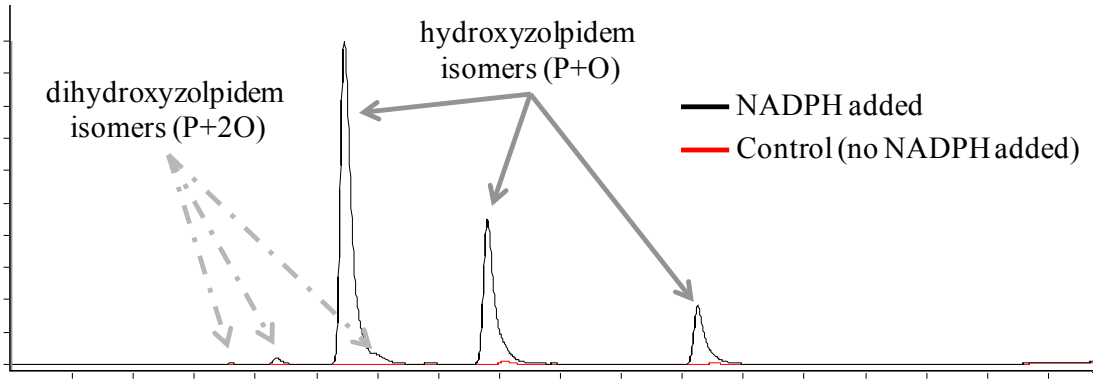


**Figure 18: Representative Phase I metabolism positive control showing the formation of hydroxyzolpidem isomers after 24 h incubation of zolpidem in HLM assay system**

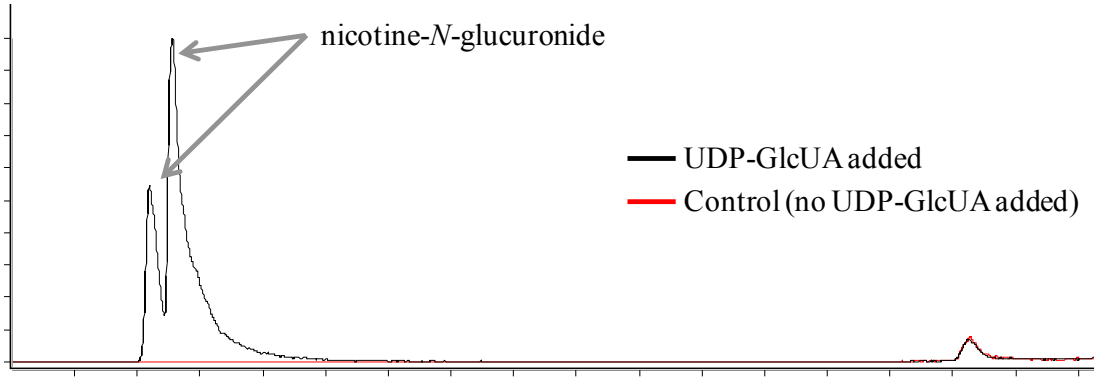


**Figure 19: Representative Phase II metabolism positive control showing the formation of nicotine-*N*-glucuronide from nicotine after 24 h incubation in HLM assay system**

### 4.2.1. **Cocaine**

Examination of metabolite profiles across *in vitro* systems showed distinct differences between assays arising from enzymatic components contained within each system. Of the 50 compounds targeted by the analytical method, 13 were confirmed in one or more of the metabolic systems. Metabolites detected include ecgonine; ecgonine methyl ester; benzoylnorecgonine; benzoylecgonine; norcocaine; 2-, 3-, and 4-hydroxybenzoylecgonine; 3- and 4-hydroxynorcocaine; and 2-, 3-, and 4-hydroxynorcocaine. As was expected, cocaethylene and the corresponding ethyl ester metabolites did not appear in any of the metabolic systems, since ethanol was not present in the reaction mixtures. Table 12 details the relative levels of primary and secondary Phase I metabolites formed in the absence of enzyme and with each *in*

*vitro* metabolic system after 24 h incubation. The presence of benzoylecgonine and ecgonine in control (no enzyme) preparations and the lack of impact of metabolic enzyme inclusion on relative levels of these metabolites indicate that their formation was not dependent on enzymatic biotransformation but instead occurred primarily via nonenzymatic hydrolysis. In addition, metabolite profiles noted in the cytosol-based systems were indistinguishable from control preparations, indicating that components of cytosol alone did not catalyze specific cocaine metabolism. Aside from enhanced formation of ecgonine methyl ester, metabolite profiles in HLM+2 and S9+2 mixtures were also similar in profile to those with no enzyme. In contrast, enzyme-mediated increases in relative metabolite concentrations were noted for ecgonine methyl ester, benzoylnorecgonine, norcocaine, and hydroxylated cocaine metabolites in the HLM and S9 systems. As expected, the metabolite profiles generated in HLM and S9 samples were qualitatively similar; quantitatively, the rate of metabolite generation was greater in HLM samples (see below). Since HRP lacks the *N*-demethylase activity found in HLM and S9 assays, no norcocaine, benzoylnorecgonine, or secondary hydroxynorcocaine isomers were detected in HRP incubations (Table 12).

The formation of hydroxylated cocaine metabolites did not occur in the absence of enzyme and was variably dependent upon the particular enzyme system tested (Table 12). In total, eight distinct hydroxylated cocaine metabolites were detected amongst the assay systems examined. Of the systems examined, hydroxylated metabolites were detected in those containing HLM, S9, or HRP. Hydroxylation in HLM and S9 was found to be NADPH-dependent, as was expected for an enzymatic monooxygenase-based Phase I metabolic process. HRP appeared to be the enzyme system most effective in generating hydroxylated cocaine and benzoylecgonine metabolites, in that higher concentrations of such metabolites were noted as compared to any of the other assay systems examined (Table 12; Figure 20). Systems derived from human liver fractions (HLM, S9) were found to exhibit regioselectivity in aromatic ring hydroxylation, forming hydroxylated products at the 3- and 4- positions, but not at the 2- position. In contrast, the oxidative activity of the HRP system was found to be less selective, generating all three hydroxylated isomers. Cytosol alone was not effective in the formation of any hydroxylated metabolites.

In contrast to the formation of Phase I cocaine metabolites, no evidence was obtained for hydroxylated metabolite depletion consistent with Phase II metabolism in the present study. This was the

case even after 24 h incubation in the presence of a Phase II metabolic cofactor (UDP-GlcUA). In addition, no cocaine metabolite glucuronides were directly identified by LC-MS/MS analysis.

**Table 12: Distribution of cocaine metabolites across examined *in vitro* assay systems**

| Metabolite | No enzyme | HLM+1 | HLM+2 | HLM+1/2 | CYT+1 | CYT+2 | CYT+1/2 | S9+1 | S9+2 | S9+1/2 | HRP+ |
|---|---|---|---|---|---|---|---|---|---|---|---|
| ***Primary Metabolites*** | | | | | | | | | | | |
| BE[a] | +++[b] | +++ | +++ | +++ | +++ | +++ | +++ | +++ | +++ | +++ | +++ |
| EME | + | ++ | ++ | ++ | + | + | + | ++ | ++ | ++ | + |
| NC | - | ++ | - | ++ | - | - | - | ++ | - | ++ | - |
| 2-OH-COC | - | - | - | - | - | - | - | - | - | - | ++ |
| 3-OH-COC | - | + | - | + | - | - | - | + | - | + | ++ |
| 4-OH-COC | - | + | - | + | - | - | - | + | - | + | ++ |
| ***Secondary Metabolites*** | | | | | | | | | | | |
| ECG | + | + | + | + | + | + | + | + | + | + | + |
| BNE | - | + | - | + | - | - | - | + | - | + | - |
| 2-OH-BE | - | - | - | - | - | - | - | - | - | - | ++ |
| 3-OH-BE | - | + | - | + | - | - | - | + | - | + | ++ |
| 4-OH-BE | - | + | - | + | - | - | - | + | - | + | ++ |
| 2-OH-NC | - | - | - | - | - | - | - | - | - | - | - |
| 3-OH-NC | - | + | - | + | - | - | - | - | - | - | - |
| 4-OH-NC | - | + | - | + | - | - | - | - | - | - | - |

[a] Metabolite abbreviations: BE, benzoylecgonine; EME, ecgonine methyl ester; NC, norcocaine; OH-COC, hydroxycocaine; ECG, ecgonine; BNE, benzoylnorecgonine; OH-BE, hydroxybenzoylecgonine; OH-NC, hydroxynorcocaine.

[b] Refers to qualitative prevalence of metabolite across all biotransformation systems tested; (+++) major metabolite, (++) intermediate metabolite, (+) minor metabolite, (-) not detected. Criteria for classifications were as follows: major – dominated chromatograph, intermediate – visible in total ion chromatograph, minor – only visible through MRM filtering.

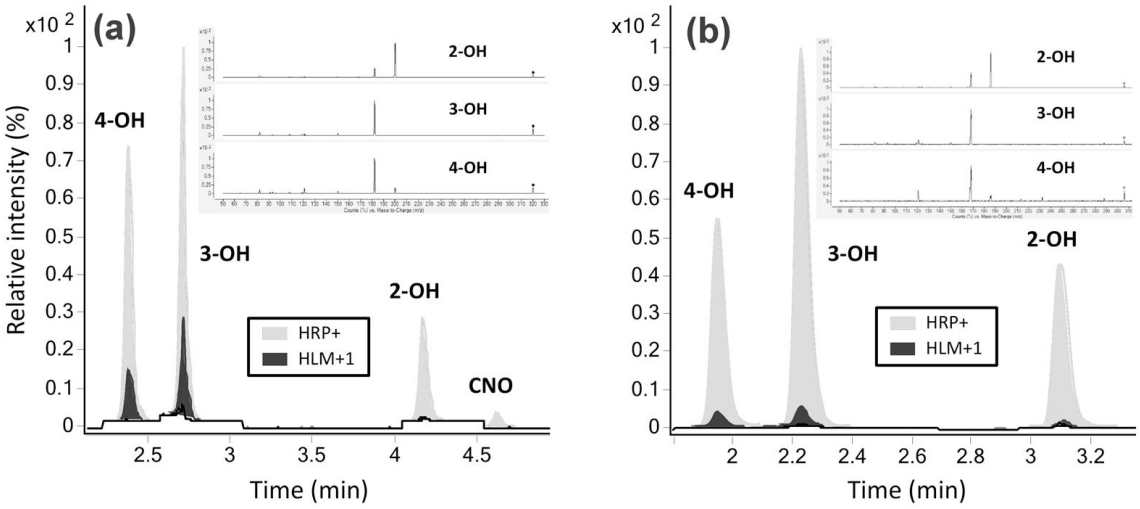


**Figure 20: LC-MS chromatograms of (a) hydroxycocaine isomers and (b) hydroxybenzoylecgonine isomers in HLM and HRP assays**

Incubation times for published *in vitro* drug metabolism assays vary widely, with typical ranges from 5 min to 24 h. In the present study, the impact of assay incubation time is illustrated by examining the production of norcocaine and benzoylnorecgonine. Figure 21a presents data showing similar levels of norcocaine in HLM systems activated with NADPH at either 0.5 or 24 h. In contrast, S9 systems activated with NADPH did not produce detectable quantities of norcocaine at the 0.5 h time point, but did after 24 h incubation. Similar patterns were noted with other primary metabolites, including 3- and 4-hydroxycocaine (Figure 22b,c). As with other primary metabolites of cocaine, 3- and 4-hydroxycocaine were produced rapidly (0.5 h incubation) in HLM incubations activated with NADPH, while detection in S9 assays required extended incubation time (24 h). Benzoylnorecgonine, a secondary metabolite of cocaine, was not as rapidly generated by HLM. Figure 21b shows that benzoylnorecgonine was not detectable in either the HLM or S9 systems at 0.5 h, but was present in both after 24 h incubation. Likewise, the secondary metabolites 3- and 4-hydroxybenzoylecgonine and 3- and 4-hydroxynorcocaine showed similar trends, requiring extended incubation time for detection in both HLM and S9 assays (Figure 23 and Figure 24).

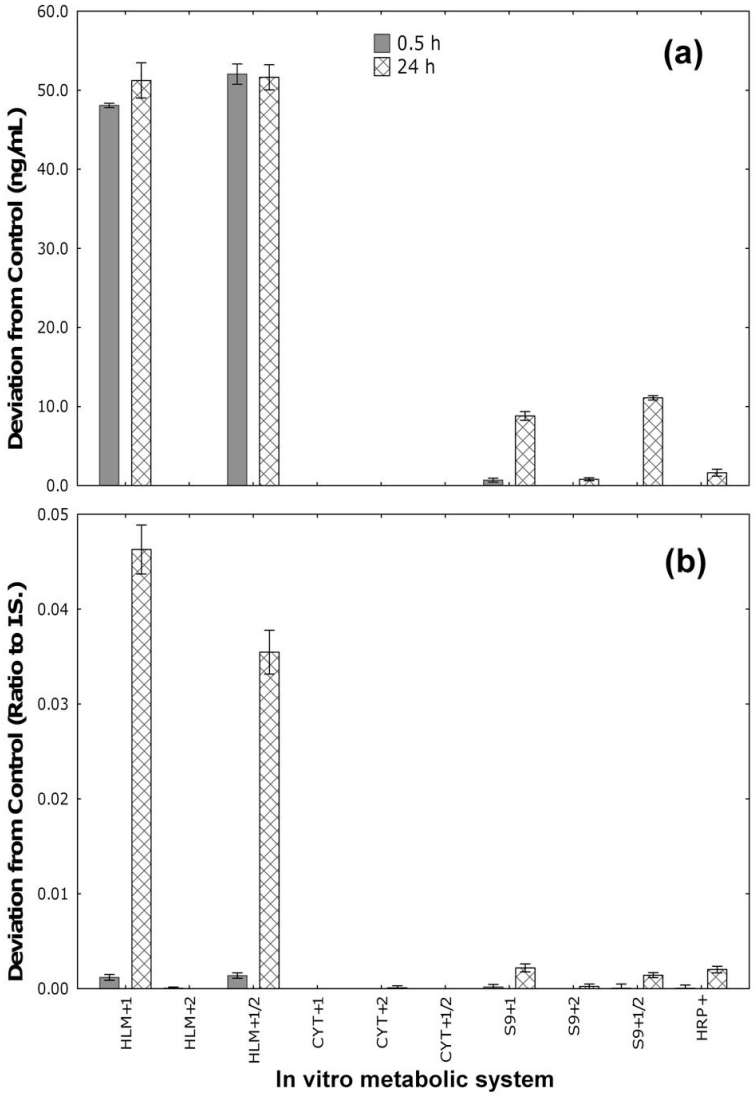


**Figure 21: Comparison of (a) norcocaine and (b) benzoylnorecgonine formation across assay systems**

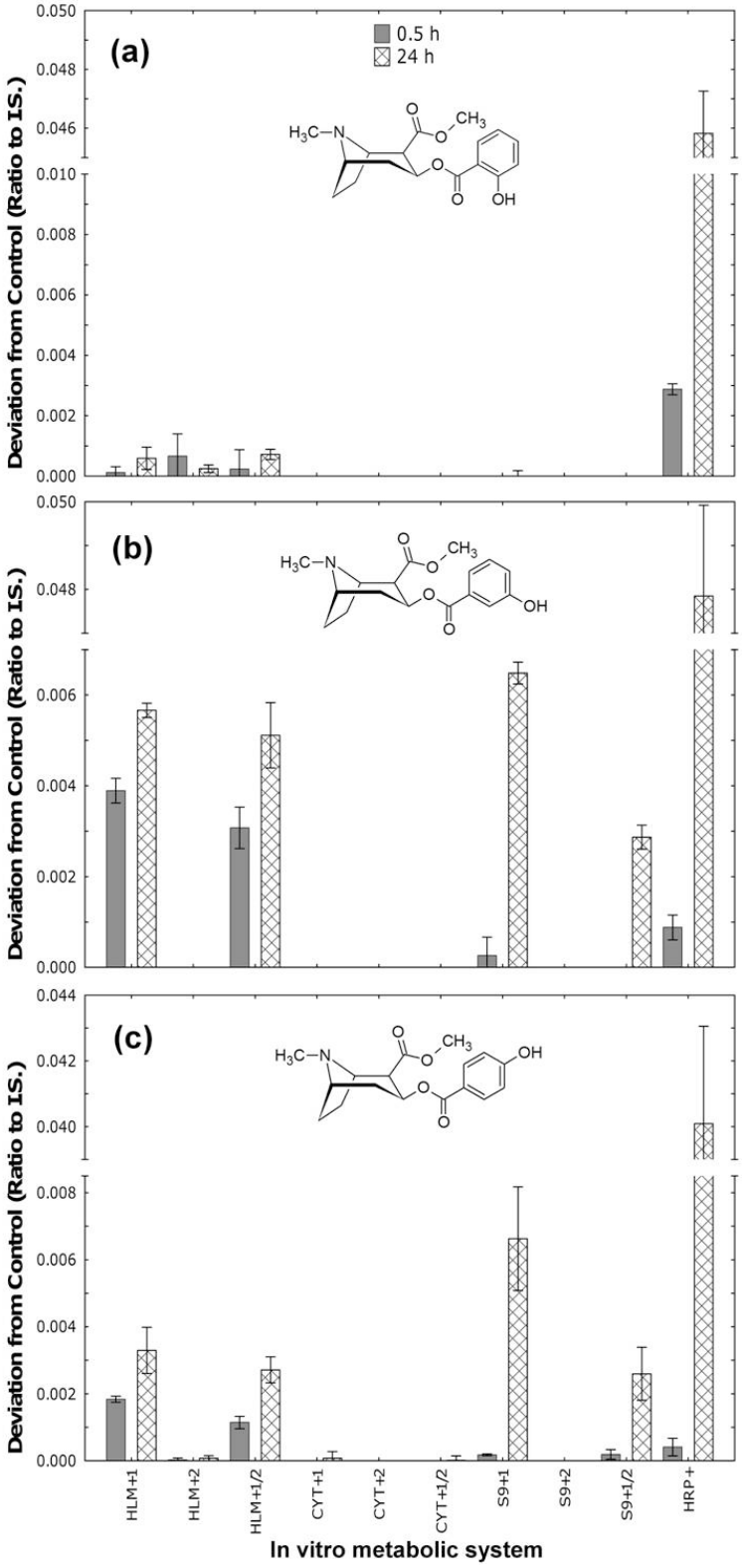


**Figure 22: Formation of (a) 2-hydroxycocaine, (b) 3-hydroxycocaine, and (c) 4-hydroxycocaine across assay systems**

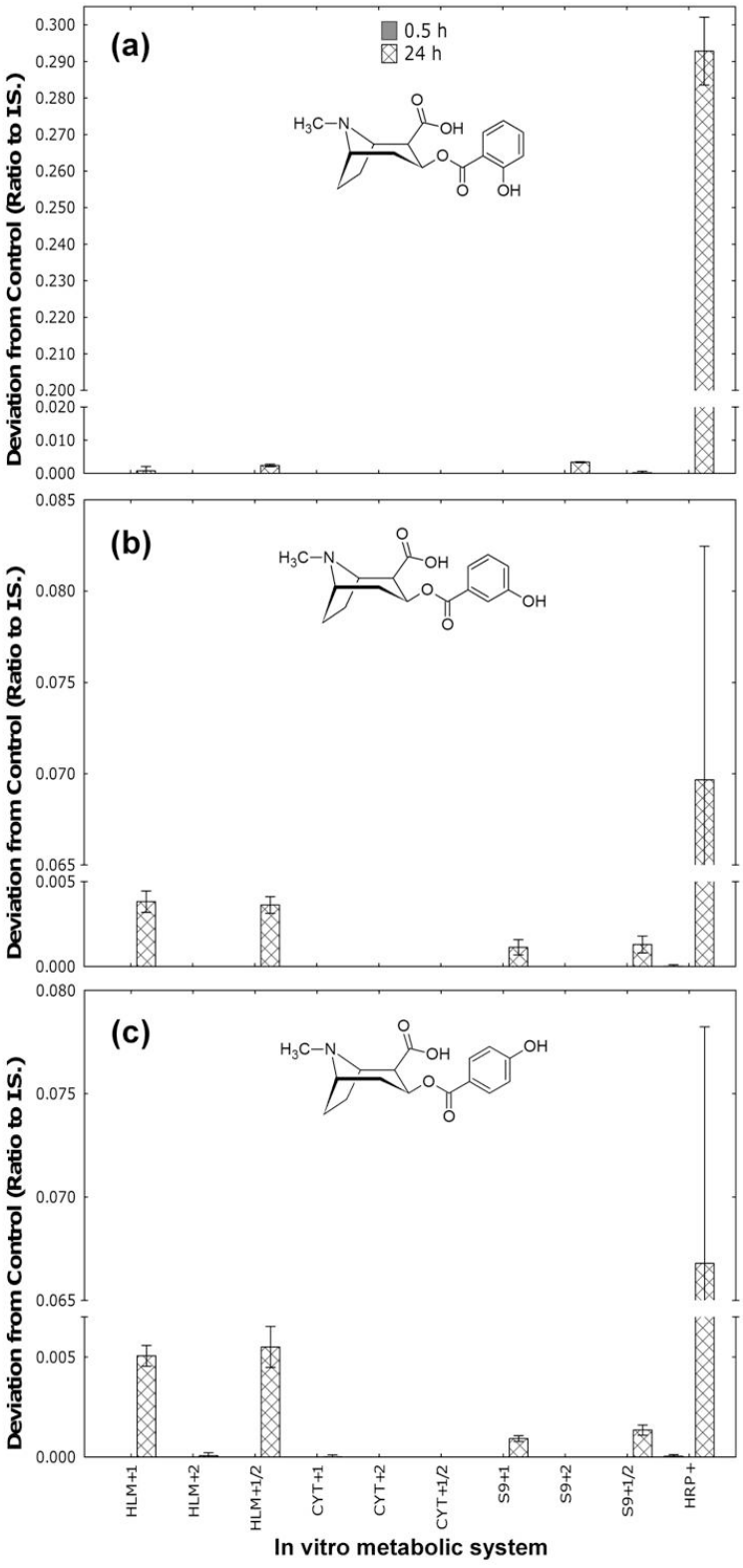


**Figure 23: Formation of (a) 2-hydroxybenzoylecgonine, (b) 3-hydroxybenzoylecgonine, and (c) 4-hydroxybenzoylecgonine across assay systems**

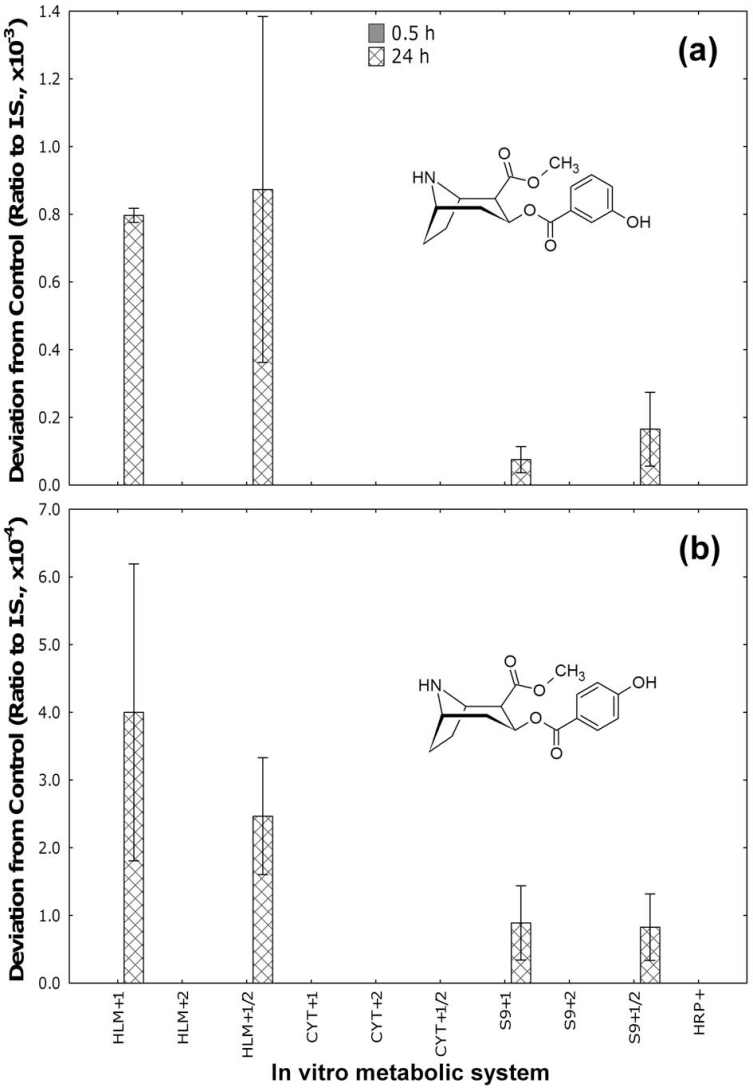


**Figure 24: Formation of (a) 3-hydroxynorcocaine and (b) 4-hydroxynorcocaine across assay systems**

### 4.2.2. **Methamphetamine**

Methamphetamine demonstrated limited metabolism within the *in vitro* systems. Of the 26 metabolites targeted by this method, four were detected among the various assays examined. These included the primary metabolites amphetamine and 2-, 3-, and 4-hydroxymethamphetamine. No secondary metabolites of methamphetamine were detected in any assay system examined in this study. Table 13 presents the relative distribution of detected Phase I metabolites formed in the control incubation (absence of enzyme) and across all *in vitro* metabolic systems after incubation for 24 h. Incubations activated solely

by UDP-GlcUA (*i.e.*, HLM+2, CYT+2, S9+2) were indistinguishable from control samples, demonstrating no basal level of Phase II glucuronidation for methamphetamine without prior biotransformation via Phase I functionalization pathways. Qualitative metabolic profiles were found to be similar in HLM, CYT, and S9 assays activated with NADPH (both +1 and +1/2 incubations), showing the formation of amphetamine, and 2-, 3-, and 4-hydroxymethamphetamine in each sample.

*N*-Demethylation of methamphetamine to produce amphetamine was shown to occur in all liver fraction systems containing NADPH and was a minor metabolic pathway in the HRP assay activated by $H_2O_2$ (Table 13; Figure 25). Maximal amphetamine production was found in the HLM system activated by NADPH, producing the metabolite at approximately nine-fold the yield generated by the CYT or S9 assays. Likewise, HLM+1 and HLM+1/2 incubations were the only assay systems to generate appreciable quantities of amphetamine after 0.5 h incubation.

All enzymatic systems were qualitatively capable of performing the aromatic hydroxylation of methamphetamine to all three isomers when activated by either NADPH (for liver-based assays; +1 and +1/2) or $H_2O_2$ (HRP+) (Figure 26). 2-Hydroxymethamphetamine was found to be generated in similar amounts in both HLM and CYT assays activated by NADPH (HLM+1, HLM+1/2, CYT+1, and CYT+1/2) and was detected in greater quantities in S9 fractions activated by NADPH (presumably as a cumulative result of enzymatic action by both soluble and membrane-associated enzymes found in the CYT and HLM, respectively). The HRP-containing assay activated with $H_2O_2$ demonstrated increased oxidative activity over all liver fraction assays, producing the 2-hydroxymethamphetamine isomer in much higher quantities. In all assay systems examined, 2-hydroxymethamphetamine was generated in larger quantities after 24 h incubation than 0.5 h incubation.

Results obtained for the production of 3-hydroxymethamphetamine across assay systems were atypical for *in vitro* production of a Phase I metabolite. The strongest oxidizing systems (*i.e.*, HLM+1, HLM+1/2, and HRP+) did produce the metabolite rapidly (see 0.5 h time point, Figure 26b). However, 3-hydroxymethamphetamine concentrations decreased in the 24 h incubation samples. Also unexpected for Phase I metabolic products, 3-hydroxymethamphetamine was produced in high levels within CYT-based systems activated with NADPH (*i.e.*, CYT+1 and CYT+1/2). Presumably, increased production of 3-

hydroxymethamphetamine in S9+1 and S9+1/2 after 24 h incubation results from the action of CYT enzymes present in the S9 fraction.

In contrast to the 3-hydroxy isomer, 4-hydroxymethamphetamine production in each *in vitro* system followed intuitive prediction. General patterns of 4-hydroxymethamphetamine were similar to the 2-hydroxy analog with minor distinctions. First, CYT-based assays containing NADPH (*i.e.*, CYT+1, CYT+1/2) were only capable of generating minor quantities of 4-hydroxymethamphetamine, while HLM-based assay systems containing NADPH (*i.e.*, HLM+1, HLM+1/2) produced the most metabolite from the liver-based fractions. It is noteworthy that the 4-hydroxy isomer is generated rapidly within HLM-based assays activated with NADPH (*i.e.*, HLM+1, HLM+1/2; demonstrating only minor increases in concentration between 0.5 and 24 h incubations) compared to 2-hydroxymethamphetamine. As with 2-hydroxymethamphetamine, the HRP assay activated with $H_2O_2$ showed greater oxidative strength than the other assays, producing more 4-hydroxymethamphetamine than any other assay system examined.

Although documented previously in authentic urine and blood specimens, subsequent glucuronidation of hydroxymethamphetamine isomers was not definitively documented in this study.[27] While minor differences in quantities of hydroxylated metabolites were noted between assays containing the cofactors necessary to form glucuronide conjugates (+1/2) and those lacking UDP-GlcUA (+1), the analysis method did not directly detect the presence of glucuronic acid conjugated metabolites.

**Table 13: Distribution of methamphetamine metabolites across examined *in vitro* assay systems**

| Metabolite | No enzyme | HLM+1 | HLM+2 | HLM+1/2 | CYT+1 | CYT+2 | CYT+1/2 | S9+1 | S9+2 | S9+1/2 | HRP+ |
|---|---|---|---|---|---|---|---|---|---|---|---|
| AMP[a] | -[b] | +++ | - | +++ | + | - | + | + | - | + | + |
| 2-OH-MET | - | ++ | - | ++ | + | - | + | + | - | + | +++ |
| 3-OH-MET | - | ++ | - | ++ | + | - | + | + | - | + | +++ |
| 4-OH-MET | - | ++ | - | ++ | + | - | + | + | - | + | +++ |

[a] Metabolite abbreviations: AMP, amphetamine; OH-MET, hydroxymethamphetamine
[b] Refers to qualitative prevalence of metabolite across all biotransformation systems tested; (+++) major metabolite, (++) intermediate metabolite, (+) minor metabolite, (-) not detected. Criteria for classifications were as follows: major – dominated chromatograph, intermediate – visible in total ion chromatograph, minor – only visible through MRM filtering.

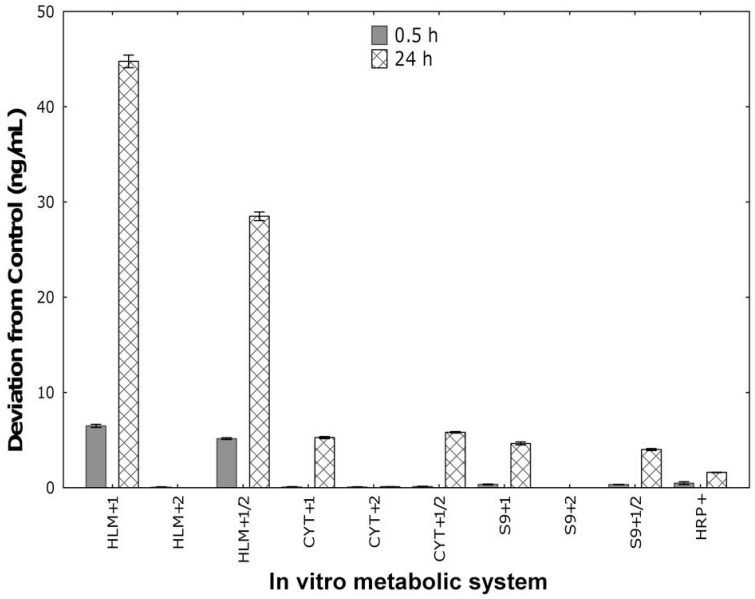


**Figure 25: Comparative biotransformation of methamphetamine to amphetamine across assay systems**

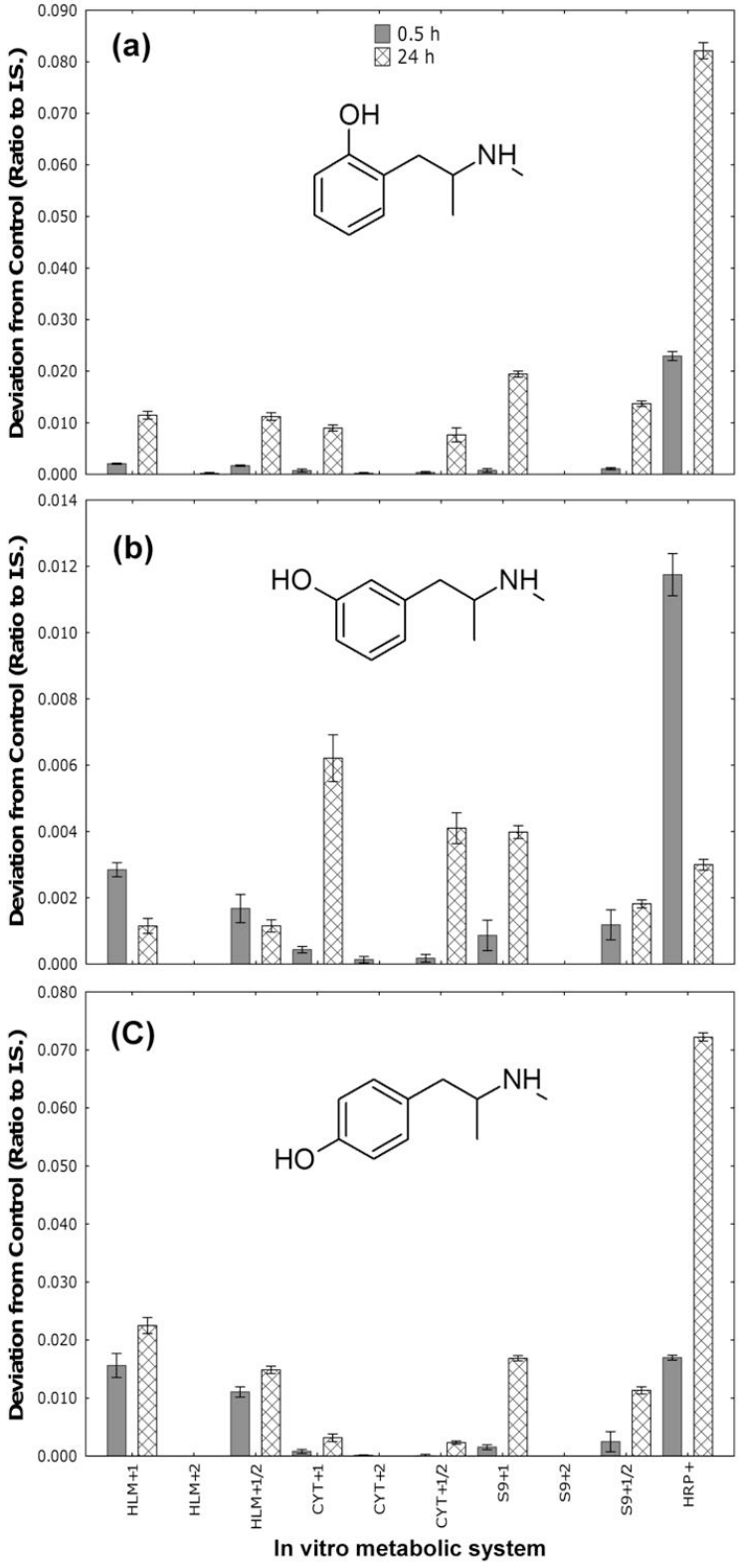


**Figure 26: Formation of (a) 2-hydroxymethamphetamine, (b) 3-hydroxymethamphetamine, and (c) 4-hydroxymethamphetamine**

### 4.2.3. **Morphine**

Morphine displayed substantial metabolite production *in vitro*, but with limited diversity of products. Of the 24 potential metabolites that were examined in this study, three were confirmed in one or more assay system. The detected metabolites were the primary morphine metabolites normorphine, morphine-3-glucuronide, and morphine-6-glucuronide. Secondary metabolites of morphine were not detected in any of the assays examined. Table 14 displays the distribution of the three detected morphine metabolites in the control incubation (*i.e.*, no enzyme) and in each active *in vitro* assay system after 24 h incubation. Incubation samples CYT+1 and HRP+ did not form any of the three metabolites and were indistinguishable from control incubations, demonstrating no metabolic contributions from NADPH-mediated metabolism in CYT or peroxide-initiated oxidative metabolism from HRP. The HLM-based assays were able to elicit both Phase I and II metabolism, generating quantitatively superior profiles over the other assay systems. CYT-containing assays only generated Phase II glucuronidation products for morphine, demonstrating no activity from soluble Phase I metabolizing enzymes within the CYT fraction. Like HLM, S9-based systems were able to produce both Phase I and II metabolites; however, product yields were diminished in comparison to analogous HLM incubations.

*N*-Demethylation of morphine to normorphine (a minor Phase I metabolic pathway of morphine) was dependent on the presence of NADPH and was only produced in the HLM and S9 systems with the former producing an approximately five-fold yield over the latter (Figure 27). No significant quantity of normorphine was produced in any CYT or HRP assay.

Morphine-3-glucuronide dominated the metabolic profiles of HLM, CYT, and S9 systems activated with UDP-GlcUA (+2 and +1/2; Figure 28a). Production of the glucuronide conjugate was maximal in the HLM system, followed by S9, and then CYT to a lesser extent. The production of morphine-6-glucuronide followed a similar distribution among *in vitro* assays examined, but in lower quantities than morphine-3-glucuronide (assuming analogous ionization efficiency between isomers; Figure 28b).

**Table 14: Distribution of morphine metabolites across examined *in vitro* assay systems**

| Metabolite | No enzyme | HLM+1 | HLM+2 | HLM+1/2 | CYT+1 | CYT+2 | CYT+1/2 | S9+1 | S9+2 | S9+1/2 | HRP+ |
|---|---|---|---|---|---|---|---|---|---|---|---|
| NM[a] | -[b] | ++ | - | ++ | - | - | - | + | - | + | - |
| M3G | - | - | +++ | +++ | - | ++ | ++ | - | ++ | ++ | - |
| M6G | - | - | ++ | ++ | - | + | + | - | + | + | - |

[a] Metabolite abbreviations: NM, normorphine; M3G, morphine-3-glucuronide; M6G, morphine-6-glucuronide

[b] Refers to qualitative prevalence of metabolite across all biotransformation systems tested; (+++) major metabolite, (++) intermediate metabolite, (+) minor metabolite, (-) not detected. Criteria for classifications were as follows: major – dominated chromatograph, intermediate – visible in total ion chromatograph, minor – only visible through MRM filtering.

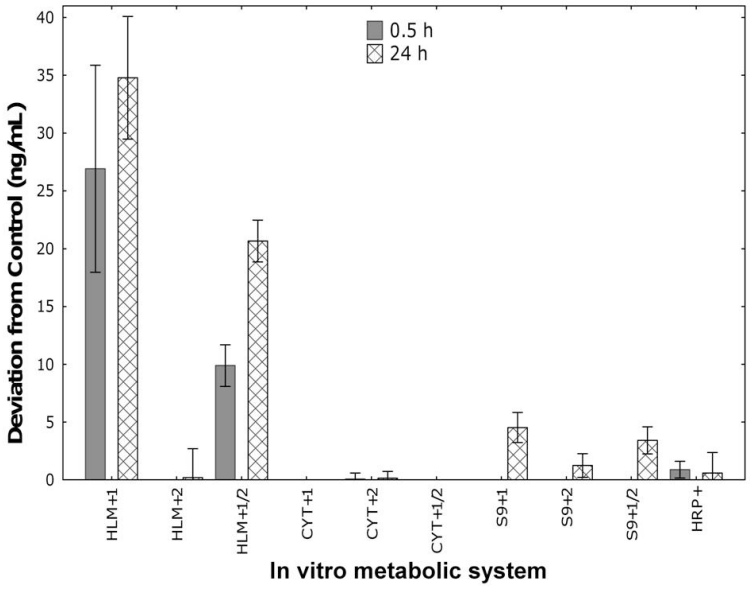


**Figure 27: Formation of normorphine from morphine across assay systems**

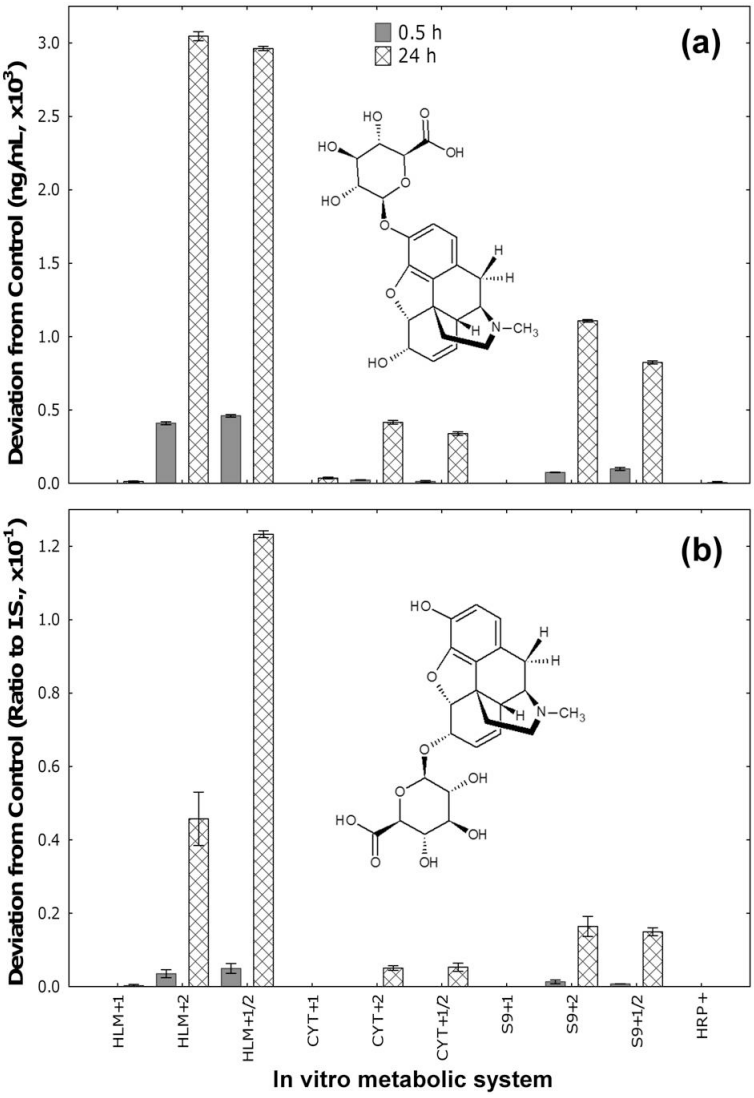


**Figure 28: Formation of (a) morphine-3-glucuronide and (b) morphine-6-glucuronide**

### 4.2.4. **Discussion of Drug of Abuse *In Vitro* Metabolism Results**

*In vitro* metabolic systems are of great use for a variety of applications in drug development and monitoring, including metabolic profiling and toxicity assessment.[30,114] The selection of the metabolic system itself in addition to variables such as cofactors and incubation time directly impacts the metabolic profile obtained. Commonly incorporated metabolic components include microsomes, cytosol, S9 fraction, and purified biotransformation enzymes. In addition, supplementation with additives can drastically impact the efficacy of these assays. For example, divalent cations (*e.g.*, $Mg^{+2}$) and/or a NADPH regeneration

system can significantly improve the functionality of certain metabolic pathways.[115] When Phase II glucuronide metabolites are desired, UDP-GlcUA must also be present as a cofactor. In addition, since UGTs are membrane-bound enzymes with active pockets located within the lumen of the ER, introducing a means of traversing the ER membrane can dramatically increases system functionality. The peptide antibiotic Alm is commonly employed for this purpose.[35,37] The present study evaluated assay systems and the influence of time and cofactors in the *in vitro* metabolism of cocaine, methamphetamine, and morphine.

Unlike in the case of licit drugs, few data have been reported on the application and utility of *in vitro* biotransformation systems for generating metabolites of drugs of abuse relevant to *in vivo* exposure. Recently, *in vitro* assays have been employed to determine major metabolites of "designer drugs," including amphetamine, phencyclidine, and tetrahydrocannabinol analogs.[116,117] These studies have facilitated the development of analytical detection methods for numerous emerging designer drug analogs whose *in vivo* metabolism has not been reported. In the present study, several such systems were effective in producing a set of biotransformation products of cocaine, methamphetamine, and morphine, including all known major primary metabolites and numerous common secondary metabolites. The data are generally consistent with the results of *in vivo* ADME studies for each important abused drug.[104,118-120] The current approach was less effective in comprehensively identifying all of the minor metabolites reportedly formed *in vivo* (see Appendix 1, Appendix 2, and Appendix 3). The inability to detect minor drug metabolites may be attributed to assay design and method sensitivity, which in the present study were optimized for rapid identification of major metabolites.

#### 4.2.4.1. **Cocaine Metabolism Discussion**

The complete enzymology of each assay system was found to influence the rate and pathways of cocaine biotransformation. Enzyme influence was illustrated by the differing relative levels of ecgonine methyl ester obtained in each assay system. Enzyme-mediated ecgonine methyl ester production primarily involves hCE-2, an esterase bound to the ER membrane in the liver[121], consistent with the finding of ecgonine methyl ester as an intermediate metabolite in assay systems containing ER membrane remnants (*i.e.*, HLM and S9). As the enzyme does not require activating cofactors such as NADPH, hCE-2 was able

to facilitate esterase activity in all HLM and S9 assay systems (*i.e.*, +1, +2, and +1/2 mixtures) in the present study. Low level formation of ecgonine methyl ester found in control (no enzyme), cytosol, and HRP assay systems likely represents non-specific hydrolysis, a phenomenon previously reported.[122] In contrast, norcocaine production is mediated by CYP *N*-demethylase activity (also localized to the ER membrane), thereby accounting for its formation exclusively in HLM and S9 assays containing NADPH. NADPH is necessary for CYP activity and is included in the +1 and +1/2 assay systems employed here. Consequently, norcocaine is absent from no enzyme, CYT, and HRP systems and from HLM+2 and S9+2 incubations.

While regioselective ring metabolism has been well documented with numerous xenobiotics in the past[123,124], this phenomenon has not been extensively investigated for drugs of abuse. Comparisons of oxidative ring metabolism of cocaine in the present study revealed distinct differences between liver derived biotransformation components and non-liver derived HRP. Specifically, regioselective hydroxylation pathways were noted for liver fractions, whereas hydroxylation by HRP was substantially less selective. In addition, the relative levels of hydroxylated metabolites produced by the HRP system were considerably greater than the hepatic systems, reaffirming the strong oxidizing power of the HRP/$H_2O_2$ system. The differences in isomer formation encountered with this system suggest that care must be taken in using the HRP assay as a model for hepatic oxidative metabolism. However, the HRP assay may be a relevant model for endogenous peroxidases localized to individual tissue types other than liver[31,125], and further studies examining the possible formation of 2-hydroxylated cocaine metabolites by tissue-specific peroxidases may validate this system as a predictor of non-hepatic *in vivo* metabolism.

In the case of cocaine metabolism, distinct differences could be seen in the production of primary vs. secondary metabolites, stressing the importance of incubation time in experimental design. Data from the current study demonstrate that, for norcocaine (a primary metabolite of cocaine), the HLM system is adept at producing the metabolite within 0.5 h, while S9 requires a longer incubation time to produce detectable quantities of norcocaine. Since benzoylnorecgonine is a secondary metabolite (*i.e.*, the result of further metabolism of the primary cocaine metabolites benzoylecgonine and norcocaine), production is slower *in vitro*. These differences in metabolic profiles among assay systems and with differing incubation

times exemplify the need for adjusting assay parameters to the specific aim or desired outcome of each individual experiment. For example, incubation time can be minimized when primary metabolites are the desired targets; however, if secondary or minor metabolites are of interest, increasing the incubation time beyond 30 min (especially with the S9 system) should be considered. Minor or secondary metabolites may be of particular interest when examining the impact of toxicophore and reactive metabolite formation for consideration in idiosyncratic toxicity studies.[69,126,127]

Similar metabolic studies on the pyrolytic cocaine product AEME reported by Toennes *et al.* and Fandino *et al.* are largely in agreement with findings from the present study regarding *in vitro* metabolism of cocaine.[128,129] Investigations into hydrolytic degradation of AEME to anhydroecgonine demonstrated passive hydrolysis exacerbated by an increase in pH. Additionally, enzymatic hydrolysis by butyrylcholinesterase was suggested on the basis of increases in anhydroecgonine production in human plasma as compared to buffer at physiological pH. These data are concordant with observations of ecgonine methyl ester formation from cocaine, where assay systems with esterase activity (*i.e.*, HLM and S9) demonstrated increased production of ecgonine methyl ester over other systems. However, even systems without active esterases (*i.e.*, no enzyme, CYT, and HRP) produced ecgonine methyl ester as a minor metabolite, likely by means of passive hydrolytic degradation. Analysis of AEME after incubation with rat liver microsomal preparations[128] showed qualitative similarity in metabolic pathways associated with AEME biotransformation as were observed in the current study with cocaine. Fandino *et al.* did note appreciable variability of enzymatic activity between microsomal preparations derived from various tissues, specifically a lack of oxidative metabolite production in kidney- and brain-based assays. However, as has been noted in other studies, xenobiotic metabolism can vary both qualitatively and quantitatively between species[117,130], suggesting caution when drawing conclusions based on cross-species assays.

The possible formation of Phase II cocaine metabolite glucuronides was also examined in the present study. Results showed no evidence for glucuronide formation (either by direct MS detection or depletion of hydroxylated metabolites) in the *in vitro* systems studied, despite the presence of an active glucuronidation mechanism. In contrast, Zhang *et al.* reported aryl-hydroxylated cocaine metabolites in authentic urine specimens after enzymatic hydrolysis, leading to their conclusion that hydroxylated

metabolites exist, at least in part, as Phase II conjugates.[104] Since the extraction procedure used in their experiments hydrolyzed both glucuronide and sulfate conjugates, it is possible that hydroxylated cocaine metabolites exist primarily as sulfonated products, whose formation was not investigated in this study.

#### 4.2.4.2. **Methamphetamine Metabolism Discussion**

The hepatic metabolism of methamphetamine has been reported to be primarily mediated by CYP enzymes[29,131] and FMOs[29]. The current *in vitro* experiments, which are generally in agreement with the influence of membrane-bound CYP and FMO enzymes on methamphetamine metabolism, demonstrated a nine-fold increase in amphetamine production in microsomal systems activated with NADPH over any other system. However, the appearance of amphetamine in CYT systems activated by NADPH suggests that not all methamphetamine metabolism is catalyzed by CYP enzymes and FMOs (which are found exclusively as membrane-coordinated enzymes in the HLM fraction). Contamination of CYT fractions with CYP enzymes can be discounted, because the analogous zolpidem hydroxylation (positive control) was limited to HLM and S9 assays. While the majority of the enzymatic components present in the CYT fraction mediate conjugative (Phase II) activities, soluble enzymes (such as methyltransferases) in the CYT fraction may contribute to the Phase I metabolism of methamphetamine.

While the oxidative activity of certain assay systems has been found to be regioselective with other drugs (including cocaine, as reported above)[123,124], the oxidation of methamphetamine to form three arene-hydroxylated isomers did not demonstrate qualitative regioselectivity in the present study. Quantitative regioselectivity could not be definitively determined due to a lack of available calibrated standards. Even though general assay regioselectivity was not observed, individual enzymatic components (*e.g.*, CYP isozymes, CYP vs. FMO) may still display regioselective activity.

It is notable that analytical schemes for methamphetamine metabolite analysis typically only test for the presence of the 4-hydroxy isomer when hydroxymethamphetamine is examined. Indeed, there is no mention of 2- or 3-hydroxymethamphetamine in human-based metabolism literature to date. However, it is unclear whether the 2- or 3-hydroxy isomers have previously been targeted as potential metabolites. 4-Hydroxymethamphetamine may be favored as the preferential hydroxyl metabolite because of its

comparatively rapid production (as demonstrated in the present study) or potential quantitative superiority over 2- and 3-hydroxy isomers. Although the 2- and 3-hydroxy derivatives were clearly present, the present data are insufficient to assess quantitative distributions of hydroxymethamphetamine isomers among the assay systems examined.

Metabolism of methamphetamine to 3-hydroxymethamphetamine displayed characteristics atypical for aryl hydroxylation products. First, data from systems typically exhibiting high oxidative activity (*i.e.*, HLM+1, HLM+1/2, and HRP+) showed a decrease in the concentration of this metabolite from 0.5 to 24 h incubation. The observed phenomenon may suggest preferential secondary oxidative metabolism of the 3-hydroxy isomer and/or molecular instability leading to further transformation of product. Also atypical for oxidative products, the predominant human liver fraction producing 3-hydroxymethamphetamine after 24 h incubation was determined to be CYT. Oxidative metabolism is typically catalyzed by monooxygenases (*e.g.*, CYPs, FMOs), which are almost exclusively located in the microsomal fraction. These data suggest the possible influence of additional classes of enzymes outside the CYP and FMO superfamilies contributing to the comprehensive metabolism of methamphetamine biotransformation.

Literature reports have demonstrated the formation and direct detection of glucuronide and sulfate conjugates of aryl-hydroxylated metabolites of methamphetamine in authentic blood and urine specimens from drug users.[27] In accordance, Phase II glucuronide products of methamphetamine metabolism were targeted by the comprehensive methamphetamine metabolism analysis method employed in the present study. In contrast to human specimen data reported in previous work, direct LC-MS analysis in the present study was unable to detect methamphetamine metabolite glucuronide formation in any *in vitro* system examined, despite the presence of active Phase I oxidation and Phase II glucuronidation mechanisms. However, decreases in hydroxymethamphetamine isomer concentrations between assays containing only active Phase I systems and those with both active Phase I and II mechanisms were noted. Observed discrepancies in hydroxymethamphetamine concentrations between assay systems containing UDP-GlcUA and those without would be consistent with secondary glucuronide conjugation. Inability of the MS-based analytical method used in this study to directly detect glucuronide products may have been the result of less

than optimal ionization and fragmentation parameters, due to the lack of analytical standards for these metabolites.

#### 4.2.4.3. **Morphine Metabolism Discussion**

In contrast to the biotransformation of cocaine and methamphetamine, the metabolism of morphine by the four *in vitro* systems was primarily mediated by Phase II glucuronidation. Glucuronide formation is generally known to be catalyzed by ER-bound UGT enzymes found mainly in the microsomal fraction, a fact corroborated by high concentrations of morphine-3- and morphine-6-glucuronide in HLM+2, HLM+1/2, S9+2, and S9+1/2 incubations in the present study. However, the appearance of glucuronide metabolites in CYT assays containing the cofactor UDP-GlcUA also suggests the presence of glucuronide-forming enzymes in the cytosol. This phenomenon may reflect either incomplete sequestering of UGT enzymes to the microsomal fraction during differential centrifugation or the existence of distinct enzymes in the cytosolic fraction that represent a minor contribution to the process of morphine glucuronidation. In contrast, incubation of nicotine as a positive control did not reveal glucuronide production in CYT incubations; nicotine-*N*-glucuronide was exclusively produced in HLM and S9 assays containing UDP-GlcUA. Lack of nicotine-*N*-glucuronide in CYT fractions activated with UDP-GlcUA suggests that incomplete sequestering of UGT enzymes to the microsomal fraction is unlikely to be the causal factor responsible for morphine glucuronidation in CYT assay systems. These data suggest that morphine glucuronidation may be influenced by non-microsomal enzymes that have not been documented in morphine metabolism-based literature.

Though Phase I biotransformation represents only a small fraction of morphine metabolism, the *N*-demethylation product normorphine was detected in HLM and S9 assays activated by NADPH. This is consistent with previous reports demonstrating the influence of CYP enzymes on the *N*-dealkylation of morphine in humans.[132] Furthermore, previous reports have demonstrated the formation of the morphine reduction product morphinone in human liver tissues.[82] However, the intrinsic reactivity of compounds containing α,β-unsaturated carbonyls such as morphinone would likely result in binding to nucleophilic targets in cellular media *in vivo* (*e.g.*, glutathione, free thiols within proteins).[133,134] While morphinone was

not detected in free fraction by the methods used in this study, it may be that any morphinone produced would be protein bound, with the free fraction of morphinone remaining below the detection limits of this method.

### 4.3. **rhCYP Assays**

#### 4.3.1. **Positive Control Probes**

Isoform viability was confirmed using samples incubated with a cocktail of known substrates for each CYP isoform (melatonin, bupropion, amodiaquine, tolbutamide, omeprazole, and dextromethorphan). The production of anticipated metabolites from each substrate probe (see Table 7) was catalogued for each isoform (Figure 29). While certain substrate-to-metabolite transformations were conserved across multiple isoform incubations (*i.e.*, *N*-demethylation of omeprazole to desmethylomeprazole, Figure 29), maximal formation of each resultant metabolite was as anticipated on the basis of published CYP isoform data.

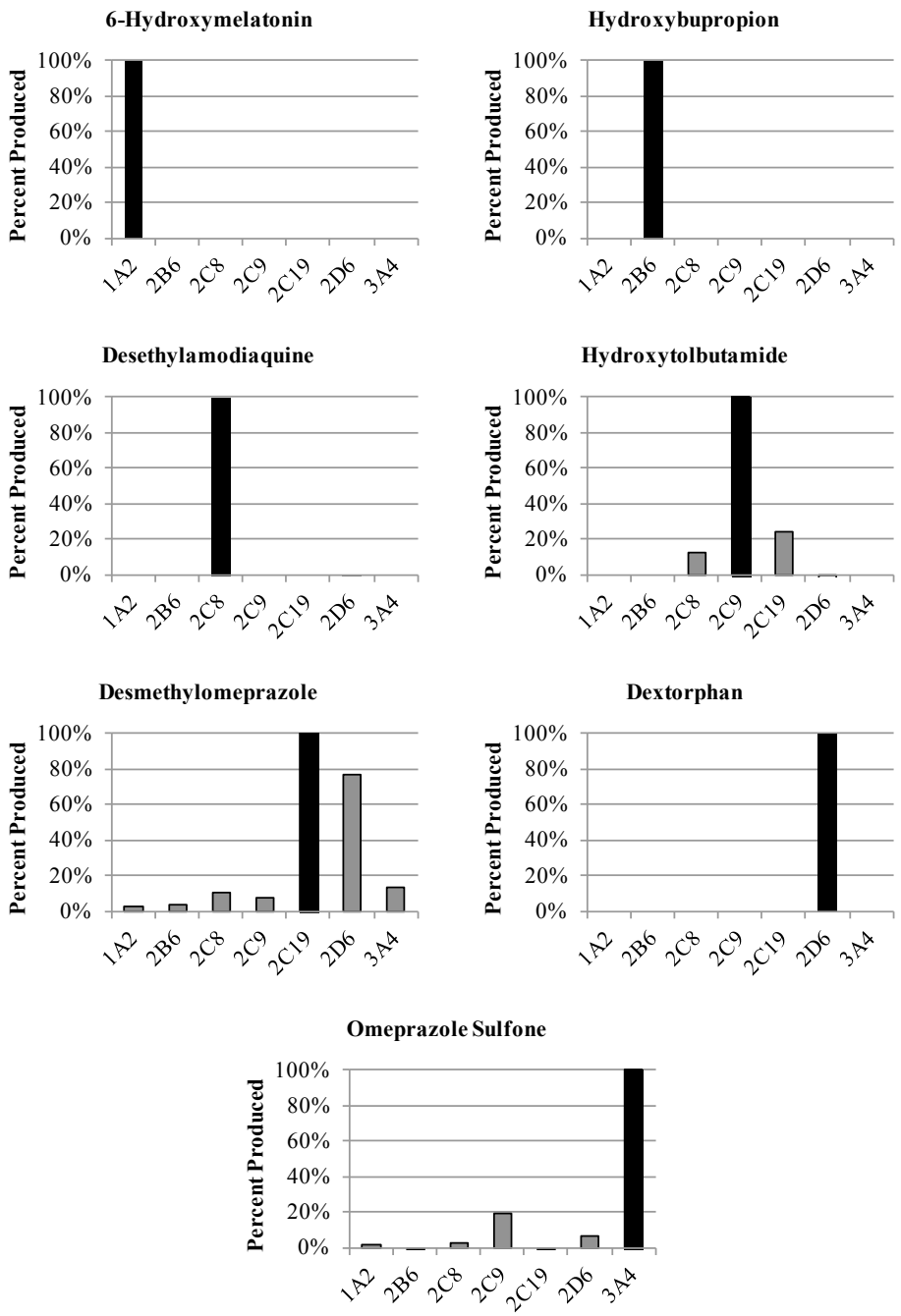


**Figure 29: rhCYP positive control assays**

**Expected metabolic event from literature: CYP1A2, melatonin→6-hydroxymelatonin; CYP2B6, bupropion→hydroxybupropion; CYP2C8, amodiaquine→desethylamodiaquine; CYP2C9, tolbutamide→hydroxytolbutamide; CYP2C19, omeprazole→ desmethylomeprazole; CYP2D6, dextromethorphan→dextorphan; CYP3A4, omeprazole→ omeprazole sulfone. Dark bars designate CYP isoform targeted by each specific metabolic transformation.**

### 4.3.2. **Cocaine**

Concordant with existing reports of cocaine ester cleavage resulting from various esterases (*e.g.*, carboxylesterases, cholinesterases), assay data demonstrated that none of the CYP isoforms examined significantly influenced the hydrolytic pathways of cocaine biotransformation.

Norcocaine production is known to be mediated by CYP enzymes, with reports having designated CYP3A4 as a contributing isoform in humans for oxidative *N*-demethylation.[135] Results from the present study confirmed the generation of norcocaine from cocaine by CYP3A4 and determined that the CYP2C family (*i.e.*, 2C8, 2C9, 2C19) also plays a significant role in the *N*-demethylation of cocaine. Figure 30 displays data collected for the contribution of each CYP isoform examined to norcocaine production.

The pathways responsible for the aromatic hydroxylation of cocaine have the potential to be complex due to regioselective oxidative activity documented in some CYP enzymes.[123,136] Therefore, the phenotyping of biotransformation pathways responsible for each hydroxylated isomer was examined individually. As such, the reactions of 2-, 3-, and 4-hydroxylated isomers of cocaine were phenotyped separately. As was reported above (Section 4.2.1), 2-hydroxycocaine is not a metabolite generated via hepatic biotransformation processes in humans. In accordance with these previous findings, the present experiment showed that 2-hydroxycocaine is not formed by any of the human CYP isozymes examined in the phenotyping panel. Likewise, 3-hydroxycocaine production could not be attributed to any of the isoforms studied, suggesting the possible influence of other enzyme classes (*e.g.*, FMOs) or one of the CYP isoforms not investigated in this study. 4-Hydroxycocaine production was found to be almost exclusively mediated by CYP2C19 with minor influences from CYPs 2C9 and 3A4 (Figure 30).

Incorporating existing knowledge with the data presented herein, Figure 31 displays a comprehensive list of known enzymatic contributors (focusing on individual CYP isoforms) for the primary Phase I biotransformation pathways affecting cocaine metabolism.

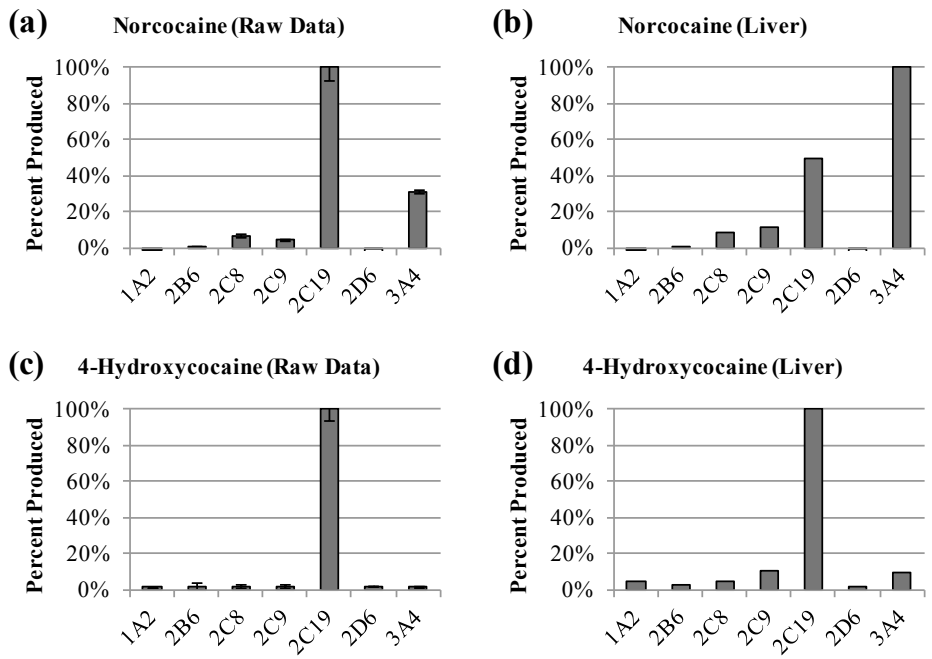


**Figure 30: Cytochrome P450 isoform panel for cocaine primary metabolite formation (a) and (c) present raw data for norcocaine and 4-hydroxycocaine formation within the CYP isoform panel. (b) and (d) present the same data after transformation to account for relative CYP concentrations in human liver tissue.**

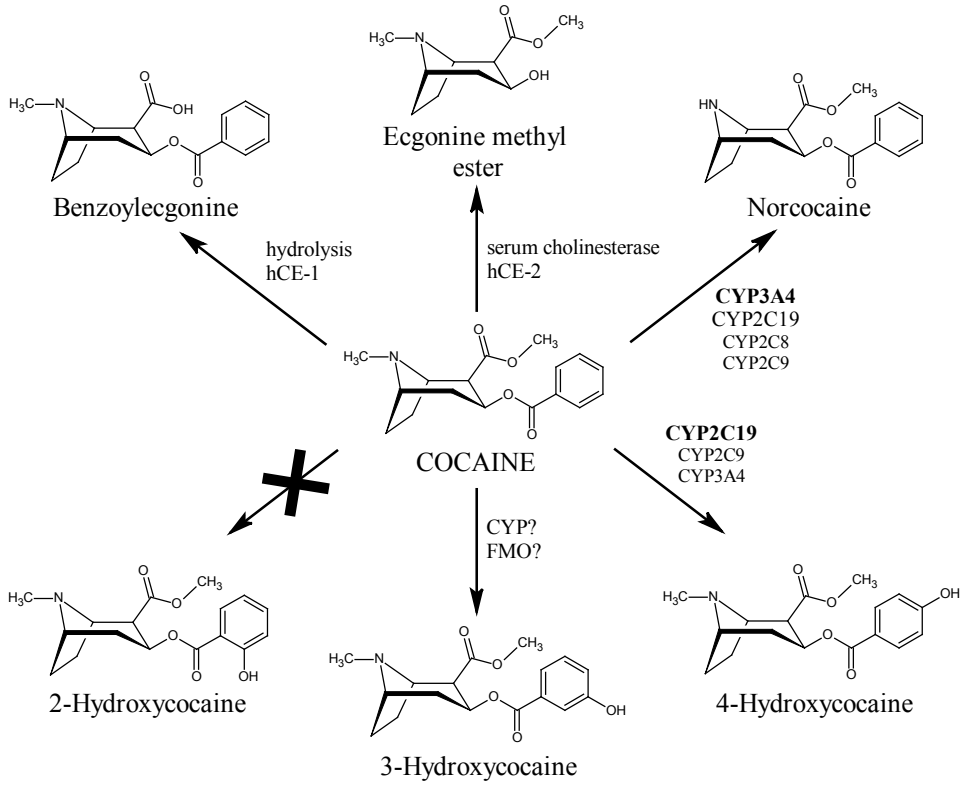


**Figure 31: Enzymology of primary cocaine biotransformation pathways in humans**

### 4.3.3. **Methamphetamine**

Since methamphetamine and amphetamine typically undergo analogous biotransformation processes due to structural similarity, it was anticipated that methamphetamine could undergo α-hydroxylation to form ephedrine in the same way that amphetamine has been documented to undergo α-hydroxylation to form norephedrine in humans and other species.[137,138] However, *in vitro* rhCYP assay incubations of methamphetamine did not demonstrate CYP-mediated formation of ephedrine. Indeed, this data is in agreement with microsomal incubation results (see Section 4.2.2) where neither ephedrine nor norephedrine were detected in any *in vitro* metabolic model system examined.

The primary Phase I metabolic pathway of methamphetamine metabolism in humans is *N*-demethylation to form the pharmacologically active product amphetamine. Existing literature has demonstrated the contribution of CYP2D6[29,131] in the metabolism of methamphetamine to amphetamine; however, complete reaction phenotyping with other major CYP isoforms has not been reported. Data collected here corroborated the primary impact of CYP2D6 previously reported in the literature. Additionally, CYPs 2C9 and 2C19 were found to mediate the *N*-demethylation of methamphetamine to amphetamine (Figure 32).

Existing literature reporting the aromatic hydroxylation of methamphetamine and other phenethylamine congeners has unilaterally focused on the 4-hydroxylated product without mentioning either the 2- or 3-hydroxylated isomers. These reports have also identified CYP2D6 as a contributor to the production of 4-hydroxymethamphetamine; however, as with CYP designation for amphetamine, comprehensive examinations of contributions from other CYP isoforms were not performed. As a result of data from the present study indicating the formation of all three hydroxymethamphetamine isomers within *in vitro* microsomal metabolic model systems (see Section 4.2.2), the biotransformation of methamphetamine to each hydroxymethamphetamine isomeric product was phenotyped individually. While minor quantities of the 2- and 3-hydroxylated isomers were formed in many of the CYP assays, no specific mediating isoform could be determined for the production of either 2- or 3-hydroxymethamphetamine. In contrast, the production of 4-hydroxymethamphetamine was found to be mediated by numerous CYP isoforms. Data collected in the current study confirmed the primary role of

CYP2D6 concordant with existing literature, but also catalogued the influences of CYP3A4 and the CYP2C subfamily (CYPs 2C8, 2C9, and 2C19; see Figure 32).

Incorporating existing knowledge with data presented herein, Figure 33 displays a comprehensive list of known enzymatic contributors (focusing on individual CYP isoforms) for the primary Phase I biotransformation pathways affecting methamphetamine metabolism.

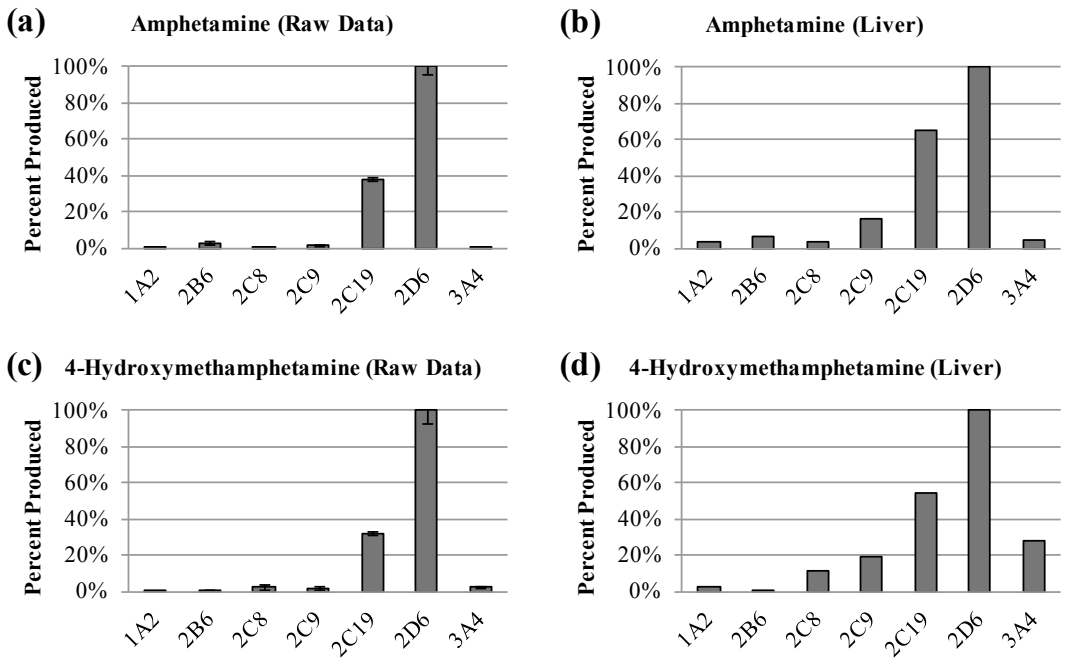


**Figure 32: Cytochrome P450 isoform panel for methamphetamine primary metabolite formation (a) and (c) present raw data for amphetamine and 4-hydroxyamphetamine formation within the CYP isoform panel. (b) and (d) present the same data after transformation to account for relative CYP concentrations in human liver tissue.**

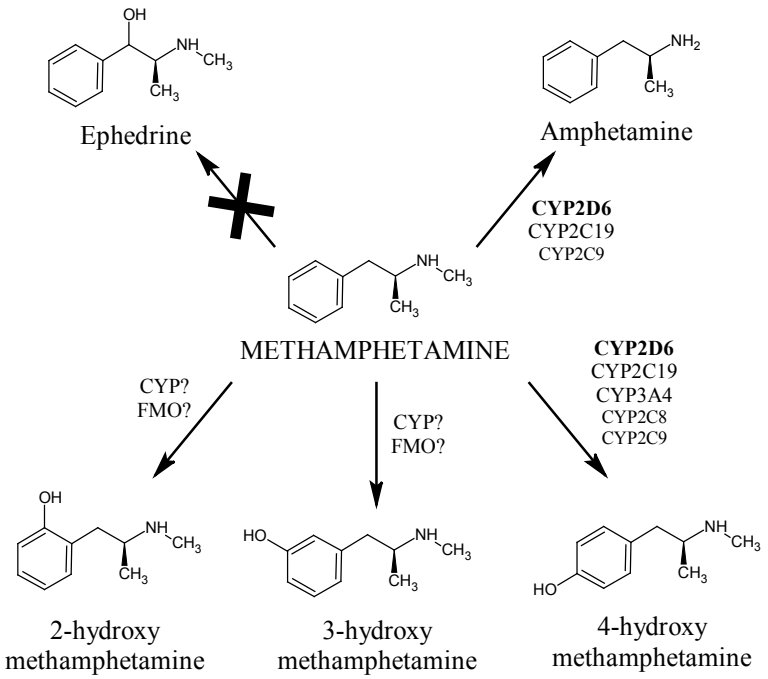


**Figure 33: Enzymology of primary methamphetamine biotransformation pathways in humans**

### 4.3.4. **Morphine**

As was documented in microsomal incubations, morphine undergoes minimal Phase I biotransformation detectable via the direct analysis methods utilized in these experiments (see Section 4.2.3). However, it is known that catalytic oxidation of the C6 hydroxyl group on morphine to form the α,β-unsaturated carbonyl metabolite, morphinone, is facilitated by the enzyme morphine-6-dehydrogenase and free hydroxyl radicals. Consistent with data from microsomal incubations performed earlier in this project (see Section 4.2.3), morphinone was not detected in any CYP isoform incubation performed, further supporting the singular role of the enzyme morphine-6-dehydrogenase in catalyzing the transformation of morphine to morphinone.[82-84]

Previous research by Projean *et al.* investigated the isoforms responsible for *N*-demethylation of morphine to normorphine using rhCYP extrapolated enzyme kinetics and microsomal inhibition data, confirming the primary influence of CYPs 3A4 and 2C8 and minor influences by CYPs 2C9, 2C19, and 2D6.[132] Results obtained by *in vitro* incubation of morphine with individual rhCYP isozymes in the current study determined the primary influence of CYPs 2C8 and 3A4 with minor influences of CYPs 2C9 and

2C19 (Figure 34). Thus, the data obtained are generally concordant with existing literature for the *N*-demethylation of morphine, demonstrating the usefulness of the simplified reaction phenotyping procedure used in this study for designation of the principal CYP isoforms mediating individual biotransformation pathways.

Incorporating existing knowledge with data presented herein, Figure 35 displays a comprehensive list of known enzymatic contributors (focusing on individual CYP isoforms) for the primary Phase I biotransformation pathways affecting morphine metabolism.

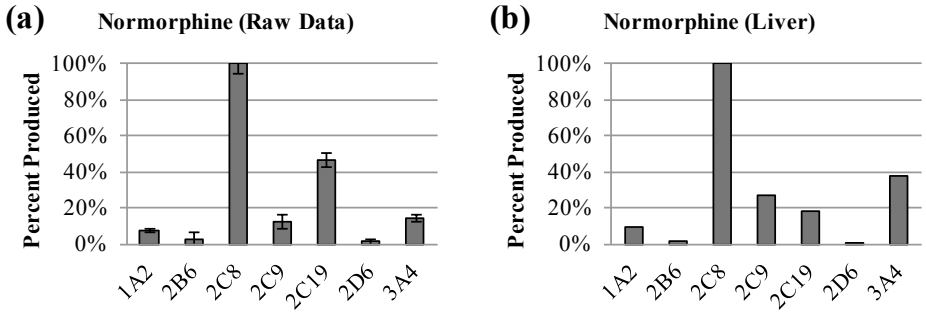


**Figure 34: Cytochrome P450 isoform panel for morphine primary metabolite formation (a) presents raw data for normorphine formation within the CYP isoform panel. (b) presents the same data after transformation to account for relative CYP concentrations in human liver tissue.**

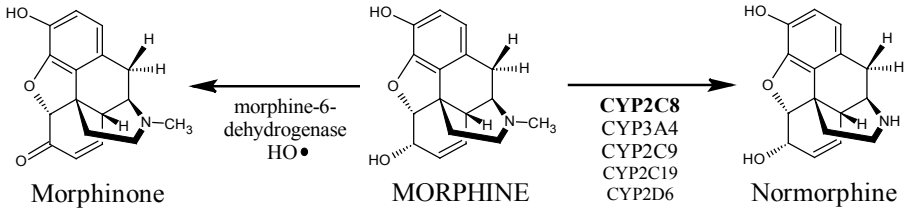


**Figure 35: Enzymology of primary morphine biotransformation pathways in humans**

### 4.3.5. **Discussion of Results from Drug of Abuse rhCYP Reaction Phenotyping**

Results obtained from CYP phenotyping of the metabolic pathways associated with primary metabolites of cocaine, methamphetamine, and morphine demonstrated the variety of enzymatic contributors that can play a role in the metabolism of a xenobiotic. Specific knowledge of the primary CYP isoforms responsible for metabolic pathways can be critical during exposure to multiple drugs. While

cocaine and methamphetamine are not typically prescribed medically, administration of morphine with other pharmaceuticals is common. Likewise, clinicians prescribing pharmaceuticals to individuals illegally abusing cocaine, methamphetamine, or morphine could greatly benefit from such phenotyping data, as the chronic use and high doses often associated with drug abuse can have a severe impact on the patient's physiology and therapeutics.[139] Additionally, known genetic predispositions (*i.e.*, enzymatic overexpression, under expression, or variance in enzyme function) can act as biomarkers of susceptibility to effects associated with drug impact on pharmacokinetics, pharmacodynamics, toxic metabolite production, and other toxicological descriptors.

Data collected in this study for morphine are in good agreement with existing literature describing the CYP phenotyping of *N*-demethylation pathways that generate the Phase I metabolic product normorphine. While the present study did not determine CYP2D6 to be a contributing isoform based on criteria utilized, the combination of Michaelis-Menten kinetic parameters determined by Projean *et al.* (*i.e.*, relatively high $K_m$ of 10.1 mM and low $V_{max}$ of 6.57 pmol/min/pmol CYP)[132] coupled with the relatively low expression of CYP2D6 in human liver (*i.e.*, 2.0% total CYP content in liver) could explain this discrepancy with existing literature. In contrast, the simplified method utilized here was successful in assigning the influence of CYPs 2C8, 3A4, 2C9, and 2C19 in concordance with existing literature, again demonstrating the value of the assay.

In the case of the important drug of abuse cocaine, CYP3A4 has previously been catalogued as a major contributor to the overall metabolism of this drug in humans. Data reported above confirm the impact of CYP3A4 on biotransformation pathways responsible for norcocaine and 4-hydroxycocaine. Additionally, norcocaine and 4-hydroxycocaine production were determined to be mediated by the CYP2C subfamily, with CYPs 2C19, 2C8, and 2C9 contributing to the *N*-demethylation of cocaine and CYPs 2C19 and 2C9 as contributors to regioselective hydroxylation to 4-hydroxycocaine. Interestingly, while individual isoform contribution to hydroxylation at the 4-position of the benzoyl ring could be attributed to specific CYP isoforms, analogous reaction to form 3-hydroxycocaine was not determined to be mediated by any of the CYPs examined. In concordance with data presented in Section 4.2.1, individual CYP phenotyping did not demonstrate the formation of 2-hydroxycocaine in any of the human CYP-containing

assays examined, supporting the conclusion that regioselective enzyme activity in human liver tissue does not allow for the hydroxylation of cocaine at the 2-position of the cocaine benzoyl moiety. Also in support of existing data, the formation of the esterase products benzoylecgonine and ecgonine methyl ester was not exacerbated by any CYP isoform examined in this study. While benzoylecgonine and ecgonine methyl ester were detected as products in rhCYP isoform assays, their presence can reasonably be attributed to the passive hydrolytic cleavage of labile cocaine ester bonds (see Section 4.2.1). Levels of the hydrolysis products in systems containing NADPH and control samples (*i.e.*, no NADPH added) were indistinguishable, demonstrating the lack of influence of NADPH-initiated CYP monooxygenase activity on their formation.

Designation of CYP2C19 as a mediating factor in 4-hydroxycocaine production may have implications on cocaine-associated pathology and its relationship to genetic predisposition for addiction. It has been suggested that the cascade associated with cocaine addiction is mediated by the binding of cocaine to dopamine transporters and downstream physiological effects that result from this binding.[140-142] Singh *et al.* have demonstrated that 2- and 4-hydroxycocaine have 9.9- and 1.6-fold higher affinity, respectively, for dopamine transporter binding as compared with cocaine (3-hydroxycocaine has only 0.2-fold the affinity for dopamine transporters compared to cocaine).[143] In compliance with the dopamine transporter binding theory of cocaine addiction, increased concentration of 4-hydroxycocaine in humans would elicit stronger dopaminergic response, thereby stimulating the addiction pathway. Individual genetic or epigenetic factors causing increases or decreases in CYP2C19 expression and/or activity may act as biomarkers of susceptibility for the development of cocaine addiction. While production of 2-hydroxycocaine would result in more dramatic shifts in addiction pathology (as its dopamine transporter binding is 9.9-fold more potent than cocaine and 6.1-fold more potent than 4-hydroxycocaine), data from this study suggests that 2-hydroxycocaine is not a metabolic product of human CYP enzymes after cocaine exposure. However, non-hepatic oxidative enzymes (*e.g.*, tissue-specific peroxidases) may bring about oxidation at the 2-position of the cocaine arene moiety, causing localized production of 2-hydroxycocaine and possible downstream impact on dopamine transporter binding and addiction.

Like cocaine, limited reports of individual isoform contribution to methamphetamine metabolism are available in the literature to suggest the involvement of CYP2D6 on the biotransformation pathways that result in amphetamine and 4-hydroxymethamphetamine production in humans. Data collected in this study confirm and extend existing data, designating CYP2D6 as the major CYP isoform responsible for both amphetamine and 4-hydroxymethamphetamine production. Additionally, results demonstrate that the *N*-demethylation of methamphetamine to amphetamine is also mediated by CYPs 2C19 and 2C9, while hydroxylation to 4-hydroxymethamphetamine can be attributed to contributions by CYPs 2C19, 3A4, 2C8, and 2C9. As was the case with cocaine oxidation, the production of hydroxylated isomers aside from 4-hydroxymethamphetamine (*i.e.*, 2- and 3-hydroxymethamphetamine) could not be attributed to any specific CYP isoform examined in this study. On the basis of the observation that both 2- and 3-hydroxymethamphetamine are formed in human liver microsomal incubations (see Section 4.2.2), it is probable that either the FMO superfamily of monooxygenase enzymes are responsible for the microsomal production of these products or that one of the CYP isoforms not examined in the present study (*e.g.*, CYP2E1) is the catalytic enzyme in these biotransformation pathways. Lastly, the production of ephedrine was examined as a possible metabolic route for methamphetamine catalyzed by CYP enzymes. In agreement with data from microsomal incubations, where ephedrine was not detected in any *in vitro* metabolic model system examined, rhCYP isoform assays also did not generate detectable concentrations of ephedrine. Lack of ephedrine detection supports the assertion that the aliphatic hydroxylation of methamphetamine to ephedrine may not be a metabolic process that occurs in humans, even though there is documented evidence for the formation of norephedrine (purportedly from the aliphatic hydroxylation of amphetamine as a secondary metabolite of methamphetamine biotransformation) in humans.[138]

### 4.4. **Reactive Metabolite Trapping and Protein Adduction Model Systems**

Positive control incubations in the presence of clozapine or benzyl bromide confirmed the formation of postulated covalent adduction products of these drugs (see Figure 36 and Figure 37).[144,145] Trapped reactive electrophiles within positive control incubations included a combination of reactive parent

compound and/or reactive metabolites, demonstrating the functionality of both pathways within these assays.

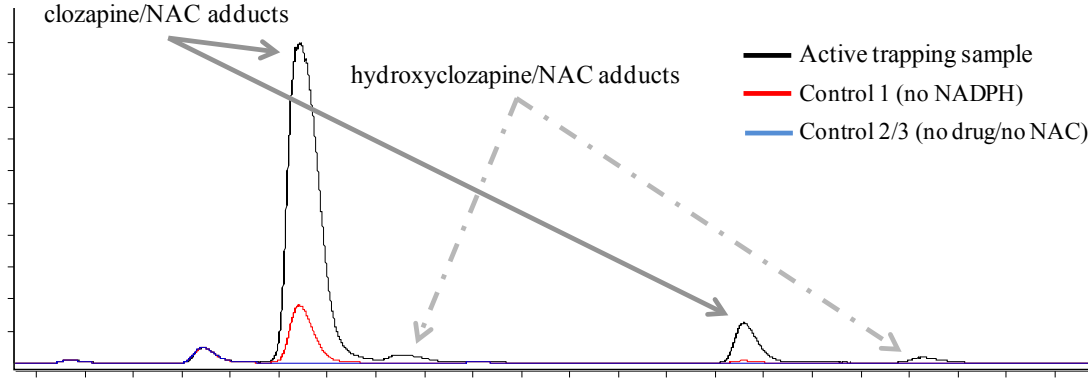


**Figure 36: Positive control incubation demonstrating passive and metabolism-mediated adduction by clozapine**

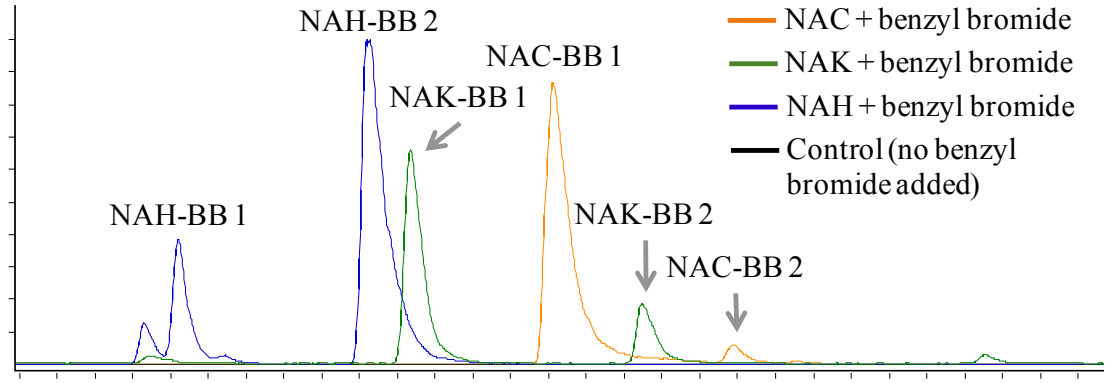


**Figure 37: Positive control incubation demonstrating passive adduction by benzyl bromide**
**Abbreviation: BB, benzyl bromide**

Preliminary screening of drug of abuse substrates (*i.e.*, cocaine, methamphetamine, or morphine) for adduction potential in the presence of an active Phase I metabolic system and trapping agent (*i.e.*, NAC, NAK, or NAH) showed the presence of numerous adduction products consistent with the *m/z* values of the hypothetical products presented in Table 9. Subsequent MS/MS investigation of each suspected adduction product further narrowed the pool of potential candidates by eliminating compounds when $MS^2$ fragmentation data was not consistent with a conjugated product resulting from substrate-trapping agent interaction. Table 15 presents a summary of preliminary screening assay data, where only cocaine/NAC

and morphine/NAC systems were found to produce adduction products with corroborating MS/MS spectra. All potential compounds detected in systems containing methamphetamine, NAK, or NAH were eliminated because of MS/MS data that was unsupportive of adduction products containing respective substrate/trapping agent moieties.

Rigorous investigations into the structure and mechanism of formation for putative adducts were performed according to the stepwise method optimization and probing assays described in the Methods section (see Section 3.6). Data and analysis are presented in the following section, organized according to individual substrate/trapping molecule systems. Chromatographic methods corresponding to each substrate/trapping molecule system are summarized in Appendix 8.

**Table 15: Summary of preliminary screening assays for potential adduction products**

| Drug Substrate | Trapping Agent | Conjugation Products with MS/MS Data Consistent with Adduction |
|---|---|---|
| **Cocaine** | NAC | *m/z* 483 |
| | NAK | ND[a] |
| | NAH | ND |
| **Methamphetamine** | NAC | ND |
| | NAK | ND |
| | NAH | ND |
| **Morphine** | NAC | *m/z* 447, 449 |
| | NAK | ND |
| | NAH | ND |

[a] ND = none detected

### 4.4.1. Cocaine Adduction Products

#### 4.4.1.1. Cocaine – *N*-Acetylcysteine Adduction

Chromatographic separation via UHPLC resulted in the designation of eight distinct analytes arising from interaction between cocaine and *N*-acetylcysteine (labeled COC-NAC 1-8 in Figure 38). Exact mass analysis performed by QTOF-MS of each analyte revealed qualitatively similar molecular mass and formula (molecular formula for all analytes determined to be $C_{22}H_{30}N_2O_8S$ via Agilent MassHunter software; see Table 16). MS/MS fragmentation of parent ions resulted in similar spectra, with a

representative spectrum presented in Figure 39. Fragmentation of *m/z* 483 precursor ions yielded fragments consistent with hydroxycocaine isomers, specifically *m/z* 121 (Figure 39 inset), a mass indicative of $[OCC_6H_4OH]^+$, an ion designating hydroxylation on the arene ring. Likewise, the fragment ion at *m/z* 182 is indicative of an intact methyl ester tropane, discounting the potential for formation by means of *N*-oxidative processes (*i.e.*, nitrosonium ion adduction). In accordance, the eight analytically determined products of cocaine–*N*-acetylcysteine adduction were assigned as isomers of the structure presented in Figure 40. Thiol-adduction products similar to that shown in Figure 40 have been previously characterized (*e.g.*, with benzylamine)[107], demonstrating the stability of conjugated enols that do not undergo subsequent dehydration to re-establish aromaticity.

Adduction products were not detected in three control samples incubated without NADPH, cocaine, and NAC, respectively, demonstrating that adduct formation is NADPH-, cocaine-, and NAC-dependent. NADPH-mediated adduct formation suggests the involvement of CYP and/or FMO enzyme families.

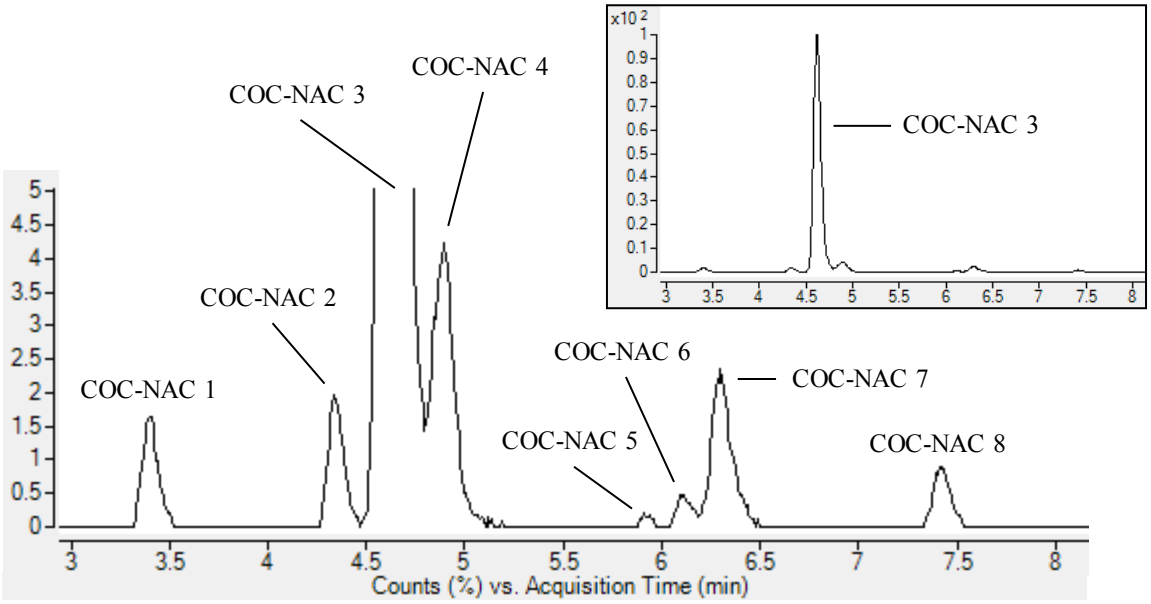


**Figure 38: Chromatographic separation of cocaine–*N*-acetylcysteine adducts (labeled COC-NAC 1-8; inset is expansion to show dominance of COC-NAC 3)**

**Table 16: Comparison of theoretical and observed $[M+H]^+$ ions for cocaine–*N*-acetylcysteine adducts**

| Adduction Product | Retention Time (min) | Theoretical Mass (m/z) | Observed Mass (m/z) | Difference (ppm) |
|---|---|---|---|---|
| **COC-NAC 1** | 3.41 | 483.1796 | 483.1794 | 0.41 |
| **COC-NAC 2** | 4.34 | 483.1796 | 483.1797 | 0.21 |
| **COC-NAC 3** | 4.61 | 483.1796 | 483.1801 | 1.03 |
| **COC-NAC 4** | 4.90 | 483.1796 | 483.1797 | 0.21 |
| **COC-NAC 5** | 5.91 | 483.1796 | 483.1793 | 0.62 |
| **COC-NAC 6** | 6.11 | 483.1796 | 483.1800 | 0.83 |
| **COC-NAC 7** | 6.30 | 483.1796 | 483.1797 | 0.21 |
| **COC-NAC 8** | 7.42 | 483.1796 | 483.1796 | 0.00 |
| **Average** | - | 483.1796 | 483.1797 ± 0.0003 | 0.21 |

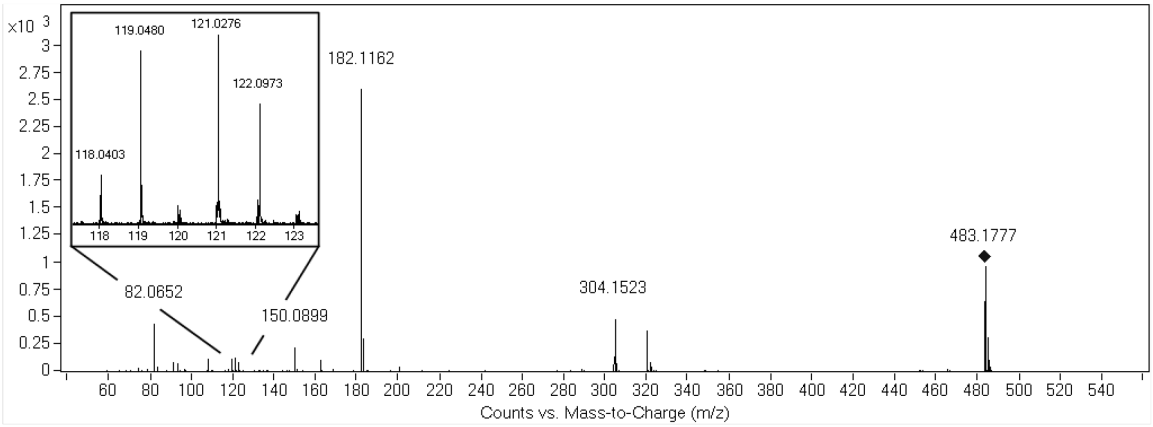


**Figure 39: MS/MS spectrum of cocaine–*N*-acetylcysteine adduct**

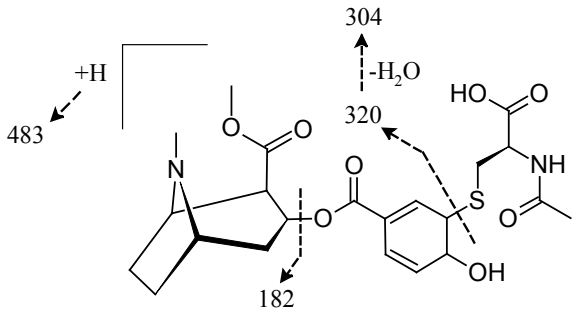


**Figure 40: Fragmentation pattern of cocaine–*N*-acetylcysteine adduct**

Investigation into the effect of varying incubation time and secondary supplementation with additional NADPH are summarized in Figure 41 using COC-NAC 3 as a model (analogous trends were documented across all eight COC-NAC isomers). Data demonstrated a linear relationship between incubation time and adduct production, with the 6 h incubation generating maximal adduct levels. In addition, it was found that, overall, a 6 h incubation with secondary NADPH supplementation at 3 h was more effective at quantitative generation of adduction products, generating 230% the amount of adduct than a 1.5 h incubation without supplementation (assuming a linear relationship between peak area count and adduct concentration).

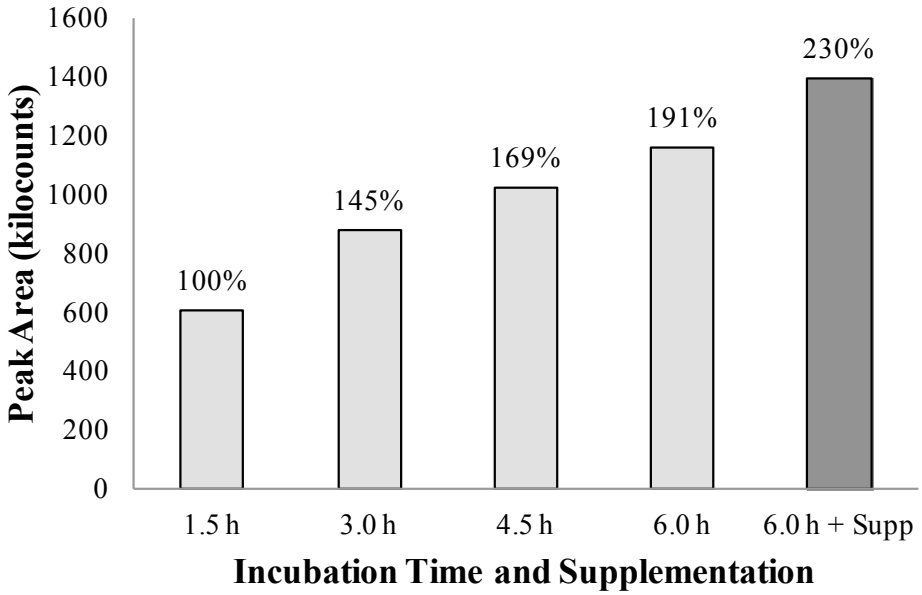


**Figure 41: COC-NAC 3 formation as a factor of incubation time and secondary NADPH supplementation**

#### 4.4.1.2. **Cocaine–*N*-Acetylcysteine Adduct Cytochrome P450 Enzyme Designation**

Examination of cocaine–*N*-acetylcysteine adduct formation within rhCYP assay systems revealed that CYPs 1A2, 2C19, and 2D6 were the primary contributing isoforms. While slight differences in quantitative isomer distribution between isoforms were observed, all contributing CYP isoforms were capable of producing each of the eight cocaine–*N*-acetylcysteine isomers. Figure 42 displays the relative quantities of adduct generated between *in vitro* assays using COC-NAC 3 as a model (labeled "Raw Data")

and the calculated relative contribution of each isoform expected in human liver tissue based on native isoform concentrations (labeled "Liver"). It is noteworthy that isoform panels examining 3- and 4-hydroxycocaine formation did not coincide with cocaine–*N*-acetylcysteine adduct formation even though hypothesized mechanisms for both rely on the same postulated cocaine-3,4-epoxide reactive intermediate. While CYP2C19 was conserved as a mediating isoform for both the 4-hydroxycocaine metabolite and cocaine adduction products, observed differences in isoform panels may be the result of enzymatic factors, specifically a preference for adduct formation over hydroxylated metabolite formation (for CYPs 1A2 and 2D6) or enzyme-substrate interactions influencing reaction kinetics within *in vitro* systems. The absence of CYP3A4 as a mediating factor in the formation of cocaine–*N*-acetylcysteine adducts does suggest that tropane nitrogen oxidation (known to be CYP3A4-mediated; demonstrated in norcocaine rhCYP assay, see Figure 30) is not a likely formation mechanism. While this data does confirm the influence of CYP enzymes in the production of metabolically induced cocaine thiol adduction, it does not preclude the contribution of the FMO superfamily of enzymes within microsomal assays.

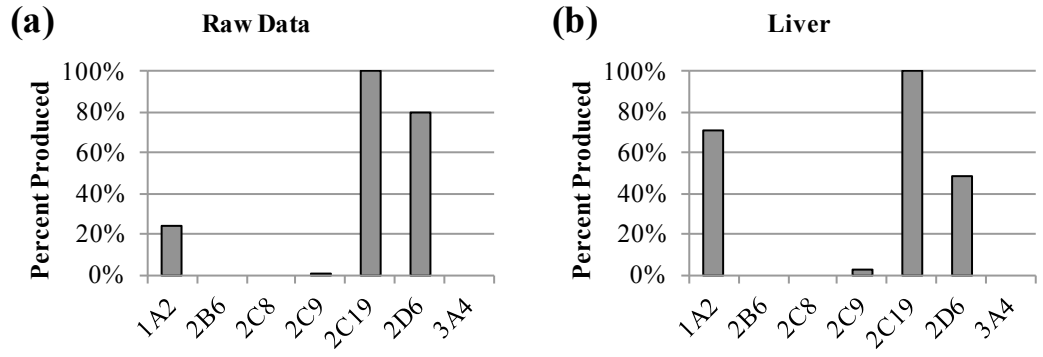


**Figure 42: Cytochrome P450 isoform panel for cocaine–*N*-acetylcysteine adduct formation (a) presents raw data for cocaine–*N*-acetylcysteine adduct formation within the CYP isoform panel. (b) presents the same data after transformation to account for relative CYP concentrations in human liver tissue.**

#### 4.4.1.3. **Putative Mechanism for Cocaine-Derived Thiol Adduction**

Structural designation of monohydroxylation at the arene moiety on cocaine in addition to knowledge of NADPH-mediated formation suggests that bioactivation of the benzoyl group yields a reactive electrophilic intermediate capable of reacting with a nucleophilic agent such as the sulfhydryl group on cysteine. Epoxide intermediate formation via FMO- or CYP-mediated oxidation (well-known

mechanisms resulting in the hydroxylation of arenes) is concordant with all data on mechanism and structure accrued in this study (Figure 43). Specific designation of the CYP isoforms 1A2, 2C19, and 2D6 confirm the role of CYPs in the adduction mechanism but do not preclude a potential influence of FMOs in the comprehensive adduction scheme. Adduct formation via an arene epoxide intermediate would involve the nucleophilic attack of the reactive epoxide intermediate by a cysteine thiol, resulting in epoxide ring opening and reduction of the oxygen to form a monohydroxylated thiol-adducted product with a stable conjugated enone. As nucleophilic attack of the epoxide can occur from numerous directions, this mechanism is also concordant with the generation of several structural isomers varying by site of hydroxylation and thiol attachment on the arene moiety.

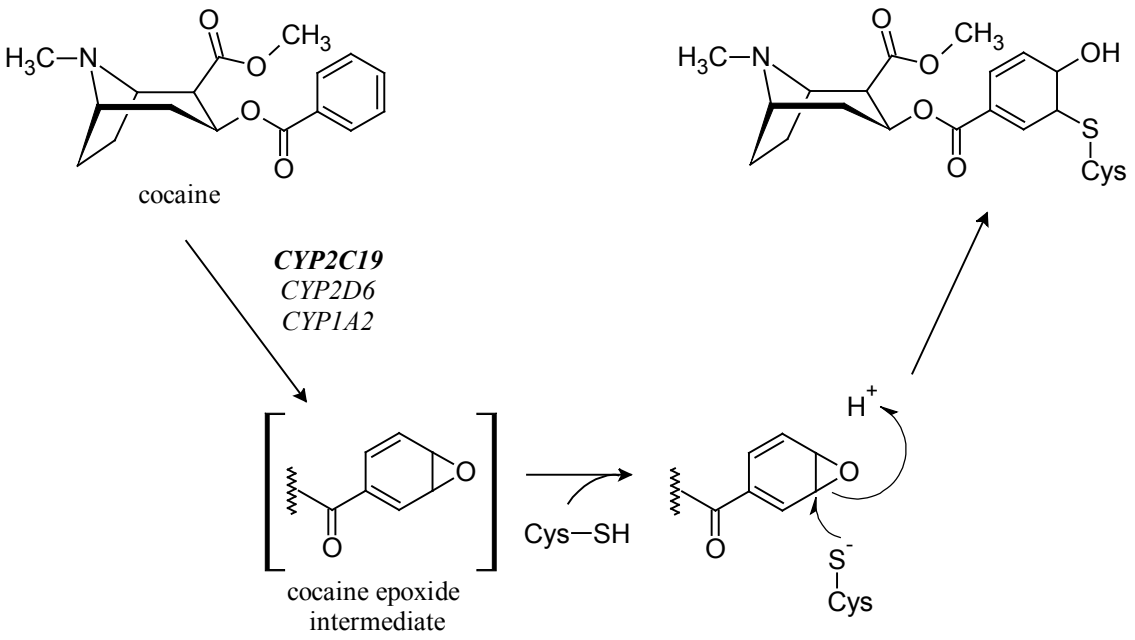


**Figure 43: Proposed mechanism for cocaine metabolism to reactive intermediate and thiol adduction**

#### 4.4.1.4. **Cocaine– Glutathione Adduction**

*In vitro* incubations supplemented with GSH as a reactive metabolite trapping agent revealed a series of cocaine– GSH adduction products consistent with the formation mechanisms proposed for cocaine– NAC adducts. LC-QQQ-MS analysis resulted in designation of three adduction products

(designated COC-GSH 1-3, Figure 44; native GSH MS/MS fragmentation included for reference in Appendix 9a). Isocratic elution at 4% B revealed COC-GSH 1-3 to be unresolved peaks (most likely arising from co-eluting structurally similar isomers; see Figure 44 inset). However, since MS/MS analysis of all peaks revealed uniform spectra (representative spectrum presented in Figure 45) and baseline separation could not be achieved even under isocratic conditions, attempts to better separate isomeric structures were not pursued, since MS/MS spectra alone are insufficient to designate individual structural isomers. Exact mass analysis by QTOF-MS revealed similar masses, with an average $[M+H]^+$ *m/z* of 627.2329 ± 0.0020. Agilent MassHunter software estimated the molecular formula to be $C_{27}H_{38}N_4O_{11}S$ with empirical data deviating 0.32 ppm from theoretical mass (*m/z* 627.2331).

Control incubations which sequentially eliminated NADPH, cocaine, and GSH did not generate any cocaine–GSH adduction products. Data demonstrated cocaine–glutathione adduction to be NADPH-, cocaine-, and GSH-mediated, analogous to cocaine–NAC adduction. An adduction mechanism requiring coordination of NADPH, cocaine, and GSH, in addition to exact mass data and analysis of MS/MS spectra, led to the designation of COC-GSH 1-3 as structural isomers of the compound displayed in Figure 46 (MS/MS fragmentation also justified in Figure 46).

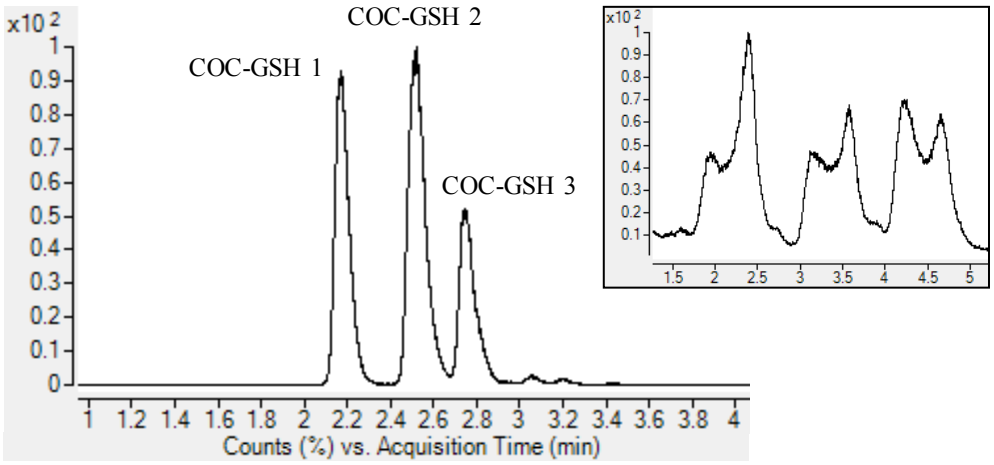


**Figure 44: Chromatographic separation of cocaine–glutathione adduction products (labeled COC-GSH 1-3; inset shows unresolved co-eluting peaks using isocratic elution)**

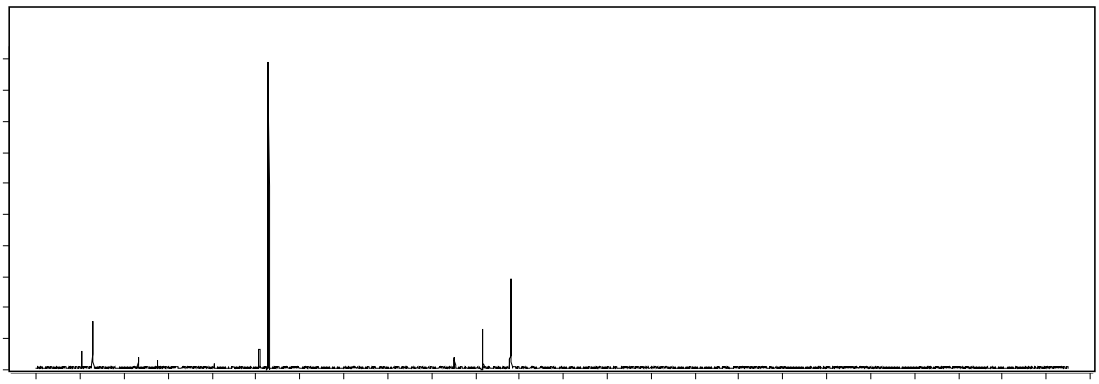

**Figure 45: MS/MS spectrum of cocaine– glutathione adduct**

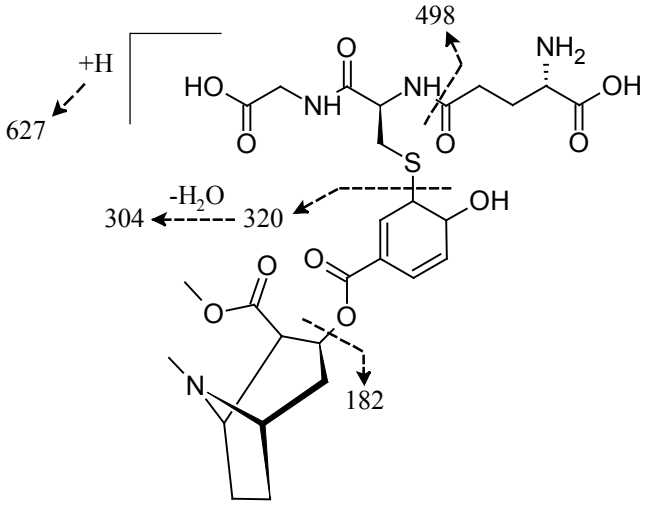


**Figure 46: Fragmentation pattern of cocaine– glutathione adduct**

4.4.1.5. **Cocaine– AcPAACAA Adduction**

Covalent adduction of cocaine to higher order biological thiols was confirmed by assessment of binding to a model hexapeptide containing a central cysteine residue (AcPAACAA; MS/MS fragmentation of native peptide included for comparison in Appendix 9b). Increasing macromolecular complexity as compared to cocaine– NAC and cocaine– GSH adduction products resulted in diminishing capacity of the chromatographic system to separate potential isomeric structures. As such, only two distinguishable products were isolated utilizing the separation conditions described in Appendix 8 (designated COC-PEP 1 and 2, Figure 47). Exact mass analysis of products revealed an empirical average $[M+H]^+$ ion of 864.3776

± 0.0007 Da, deviating from the theoretical $[M+H]^+$ of 864.3808 Da ($C_{39}H_{57}N_7O_{13}S$) by 3.70 ppm. As before, COC-PEP 1 and 2 produced qualitatively similar MS/MS spectra, displaying characteristic peptide fragmentation patterns in conjunction with ions consistent with the primary fragmentation of hydroxycocaine (Figure 48). Indeed, MS/MS fragmentation patterns support analogous adduction mechanisms for covalent binding of cocaine to higher order biological thiols as were observed for NAC and GSH assays (Figure 49).

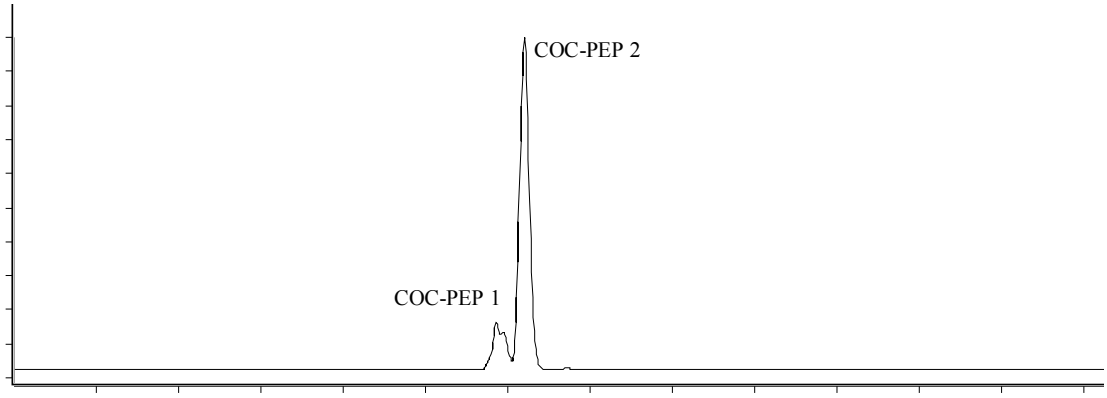


**Figure 47: Chromatographic separation of cocaine– AcPAACAA adduction products (labeled COC-PEP 1-2)**

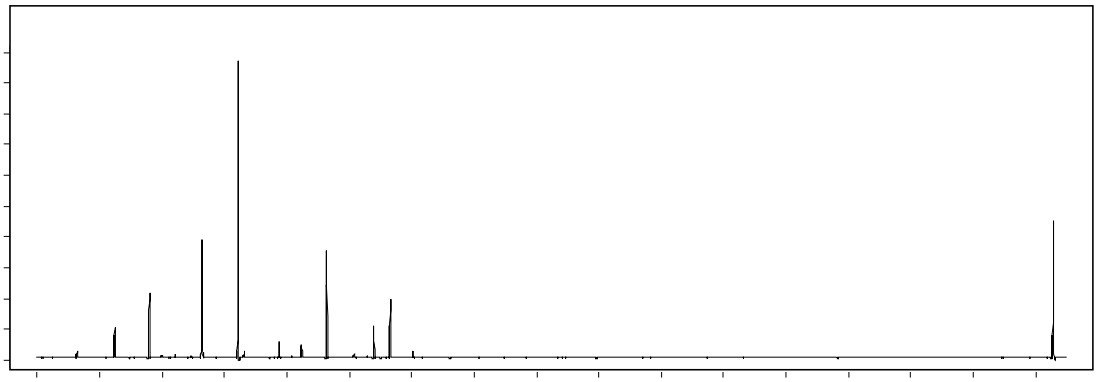

**Figure 48: MS/MS spectrum of cocaine– AcPAACAA adduct**

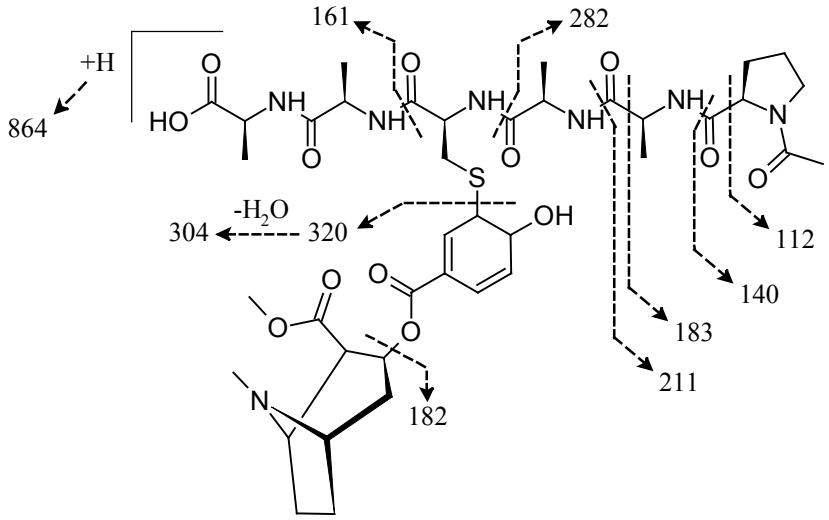


**Figure 49: Fragmentation pattern of cocaine– AcPAACAA adduct**

4.4.1.6. **Discussion of Cocaine Thiol Adduction Results**

Data collected from *in vitro* assay incubations of cocaine in the presence of thiol-containing trapping agents (*i.e.*, NAC, GSH, and AcPAACAA) in conjunction with MS/MS-based structural investigations suggest a novel metabolic pathway in the metabolism of cocaine that is of particular interest to analytical and forensic toxicologists and pathologists. While investigations were performed to examine the interaction of cocaine metabolites with other know nucleophilic amino acids in addition to cysteine (*i.e.*, histidine and lysine), no evidence was found in the current study to suggest binding of cocaine biotransformation products to biological nucleophiles other than sulfhydryls. Chromatographic and mass spectrometric investigations of products arising from cocaine interaction with biological thiols revealed the production of numerous stereospecific analytes. Each sulfhydryl-containing trapping agent generated more than one chromatographically distinct product that maintained high MS/MS qualitative similarity among each trapping agent product group. As such, it was determined by means of exact mass analysis and MS/MS fragmentation patterns that the resulting products represented structural isomers. Step-wise assay modification determined the adduction products to be NADPH-dependent, suggesting monooxygenase (*e.g.*, CYP and/or FMO superfamilies) contributions to the metabolic activation and subsequent adduction mechanism. Indeed, rhCYP assay incubations conclusively demonstrated the influence of CYPs 1A2,

2C19, and 2D6 in the production of the observed adduction products arising from cocaine biotransformation. FMOs can often accomplish oxidative events analogous to CYP biotransformation; as such, designation of CYP influences on adduct production does not preclude the contribution of the FMO superfamily within the hepatocellular microenvironment.

The proposed formation of irreversibly bound oxidation products from cocaine biotransformation is not a novel toxicological finding per se, with previous research groups having documented their existence (see summary in Figure 11). However, data collected from the current study are not consistent with any proposed mechanism of covalent cocaine adduction that exists in the literature. In contrast, rigorous exact mass MS and MS/MS investigations coupled with CYP isoform designation yielded evidence for a novel metabolic pathway and covalent attachment mechanism. The data support oxidative bioactivation of cocaine to an aryl epoxide reactive electrophilic intermediate, followed by nucleophilic thiol-induced ring opening resulting in the formation of a monohydroxylated thiol-adducted product. The observed MS/MS product ions *m/z* 121 and 182 of NAC-bound cocaine metabolites are indicative of hydroxylation on the arene ring and an intact methyl ester tropane, respectively. Because of the observed product ions, oxidative activation of the tropane nitrogen was discounted as a potential mechanism of adduct formation. Indeed, oxidation of the cocaine aryl group purports the existence of a reactive intermediate (*i.e.*, an aryl epoxide) directly resulting in nucleophile binding at the site of oxidation.

Investigation of adduction products arising from nitrogen oxidation as well as methyl ester activation as reported in the literature[23,95-99] were performed in the current study; however, the *in vitro* systems utilized were unable to confirm these previously proposed mechanisms. Other research has employed immunogenic detection using antibodies raised against tropane nitrogen haptenized cocaine as evidentiary support for adduct formation via tropane nitrogen oxidation.[95,96] Myriad factors may have contributed to the lack of detected products arising from this route of biotransformation in the present study, including electrophilic interaction with nucleophilic sites on proteins other than those examined, differences in ionization states of nucleophilic residues *in vivo* vs. *in vitro* (*e.g.*, impact of the immediate microenvironment on ionization state), low stoichiometric binding leading to product concentration below

method detection limits, adduction product structure with a molecular ion outside the menu utilized within this study (see Table 9), or the combined effects of more than one of these factors.

Likewise, studies by Deng *et al*. utilized MS and nuclear magnetic resonance (NMR) analysis to designate the structure of an adduction product putatively arising from the interaction of a self-acid-catalyzed electrophilic ester with nucleophilic lysine residues.[98] Since autoradiography and Western blot immunodetection were the primary methods utilized, it is possible that the present approach was unable to detect the expected product due to analyte abundance below the method detection limit. While attempts were made to boost the yield of lysine adduction products by increasing the incubation pH to increase the percent of NAK in the reactive neutral state, modification of pH above the $pK_a$ of cocaine's tropane nitrogen ($pK_a$ of 8.6) would significantly decrease the proportion of cocaine molecules with the protonated ammonium tropane. Since the ammonium tropane is necessary for self-acid-catalyzed ester activation, increasing media pH would still be detrimental to the adduction process even if it resulted in the increased concentration of neutral reactive lysine residues. However, lysine residues *in vivo* with depressed $pK_a$ values are not uncommon, which suggests that this mechanism could be more relevant to *in vivo* cocaine metabolism than is suggested by the *in vitro* results of the present study.

The novel pathway for cocaine adduction to biological thiols described in this study has significant implications for cocaine-associated toxicity and the sequelae associated with cocaine biotransformation. Numerous toxicity studies investigating cocaine biotransformation have catalogued the depletion of hepatocellular GSH, with the mechanism responsible for this event purported to involve oxidative stress.[23,94] While generation of reactive oxygen species during the CYP-catalyzed metabolism of cocaine is likely and expected as a result of "leaky" oxidative pathways (see Figure 2), data from the current study suggests that specific targeting of GSH thiols by reactive cocaine intermediates is also a possible compounding mechanism behind *in vivo* GSH depletion. Additionally, covalent binding to reactive thiols present within the structure of endogenous proteins may be detrimental to protein activity or cause complete protein deactivation, especially when the adducted thiol is imperative to protein function. Indeed, macromolecular binding and GSH depletion may be causal factors in the observed hepatocellular necrosis in chronic cocaine abusers.[23,146]

### 4.4.2. **Morphine Adduction Products**

#### 4.4.2.1. **Morphine– *N*-Acetylcysteine Adduction**

UHPLC chromatographic separation and MS analysis demonstrated the presence of seven distinguishable analytes resultant from NAC interaction with morphine (designated MOR-NAC 1-7, Figure 50). The products MOR-NAC 1-4 had parent $[M+H]^+$ ions with *m/z* 447 and were determined to have the chemical formula$C_{22}H_{26}N_2O_6S$ by Agilent MassHunter software based on exact mass data from QTOF-MS (see Table 17). MS/MS fragmentation of MOR-NAC 1-4 parent ions (*m/z* 447) yielded two distinct subsets of fragments, with Figure 51a depicting a representative spectrum for MOR-NAC 1 and 3 and Figure 51b showing a representative spectrum for MOR-NAC 2 and 4. Three minor products were determined to have nominal masses of 448 Da and molecular formulas approximated as $C_{22}H_{28}N_2O_6S$ in the same manner as above (see Table 17). The three minor products (MOR-NAC 5-7) were found to have extremely similar MS/MS fragmentation patterns. A representative MS/MS spectrum obtained from parent ion (*m/z* 449) fragmentation of MOR-NAC 5-7 is presented in Figure 51c. It is noteworthy that, qualitatively, the representative spectrum for MOR-NAC 5-7 closely resembles that of MOR-NAC 2 and 4 with a mass shift of *m/z* +2 for most fragments. Spectral similarity suggests that compounds MOR-NAC 5-7 are structurally related to MOR-NAC 2 and 4 by the addition of 2H (accounting for the shift of parent ion $[M+H]^+$ from *m/z* 447 to 449 and mass shifts of *m/z* +2 for many prominent daughter ions of *m/z* 449 compared to *m/z* 447).

Control incubations without NADPH, morphine, and/or NAC provided further insight into possible mechanisms of product formation. All adduction products (MOR-NAC 1-7) were found to be dependent upon the presence of both morphine and NAC. However, only MOR-NAC 1 and 3 were found to be NADPH-dependent. MOR-NAC 2, 4, 5, 6, and 7 were generated in the absence of NADPH, suggesting reaction mechanisms not involving the CYP and FMO enzyme superfamilies.

Previous studies involving morphine's covalent adduction to biological sulfhydryls using NMR spectrometry have described two distinct products, one involving thiol attachment at C-10 of morphine[88,90] and the other at C-8[80,82,83] (represented by Figure 52a and b, respectively; see Section 2.6). Correia *et al*. determined that adduction at the C-10 position was CYP-mediated in rats, requiring NADPH as a cofactor

to elicit metabolic activation of morphine, although no specific mechanistic explanation was proposed.[88] Indeed, NADPH-mediated adduction of morphine with the model thiol, NAC, was catalogued in the present study for MOR-NAC 1 and 3, suggesting that these derivatives are the result of structural isomer formation by thiol addition at the C-10 position on morphine, resulting in the stereo isomers 10α- and 10β-*S*-(*N*-acetylcysteinyl)morphine. More complete NMR- or chiral-based analysis methods are required to definitively assign MOR-NAC 1 and 3 as 10α- and 10β-*S*-(*N*-acetylcysteinyl)morphine; however, the mechanisms of formation and MS/MS fragmentation patterns are consistent with these putative designations. It is noteworthy that isomeric structures were not identified in the studies performed by Correia *et al*. (*i.e.*, only the 10α- species was confirmed via NMR). The putative appearance of the 10β-isomeric structure in the current study may be the result of differences in species-specific regioselective thiol addition or variance in quantitative or qualitative adduct formation between *in vitro* and *in vivo* environments, or may be a product of technological advances in chromatographic separations allowing for higher resolution than was available at the time the earlier experiments were performed.

Extensive characterization of thiol adduction products at C-8 of morphine was performed to determine adduct structure and mechanism of formation. Reduction of the C-6 hydroxyl moiety yields morphinone, a Phase I metabolic product of morphine containing a Type-2 alkene in the form of an α,β-unsaturated carbonyl. This reduction event is catalyzed by the enzyme morphine-6-dehydrogenase and is not mediated by the CYP or FMO enzyme superfamilies (making the event atypical in the realm of Phase I xenobiotic biotransformation).[82,83] In place of NADPH, morphine-6-dehydrogenase utilizes $NAD(P)^+$ as an activating cofactor (with bias toward $NAD^+$ activation over $NADP^+$ in many species, including humans).[82] Research has also demonstrated the formation of morphinone from interaction with hydroxyl radicals.[84] In the current study, formation of MOR-NAC 2 and 4 is in good agreement with the structure and mechanisms described in previous studies for products resulting from morphinone adduction to thiols at C-8, being readily produced even in the absence of NADPH.

Published literature has postulated morphinone-derived adduct reduction to re-hydrogenate the C-6 keto group via biological reducing agents (*e.g.*, NADPH, GSH); however, no literature exists in which reduced products were isolated or characterized. Formation of MOR-NAC 5-7 within *in vitro* incubations

is consistent with reduction of morphinone-derived thiol adducts (see Figure 52c for reduction product structure and fragmentation). Concordance of MOR-NAC 5-7 with the hypothesized C-6 keto reduction products was confirmed by their production in the absence of NADPH and by qualitative MS/MS spectral similarity with MOR-NAC 2 and 4 fragmentations (see Figure 51b and 51c). Such reduction could be elicited by NAD(P)H generated by morphine-6-dehydrogenase during conversion of morphine to morphinone, but more likely results from reducing activity of free thiols (*i.e.*, NAC) within the samples. Theoretically, reduction could yield two stereo isomers from each morphinone-based adduct (yielding a total of four isomeric products). Detection of three distinct products (instead of the predicted four) may be the result of insufficient chromatographic separation causing coelution, stereo-selectivity in hydrogenation products, or a specific biochemical process diminishing the production of a specific adduction product isomer.

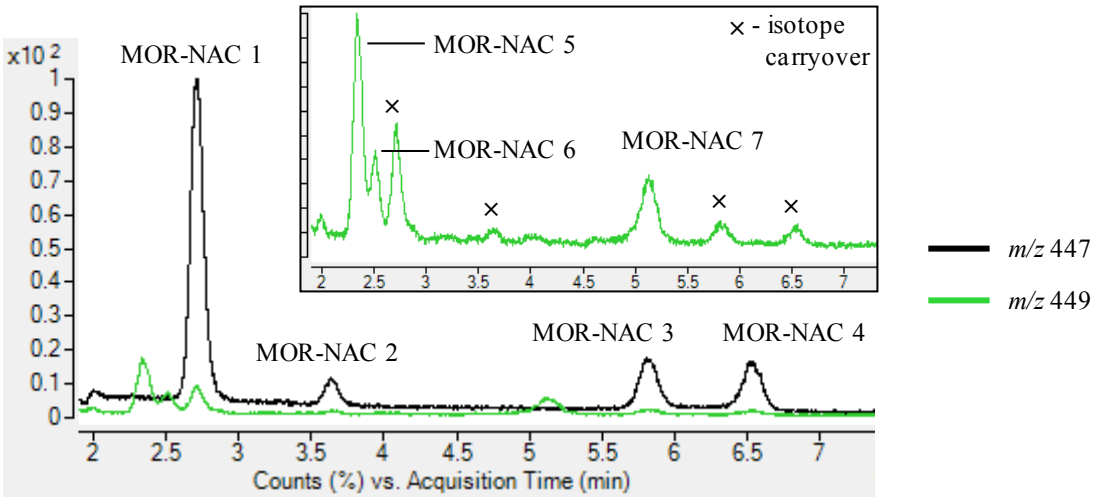


**Figure 50: Chromatographic separation of morphine− *N*-acetylcysteine adducts from *in vitro* incubation sample (labeled MOR-NAC 1-7; inset shows expansion of *m/z* 449 chromatograph)**

**Table 17: Comparison of theoretical and observed $[M+H]^+$ ions for morphine−*N*-acetylcysteine adducts**

| Adduction Product | Retention Time (min) | Theoretical Mass (m/z) | Observed Mass (m/z) | Difference (ppm) |
|---|---|---|---|---|
| **MOR-NAC 1** | 2.66 | 447.1584 | 447.1589 | 1.12 |
| **MOR-NAC 2** | 3.56 | 447.1584 | 447.1587 | 0.67 |
| **MOR-NAC 3** | 5.70 | 447.1584 | 447.1590 | 1.34 |
| **MOR-NAC 4** | 6.41 | 447.1584 | 447.1588 | 0.89 |
| **1-4 Average** | - | 447.1584 | 447.1589 ± 0.0001 | 1.12 |
| **MOR-NAC 5** | 2.32 | 449.1741 | 449.1744 | 0.67 |
| **MOR-NAC 6** | 2.48 | 449.1741 | 449.1743 | 0.45 |
| **MOR-NAC 7** | 5.10 | 449.1741 | 449.1739 | 0.45 |
| **5-7 Average** | - | 449.1741 | 449.1742 ± 0.0003 | 0.22 |

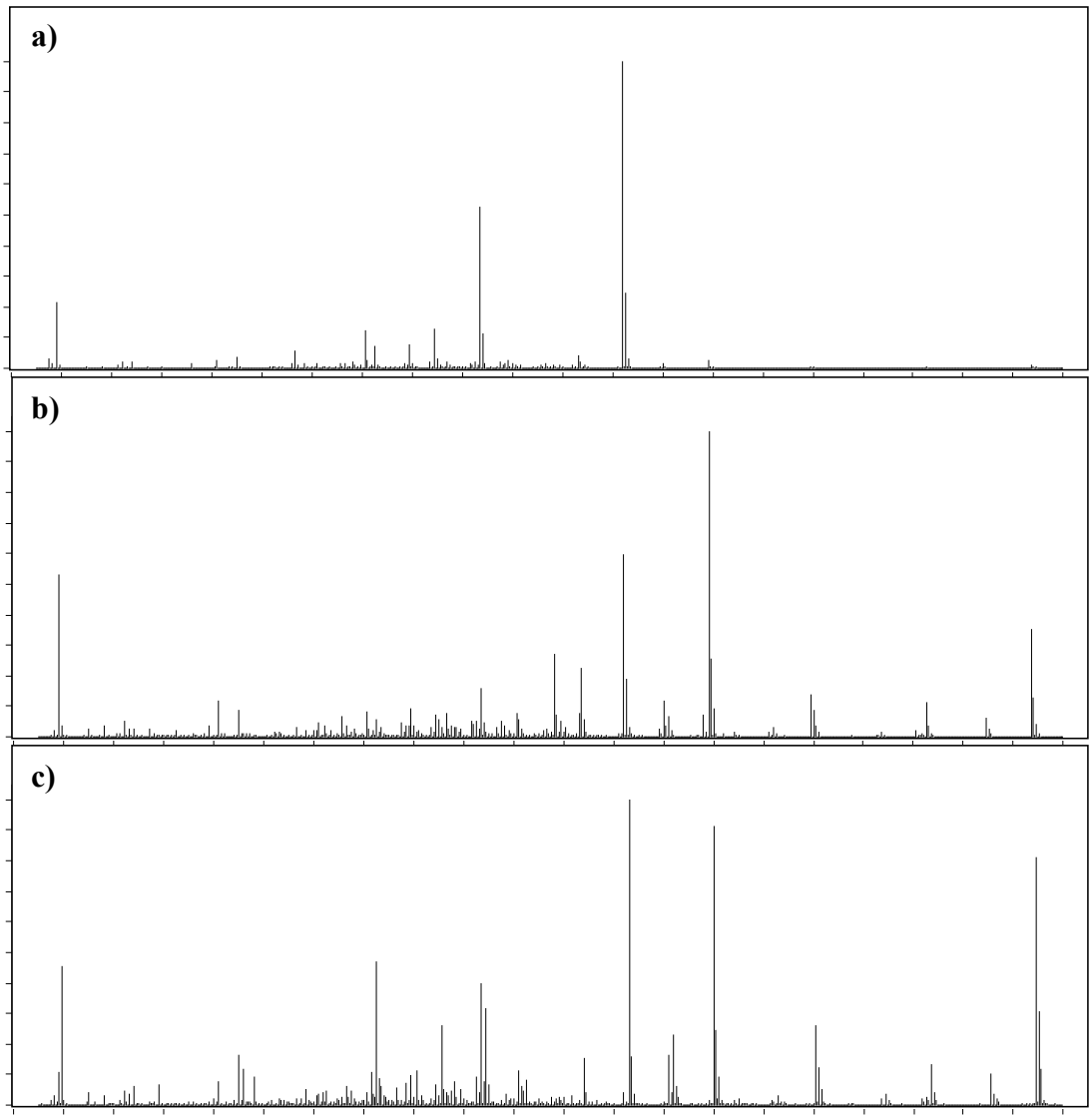


**Figure 51: MS/MS spectra of morphine– *N*-acetylcysteine adducts (a) MOR-NAC 1 and 3, (b) MOR-NAC 2 and 4, and (c) MOR-NAC 5-7**

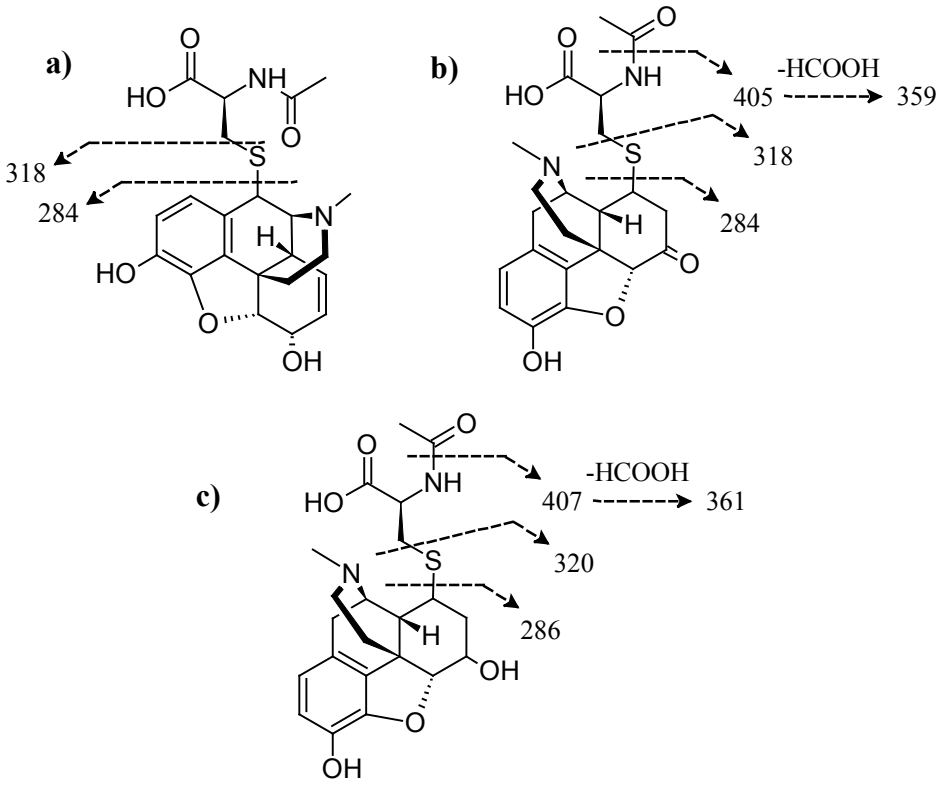


**Figure 52: Fragmentation patterns of morphine–*N*-acetylcysteine adducts (a) MOR-NAC 1 and 3, (b) MOR-NAC 2 and 4, and (c) MOR-NAC 5-7**

Morphine-derived adduct production was found to be variably dependent on incubation time. Figure 53 displays data with MOR-NAC 1 and 4 acting as representative models for NADPH-mediated and non-NADPH-mediated adduction products, respectively. Figure 54 shows data with MOR-NAC 5 as a representative model for all non-NADPH-mediated secondary reduction products. Maximum levels of all morphine-based NAC adduction products were found to be present under conditions of secondary supplementation with NADPH and 6 h incubation time. This effect was particularly apparent for the secondary reduction products MOR-NAC 5-7 (see Figure 54), where it is likely that supplemental NADPH acts as a reducing agent for oxidation products produced during the first 3 h of incubation.

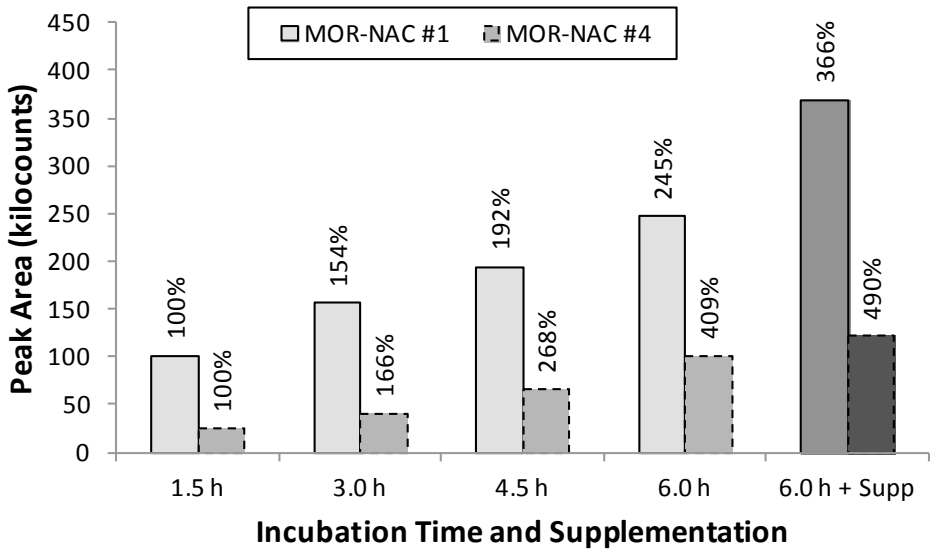


**Figure 53: MOR-NAC 1 and 4 formation as a factor of incubation time and NADPH supplementation**

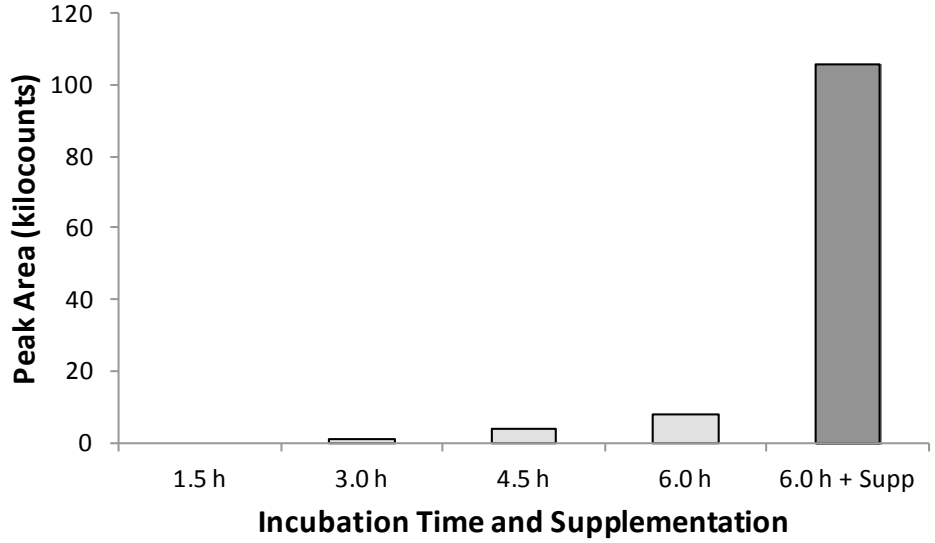


**Figure 54: MOR-NAC 5 formation as a factor of incubation time and NADPH supplementation**

#### 4.4.2.2. **Morphine– *N*-Acetylcysteine Adduct Cytochrome P450 Enzyme Designation**

As a result of data demonstrating the NADPH-independent formation of MOR-NAC 2 and 4-7, investigation of CYP isoform influences on adduct formation was performed solely for MOR-NAC 1 and 3. Qualitative and quantitative profiles of individual isoform contribution to MOR-NAC 1 and 3 formation were similar, further supporting the common mechanism of formation purported in Section 4.4.2.1 (Figure

55). Raw data demonstrated very minor contributions from the CYP2C subfamily (*i.e.*, 2C8, 2C9, 2C19), with CYPs 2D6 and 3A4 being the major isoforms responsible for NADPH-mediated morphine adduction to thiols. After correction for relative enzyme concentrations in human liver, it is evident that CYP3A4 is almost entirely responsible for the CYP-mediated formation of morphine– NAC adduction products (although this does not necessarily preclude FMO contributions to this metabolic cascade).

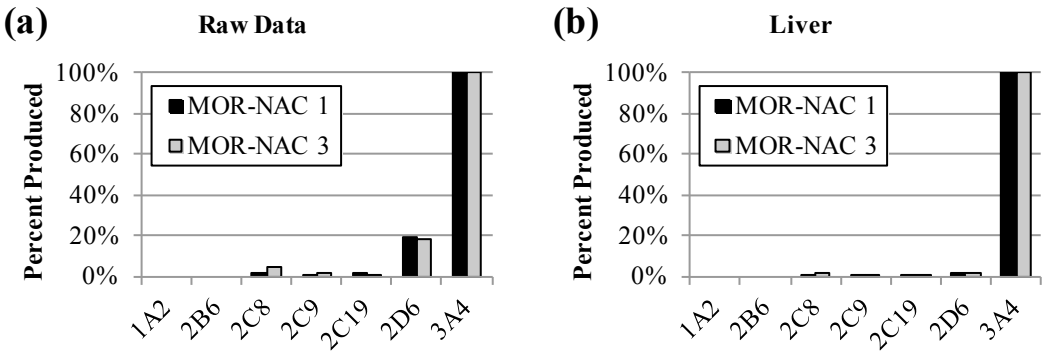


**Figure 55: Cytochrome P450 isoform panel for morphine– *N*-acetylcysteine adduct formation (a) presents raw data for morphine– *N*-acetylcysteine adducts formation within the CYP isoform panel. (b) presents the same data after transformation to account for relative CYP concentrations in human liver tissue.**

#### 4.4.2.3. **Putative Mechanisms for Morphine-derived Thiol Adduction**

In combination with existing structural and mechanistic data from literature, data from this study suggests two distinct mechanisms of protein adduct formation arising from Phase I morphine biotransformation (Figure 56). The first mechanism is consistent with dehydrogenation of the C-6 hydroxyl group by means of enzymatic oxidation by morphine-6-dehydrogenase or hydroxyl radicals to yield the known reactive metabolite, morphinone (Pathway (a), Figure 56). Subsequent biomolecular adduction of morphinone involves nucleophilic attack of the electrophilic C-8 site by a thiol resulting in 1,4 Michael addition. Tautomerism of the resultant enol to the stable keto form leads to observation of a 3,4 addition product (keto structure confirmed by previous NMR studies[85]). Secondary reduction of the C-6 keto group of adducted morphinone subsequently yields a series of enantiomeric compounds.

The second mechanism of morphine metabolism and adduction is consistent with the enzymatic oxidation of the C-3 hydroxyl moiety via FMO- or CYP-catalyzed biotransformation (Pathway (b), Figure

56). rhCYP investigation confirmed the almost exclusive influence of CYP3A4 in facilitating this pathway, but does not preclude the potential role of FMOs in the complete enzymology for this reaction. Redistribution of aromatic electrons within the conjugated ring structure of the oxidized product generates a quinone methide, a Type 2 alkene structure known to possess reactive electrophilic properties.[147] Nucleophilic attack by biological thiols on the electron-depleted C-10 site, followed by electron rearrangement along the conjugated quinone methide structure causes reduction of the C-3 oxygen (via 1,6 Michael addition).

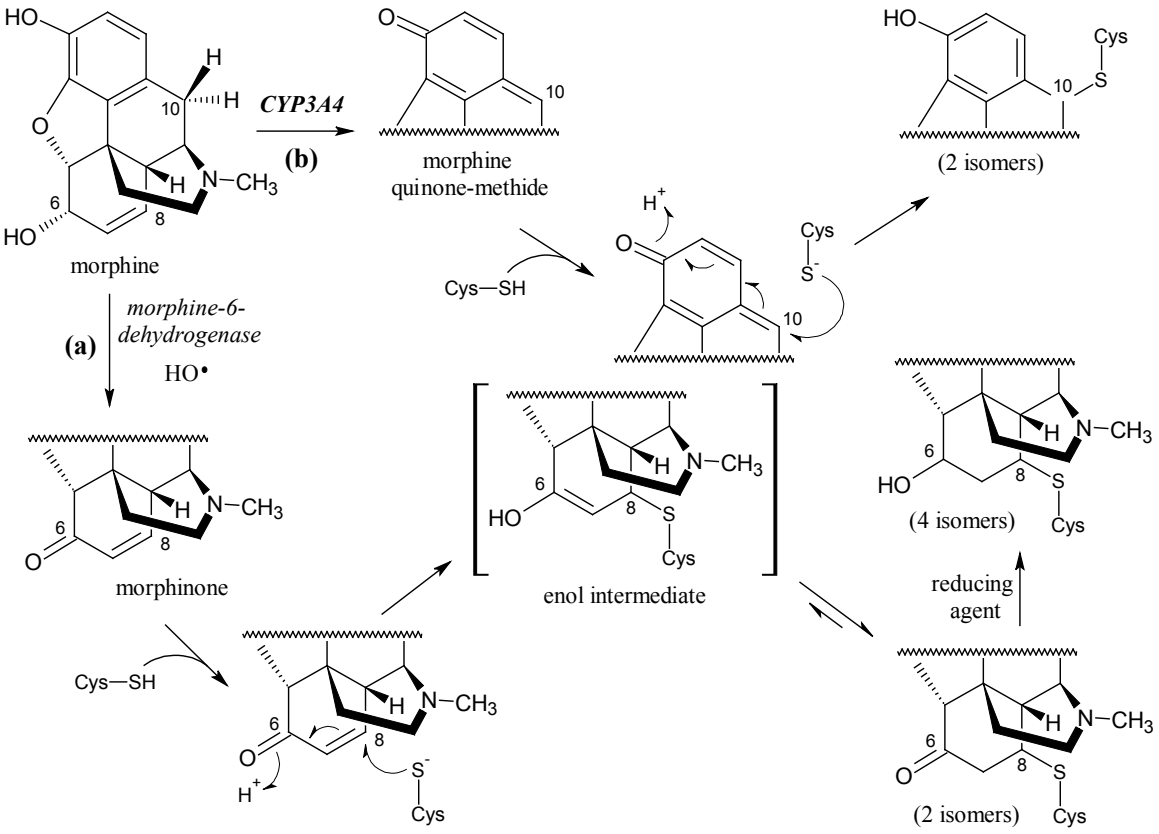


**Figure 56: Proposed mechanisms for morphine metabolism to reactive metabolites and thiol adduction**

#### 4.4.2.4. **Morphine– Glutathione Adduction**

Incubation of morphine with GSH resulted in the appearance of four adduction products (designated MOR-GSH 1-4, Figure 57; MS/MS fragmentation of native peptide included for comparison in

Appendix 9a). Exact mass QTOF-MS analysis of each adduction product revealed *m/z* consistent with the chemical formula $C_{27}H_{34}N_4O_9S$ (Table 18). MS/MS analysis of each analyte revealed two sets of products with qualitatively similar spectra: MOR-GSH 1 and 2 yielded spectra represented by Figure 58a, while Figure 58b is a representative spectrum of MOR-GSH 3 and 4 fragmentations.

Control incubations in which NADPH, morphine, and GSH were sequentially removed from assays revealed that all products were reliant on the presence of morphine and GSH while only MOR-GSH 1 and 2 required the presence of NADPH (*i.e.*, formation of MOR-GSH 3 and 4 is not NADPH-dependent). In consideration of the putative mechanisms determined by morphine incubations with NAC, it is postulated that MOR-GSH 1 and 2 are the result of CYP-mediated activation of C-10 to form 10α- and 10β- isomers (Figure 59a). Likewise, NADPH-independent formation of MOR-GSH 3 and 4 is consistent with morphine-6-dehydrogenase-mediated production of 8α- and 8β- adduction product isomer formation via the reactive metabolite, morphinone (Figure 59b). In contrast to assays containing NAC, no secondary reduction products were detected in samples containing GSH. Inability to detect such secondary reduction products may be the result of decreased production of primary adduction products in assays containing GSH (vs. those using NAC as trapping agent) thereby decreasing reduced product levels below method detection limits. Another possible factor could be steric interference directly resulting from addition of the bulky tripeptide GSH, resulting in hindered access to the C-6 keto group for reducing agents.

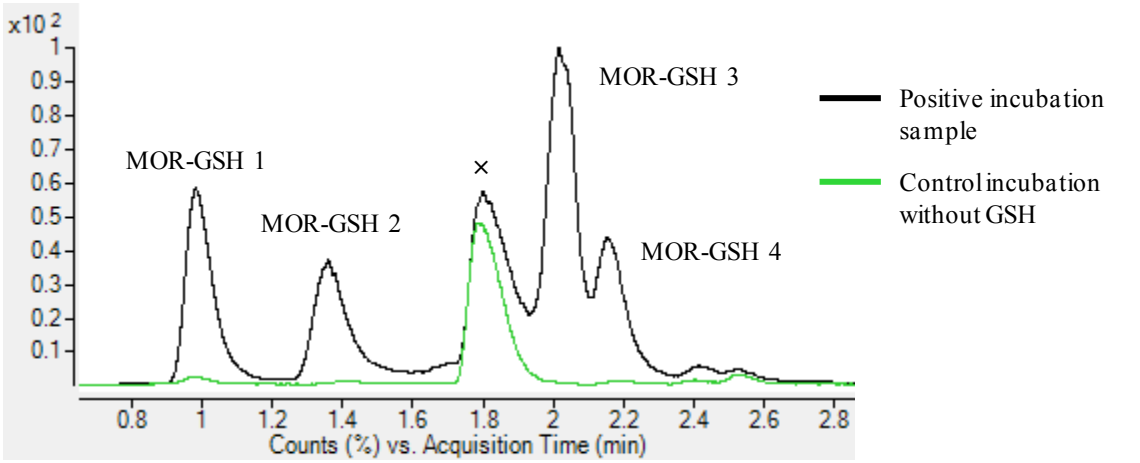


**Figure 57: Chromatographic separation of morphine− glutathione adducts (labeled MOR-GSH 1-4)**

**Table 18: Comparison of theoretical and observed $[M+H]^+$ ions for morphine–glutathione adducts**

| Adduction Product | Retention Time (min) | Theoretical Mass (m/z) | Observed Mass (m/z) | Difference (ppm) |
|---|---|---|---|---|
| **MOR-GSH 1** | 0.98 | 591.2119 | 591.2083 | 6.09 |
| **MOR-GSH 2** | 1.36 | 591.2119 | 591.2092 | 4.57 |
| **MOR-GSH 3** | 2.02 | 591.2119 | 591.2112 | 1.18 |
| **MOR-GSH 4** | 2.16 | 591.2119 | 591.2063 | 9.47 |
| **1-4 Average** | - | 591.2119 | 591.2088 ± 0.0020 | 5.24 |

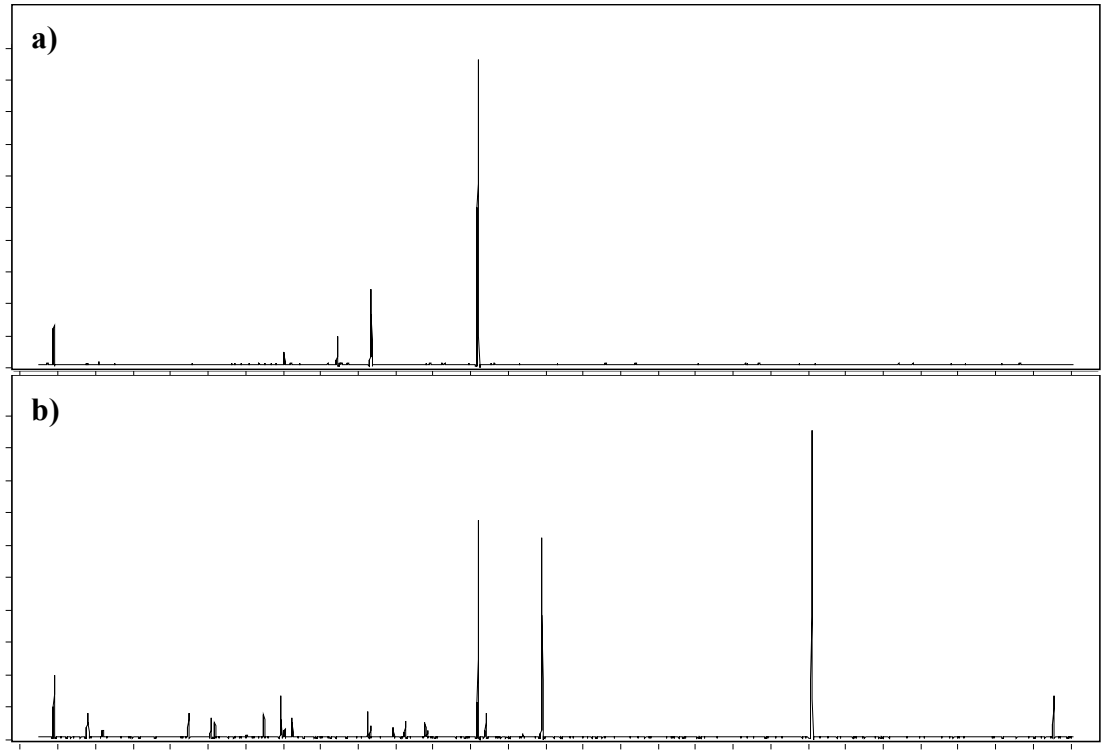


**Figure 58: MS/MS spectra of morphine– glutathione adducts (a) MOR-GSH 1 and 2 and (b) MOR-GSH 3 and 4**

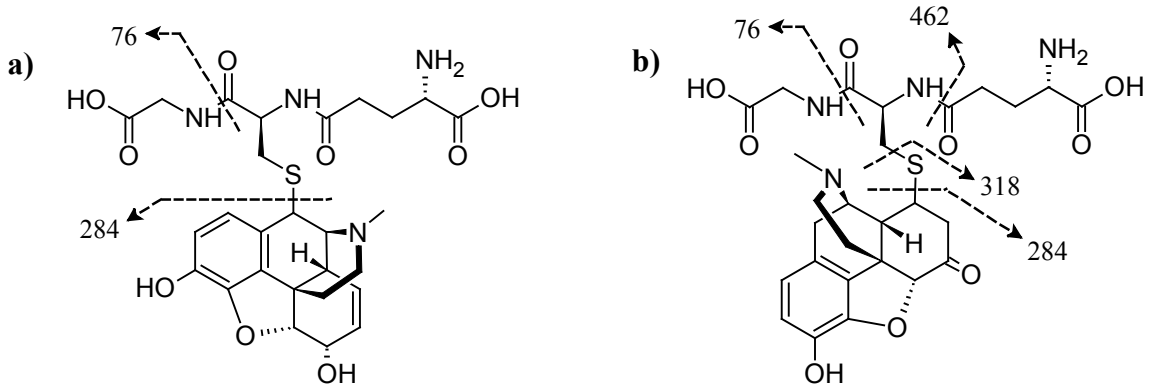


**Figure 59: Fragmentation patterns of adducts between glutathione and (a) MOR-GSH 1 and 2 and (b) MOR-GSH 3 and 4**

#### 4.4.2.5. **Morphine– AcPAACAA Adduction**

Irreversible adduction of morphine to higher order biological thiols was confirmed via assessment of binding to the model hexapeptide AcPAACAA (MS/MS fragmentation of native peptide included for comparison in Appendix 9b). As with previous studies in this project, the increase in macromolecular complexity resulted in diminished capacity of the chromatographic system to separate potential isomeric structures. In the case of morphine incubations with the AcPAACAA trapping agent, only one distinguishable product was isolated, employing the separation conditions from Appendix 8 (designated MOR-PEP 1, Figure 60). Exact mass analysis by QTOF-MS determined an empirical $[M+H]^+$ ion of *m/z* 828.3566, deviating from theoretical $[M+H]^+$ *m/z* 828.3597 ($C_{39}H_{53}N_7O_{11}S$) by 3.74 ppm. A representative MS/MS spectrum for MOR-PEP 1 is presented in Figure 61, displaying characteristic peptide fragmentation patterns in conjunction with ions consistent with the primary fragmentation of morphine. While MS/MS fragmentation patterns are not enough to distinguish between the proposed structures analogous to NAC and GSH adducts, results of collision induced dissociation of MOR-PEP 1 are consistent with either structure presented in Figure 62a and b (or possible coelution of both products).

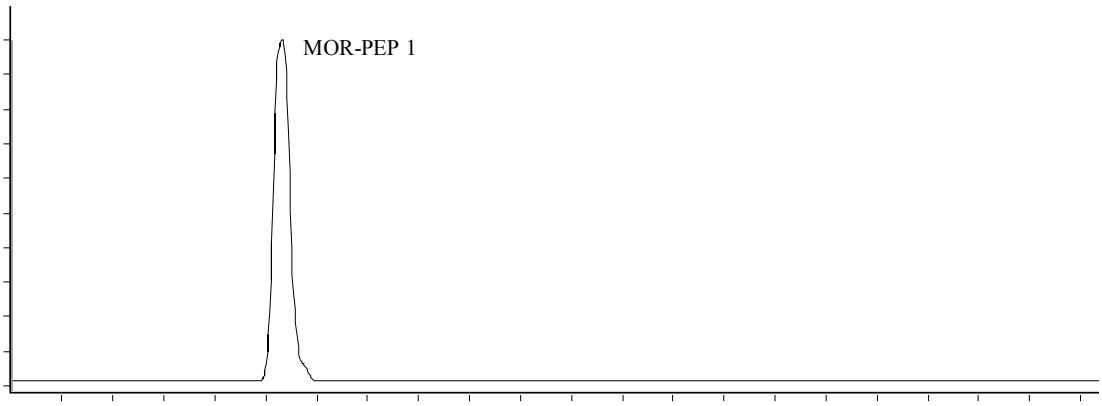


**Figure 60: Chromatographic separation of morphine– AcPAACAA adduction products (labeled MOR-PEP 1)**

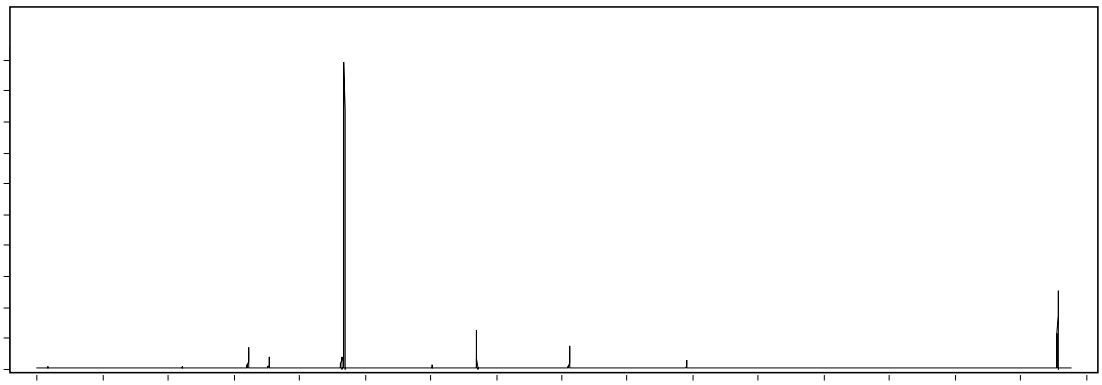

**Figure 61: MS/MS spectrum of MOR-PEP 1**

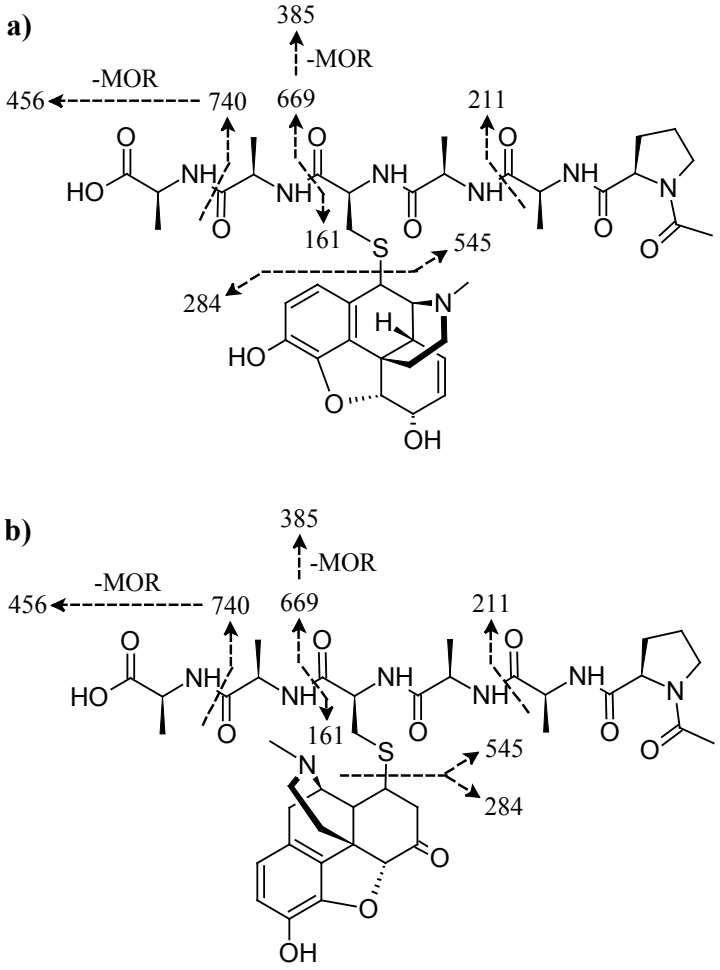


**Figure 62: Structure and MS/MS fragmentation pattern of (a) morphine quinone methide-derived adduct and (b) morphinone-derived adduct**

4.4.2.6. **Discussion of Morphine Thiol Adduction Results**

Results of the above studies from the *in vitro* trapping studies suggest a series of Phase I metabolic pathways that result in irreversible binding to biological thiol moieties. Covalent adduction products described by data in the present study are consistent with the formation of two electrophilic reactive entities resulting from the Phase I biotransformation of morphine: morphinone and morphine quinone methide. Covalent protein binding via morphinone has been documented in the literature as formation of 8α-morphinonyl thiol adducts.[85] However, results from the current study have elaborated on the mechanism of covalent attachment and the nature of resulting adduction products. Incubation of morphine with NAC

demonstrated the formation of five distinct products of morphine/NAC interaction that are not reliant on NADPH activated metabolism, consistent with morphinone production by the enzyme morphine-6-dehydrogenase. Two of these chromatographically distinguishable compounds have a molecular ion of *m/z* 447, while three have a molecular ion of *m/z* 449. The two *m/z* 447 compounds have similar MS/MS spectra, suggesting similar structures. Their mechanism of formation is consistent with the bioactivation of morphine to morphinone followed by the 1,4 Michael addition of thiol nucleophile with subsequent rearrangement of the enol to the tautomeric keto form, resulting in the formation of both the 8α- and 8β-stereo products. This accounts for the manifestation of two chromatographic peaks with identical MS/MS spectra. While previous literature only reported the formation of the 8α- isomer, chromatographic assessment of the products in those studies was performed via UV detection, which would not have allowed distinction of coeluting peaks. In contrast, improvement in chromatographic analysis and MS detection in the present study allowed for mass-to-charge filtering and consequential designation of coeluting analytes with differing molecular masses.

Existing literature does suggest the possibility of secondary reduction products resulting from hydrogenation of the C-6 keto group of morphinone; however, no specific identification of such products has been reported to date. The three detected adduction products with molecular ions of *m/z* 449 are consistent with secondary reduction of bound morphinone-derived adducts. MS/MS fragmentation patterns of each *m/z* 449 product are qualitatively similar and closely resemble the fragmentation patterns of the morphinone-derived adduction products with minor shifts in fragment masses resultant from the hydrogenation of the C-6 keto group. Theory predicts the existence of four isomeric structures resulting from the hydrogenation of the 8α- and 8β- morphinone stereo adduction products. Data from the present study conclusively demonstrated three such isomers via chromatographic methodology. The unaccounted for isomer in the present study may be the result of stereospecificity along the mechanistic pathway or may be caused by insufficient chromatographic resolving power or coelution with one of the major products of *m/z* 447 and consequential masking by carryover from the M+2 isotope peak.

In conjunction with the aforementioned products that are the result of the reactive morphine metabolite morphinone, a second pathway was examined in this study (*i.e.*, two distinct products with *m/z*

447). Consistent with the NADPH-mediated dehydrogenation of the C-3 hydroxyl group and subsequent electron shift to generate a quinone methide functional group, products of this pathway have previously been suggested, but without a purported mechanism to account for their formation. Results from the current study demonstrated the formation of two chromatographically separable products arising from NAC interaction with morphine having a molecular ion of *m/z* 447 that require the addition of monooxygenase activating cofactor NADPH. MS/MS fragmentation patterns of the two products show extreme similarity, again suggesting structural similarity. On the basis of NADPH-mediated formation, similarity in MS/MS spectra, and exact mass analysis, these two structurally similar products are proposed to be the 10α- and 10β- stereoisomers of 10-*S*-(*N*-acetylcysteinyl)morphine. The 10α- isomer has been conclusively characterized by NMR structural analysis in literature.[90] As with morphinone-derived adduction products, analysis of products arising from this mechanistic pathway were chromatographically separated and detected via UV absorbance, which may have masked additional stereoproducts beneath signals from other more abundant metabolic products of morphine.

While previous research has proposed an electrophilic reactive metabolite that is responsible for the formation of NADPH-mediated irreversible morphine adduction products, no specific pathway of activation has been proposed to date to account for such products. The purported reactivity of the hypothesized progenitor(s) of NADPH-mediated adduction products makes them difficult to identify by means of free-fraction analysis; therefore, conclusive designation of this pathway may be difficult by analytical methods. However, this study has clarified myriad aspects surrounding the formation of irreversible thiol adducts arising from monooxygenase activity on morphine. Indeed, rhCYP assay incubations conclusively determined the almost exclusive influence of CYP3A4 in the production of the NADPH-mediated adduction products cataloged in this study that arise from morphine biotransformation. While these data substantiate the role of CYP monooxygenase within this mechanism, they do not necessarily preclude the influence of FMO activity.

The two pathways of irreversible morphine adduction to biological thiols identified in this study expand the existing pool of knowledge and more completely describe the potential metabolic fate of morphine after human exposure. The data provide evidence for novel routes of toxicophore activation in

morphine and suggest that the breadth of products arising from the covalent interaction of morphine biotransformation products with biological thiols may be more diverse than postulated in existing literature. In fact, they may contribute to the discrepancy in mass balance for morphine metabolism and may be a major component of the mechanism of depletion of cellular GSH following morphine exposure.[83] Macromolecular covalent binding may also contribute to the sequelae that result in cellular damage and tissue necrosis, especially that localized to hepatic tissue, which is the primary site of reactive morphine metabolite formation.[148]

### 4.4.3. **Use of Adducts as Cocaine and Morphine Biomarkers**

In conjunction with providing insights into drug-induced toxicities, detection methods for GSH and NAC adduction products can serve as viable alternatives to direct testing of biological matrices for parent drug and metabolites. GSH conjugates are commonly excreted in bile, but there is precedence for the extraction and detection of GSH conjugates from the blood.[149,150] Perhaps more relevant to non-invasive analysis for drug of abuse exposure are NAC conjugates (also called mercapturates). Being the post-conjugation processed product of Phase III metabolic activity on GSH conjugates, mercapturates are preferentially excreted in the urine, an ideal matrix for minimally invasive confirmation of xenobiotic exposure.[15,16]

The data collected and methods developed within the present body of research form the foundation of an analytical scheme to detect both GSH conjugates and mercapurates arising from cocaine and morphine exposure. Complete MS/MS characterization of each product allows for sensitive MRM detection to be employed for the evaluation of such adducts. Furthermore, chromatographic methods established in this work may be translated to other laboratories with commercial LC-MS/MS instrumentation, making the validation of GSH- and NAC-bound drug metabolites feasible for forensic and medical investigations.

While less conventional among drug of abuse detection methods, the examination of protein adduction products may be an attractive future tract for forensic toxicological analysis. Analytical methods to detect and identify bound adducts commonly rely on enzymatic digestion and chromatographic

designation of a peptide fragment from the original protein containing an adducted moiety.[151] While protein extraction, digestion, and analytical designation of adducted thiol-containing peptides can be time-consuming, the potential to extend the window of detection for cocaine and morphine from days (the current timeline for parent drug and metabolites in the free fraction) to weeks/months (depending on the *in vivo* life-time of the protein target) is an attractive proposal for toxicologists. Such adducts may therefore be useful as longer-term and/or retrospective exposure biomarkers for these important drugs of abuse. Similarly, identification of individual protein targets and specific sites of covalent adduction by cocaine or morphine via the mechanisms described above would be useful in further illuminating the comprehensive metabolism of cocaine and morphine as well as the milieu of toxic responses attributed to each drug in the human body.

Data from the current study suggests that detection methods utilizing macromolecular biomarkers are technically feasible for both cocaine and morphine adducts. The studies presented herein describe adduction mechanisms, nucleophilic targets on proteins, and MS/MS-characterized identities of adducted moieties for cocaine- and morphine-derived adducts. In conjunction with existing proteomic technologies and peptide mapping techniques, the above results are translatable into an analytical scheme useful in characterizing the cocaine and morphine "adductome"[152] in the human body.

## 4.5. *In Silico* Estimations of Chemical Reactivity and Adduction Potential

### 4.5.1. Nucleophilicity of Reactive Amino Acids

Calculation of molecular HOMO and LUMO energies by means of DFT calculations revealed significant differences in the nucleophilic reaction potential of model nucleophiles that are directly mediated by pH/$pK_a$-dependent ionization states, a property well-documented with *in vivo* biological nucleophile research. Table 19 contains HOMO and LUMO energies determined using DFT calculations and molecular properties calculated from HOMO and LUMO energies including chemical potential ($\mu$), hardness ($\eta$), softness ($\sigma$), electrophilicity index ($\omega$), and nucleophilicity index ($\varphi$). The calculated properties are concordant with *in vitro* data generated in the present study, demonstrating increased nucleophilicity index when Cys is in the ionized thiolate form and when His and Lys are in their

deprotonated (un-charged) states. Cys-containing nucleophiles demonstrated increased chemical potential and decreased chemical hardness in their thiolate forms compared to the uncharged state. Basic His and Lys nucleophiles also showed increased chemical potential when deprotonated, but both basic residues exhibited increases in chemical hardness when un-charged. In general, nucleophiles containing thiolate Cys moieties were the softest among those examined, with glutathione in the thiolate form (GSH (-1)) being the softest nucleophile, exemplifying the axiomatic designation of Cys thiols as the softest biological nucleophiles. Concurrently, the highest calculated nucleophilicity index was GSH (-1), supporting GSH's role as a nucleophilic reservoir for reactive electrophilic species within intra- and inter-cellular media.

**Table 19: Quantum mechanical parameters for biological nucleophiles**

| Nucleophile | $E_{LUMO}$ (eV) | $E_{HOMO}$ (eV) | μ (eV) | η (eV) | σ ($eV^{-1}$) | ω (eV) | φ ($eV^{-1}$) |
|---|---|---|---|---|---|---|---|
| **Cys (0)**[a] | -0.03 | -6.86 | -3.44 | 3.42 | 0.293 | 1.74 | 0.576 |
| **Cys (-1)** | 4.05 | 0.21 | 2.13 | 1.92 | 0.521 | 1.18 | 0.845 |
| **His (+1)** | -4.88 | -10.31 | -7.60 | 2.71 | 0.368 | 10.64 | 0.094 |
| **His (0)** | -0.28 | -6.08 | -3.18 | 2.90 | 0.345 | 1.75 | 0.572 |
| **Lys (+1)** | -4.58 | -8.98 | -6.78 | 2.20 | 0.455 | 10.45 | 0.096 |
| **Lys (0)** | 0.10 | -6.26 | -3.08 | 3.18 | 0.314 | 1.49 | 0.670 |
| **NAC (0)** | -0.10 | -6.70 | -3.40 | 3.30 | 0.303 | 1.75 | 0.570 |
| **NAC (-1)** | 3.79 | -0.13 | 1.83 | 1.96 | 0.510 | 0.85 | 1.170 |
| **NAH (+1)** | -5.07 | -9.96 | -7.52 | 2.44 | 0.409 | 11.56 | 0.087 |
| **NAH (0)** | -0.33 | -6.24 | -3.28 | 2.96 | 0.338 | 1.82 | 0.549 |
| **NAK (+1)** | -4.54 | -8.88 | -6.71 | 2.17 | 0.460 | 10.37 | 0.096 |
| **NAK (0)** | 0.20 | -6.34 | -3.07 | 3.27 | 0.306 | 1.44 | 0.694 |
| **GSH (0)** | -0.80 | -6.60 | -3.70 | 2.90 | 0.345 | 2.36 | 0.424 |
| **GSH (-1)** | 1.54 | -0.06 | 0.74 | 0.80 | 1.250 | 0.34 | 2.925 |

[a] Ionization state of molecule is presented in parentheses

### 4.5.2. **Electrophilicity of Reactive Drug Intermediates and Metabolites**

To thoroughly examine the mechanisms of formation for each adduction product detected in this research, reactivity parameters of postulated electrophilic species were determined. Calculated descriptors for mechanisms of cocaine adduct formation included those for the parent compound (cocaine), the hypothesized reactive intermediate (cocaine-3,4-epoxide), and the resultant stable metabolites in humans

(3- and 4-hydroxycocaine) (see Table 20). While variations in chemical potential and chemical hardness were minimal between parent, reactive intermediate, and stable metabolic products, the higher order parameter describing electrophilicity showed an increase in molecular electrophilicity for the reactive epoxide over the stable parent and metabolites. Stereoisomeric forms of cocaine-3,4-epoxide were found to have HOMO and LUMO energies that were quantitatively identical, demonstrating that stereochemistry of the epoxide does not modify electrophilicity. Comparisons of HOMO and LUMO energies between 2-, 3-, and 4-hydroxycocaine metabolites revealed modest differences in thermodynamic and kinetic stability between isomeric products. Large HOMO-LUMO energy gaps (exemplified by larger $\eta$ values) are characteristic of hard electrophiles, which exhibit thermodynamic stability. Similarly, high-lying LUMO shells coupled with low-lying HOMO shells are characteristic of chemically inert species resistant to both self-reaction and kinetic reactions with Lewis acids and bases. Comparison of HOMO-LUMO gaps and relative energies between hydroxycocaine isomers suggests increased molecular stability for the 2- and 4-hydroxycocaine isomeric products in comparison to 3-hydroxycocaine. Relative thermodynamic stability may be a contributing factor to the observed preferential formation of 4-hydroxycocaine over 3-hydroxycocaine as reported with authentic samples.[153-155]

Similar *in silico* studies were repeated for morphine-derived adducts using the parent compound (morphine), known reactive metabolite, morphinone, and postulated reactive metabolite, morphine quinone methide (see Table 20). The reactive metabolites morphinone and morphine quinone methide were found to have increased electrophilic chemical potential and decreased hardness in comparison to morphine. Calculation of the electrophilicity index demonstrated substantial increases in electrophilic potential as a function of electronic factors, with the postulated metabolite morphine quinone methide possessing the highest electrophilicity index among the electrophiles examined.

**Table 20: Quantum mechanical parameters for drug electrophiles**

| Electrophile | $E_{LUMO}$ (eV) | $E_{HOMO}$ (eV) | μ (eV) | η (eV) | σ ($eV^{-1}$) | ω (eV) |
|---|---|---|---|---|---|---|
| **COC (+1)**[a,b] | -3.86 | -9.29 | -6.57 | 2.72 | 0.368 | 7.95 |
| **2-OH-COC (+1)**[c] | -3.71 | -8.54 | -6.13 | 2.41 | 0.414 | 7.78 |
| **3-OH-COC (+1)** | -3.82 | -8.43 | -6.12 | 2.31 | 0.434 | 8.13 |
| **4-OH-COC (+1)** | -3.72 | -8.59 | -6.16 | 2.44 | 0.410 | 7.78 |
| **COC-3,4-epoxide (+1)**[d] | -4.22 | -8.85 | -6.54 | 2.23 | 0.431 | 9.21 |
| **MOR (+1)** | -3.27 | -8.36 | -5.82 | 2.55 | 0.393 | 6.65 |
| **MN (+1)** | -4.93 | -8.71 | -6.82 | 1.89 | 0.530 | 12.32 |
| **MQM (+1)** | -6.10 | -9.47 | -7.78 | 1.69 | 0.593 | 17.98 |

[a] Electrophile Abbreviations: COC, cocaine; OH-COC, hydroxycocaine; MOR, morphine; MN, morphinone; MQM, morphine quinone methide
[b] Ionization state of molecule is presented in parentheses
[c] While 2-OH-COC is not generated in human hepatocytes, data is included for comparisons of relative stability between OH-COC isomers
[d] Postulated reactive intermediates and metabolites are highlighted for distinction from precursors and stable metabolites

### 4.5.3. *In Silico* Estimation of Nucelophile-Electrophile Interactions

While *in silico* estimations of individual nucleophile and electrophile reactivity are vital to the study of adduction potential for reactive molecules, they are limited by their unilateral view of each in isolation without consideration of nucleophile-electrophile interaction, which is a major component in HSAB theory. Simulations of system reactivity were performed by inclusion of nucleophile and reactive electrophile descriptors of chemical potential and hardness according to Equation 9 in Section 2.5. The data presented in Table 21 are higher-order descriptors of electrophile– nucleophile reactivity as a function of electronic interaction between frontier molecular orbitals. The reactive metabolites cocaine-3,4-epoxide, morphinone, and morphine quinone methide are predicted to show increased reactivity with the thiolate forms of Cys and NAC as well as with unprotonated (un-charged) His, Lys, NAH, and NAK. In the case of GSH, morphinone and morphine quinone methide were determined to be more reactive with the thiolate form, while cocaine-3,4-epoxide was calculated to have higher reactivity with the uncharged thiol. Quantitative comparisons suggests that the most reactive nucleophile– electrophile pair is Cys (-1)/ morphinone. However, morphinone was not unanimously the most reactive species among morphine

metabolites. Morphine quinone methide displayed a greater predicted reaction potential for GSH (-1), the neutral basic amino acids His (0) and Lys (0), and the analogous neutral basic *N*-acetylated amino acids NAH (0) and NAK (0). The reactive cocaine metabolite cocaine-3,4-epoxide was predicted to have an increased reaction potential with the harder basic nucleophiles than either of the reactive morphine metabolites.

**Table 21: Calculated reaction indices ($\omega^-$) for electrophile reactions with possible nucleophilic targets**

| Nucleophile | $\omega^-$ (eV) | | |
|---|---|---|---|
| | COC-3,4-epoxide (+1)[a,b] | MN (+1) | MQM (+1) |
| **Cys (0)**[a] | 13.55 | 8.35 | 10.74 |
| **Cys (-1)** | 456.66 | 72,214.25 | 1,703.02 |
| **His (+1)** | 9.80 | 1.20 | 0.04 |
| **His (0)** | 48.26 | 18.76 | 20.82 |
| **Lys (+1)** | 4.64 | 0.02 | 4.20 |
| **Lys (0)** | 25.40 | 13.27 | 15.69 |
| **NAC (0)** | 16.92 | 9.72 | 12.20 |
| **NAC (-1)** | 542.45 | 13,314.57 | 1,181.47 |
| **NAH (+1)** | 74.36 | 1.92 | 0.15 |
| **NAH (0)** | 38.47 | 16.23 | 18.55 |
| **NAK (+1)** | 1.54 | 0.16 | 5.29 |
| **NAK (0)** | 21.61 | 12.02 | 14.44 |
| **GSH (0)** | 34.61 | 13.83 | 16.43 |
| **GSH (-1)** | 9.19 | 19.31 | 37.08 |

[a] Ionization state of molecule is presented in parentheses
[b] Abbreviations: COC, cocaine; MN, morphinone; MQM, morphine quinone methide

### 4.5.4. **Discussion of Calculated Reactivity Data**

The use of *in silico* techniques to model complex chemical systems has found great utility recently, as technological advances have minimized the cost of computing systems necessary to perform iterative processes associated with such methods. In this study, *in silico* techniques were utilized to model the electronic reactivities of relevant nucleophiles and electrophiles associated with protein adducts formed with cocaine and morphine metabolic products. Data collected are in good agreement with existing

knowledge of nucleophile reactivity, especially as a property mediated by pH/$pK_a$-derived ionization states, demonstrating the applicability of these calculation-based estimators. *In silico* analysis of purported reactive electrophiles (*i.e.*, cocaine-3,4-epoxide, morphinone, and morphine quinone methide) revealed increases in molecular electrophilicity compared to parent molecules and stable metabolic products. When the electronic reactivity was exclusively based on HOMO and LUMO energies, the reactive products of morphine metabolism (*i.e.*, morphinone and morphine quinone methide) were found to be more reactive than cocaine-3,4-epoxide. However, these calculations do not fully account for the steric strain present in an aryl epoxide like cocaine-3,4-epoxide. Consequently, overall reactivity of a system involving a cocaine-derived reactive epoxide may be increased as compared to that predicted from the above data.

One motivation behind performing *in silico* reactivity estimations in the present study was to assess the feasibility of morphine quinone methide as a possible reactive electrophile and its potential role as the metabolite responsible for NADPH-mediated thiol adducts described in this study. The calculated electrophilicity of 17.98 eV for morphine quinone methide is of similar magnitude to that for the electrophile morphinone ($\omega$ = 12.32 eV), supporting not only the putative assignment of morphine quinone methide as a reactive biotransformation product of morphine, but also accounting for its formidable reactivity and consequential inability to be detected in the free fraction by methods employed in this study. Additionally, quantum mechanical calculations suggest that morphine quinone methide is a relatively soft electrophile, which would support the selectivity for reaction with Cys thiols (soft nucleophiles) as opposed to His or Lys residues (moderately hard nucleophiles) observed in *in vitro* incubations performed for adduct screening purposes.

The "reactivity index ($\omega^-$)" modeling interactions between individual electrophile– nucleophile pairs were in good agreement with general trends predicted by HSAB theory. The soft electrophiles morphinone and morphine quinone methide were found to have high reactivity with cysteine-based thiolates, especially Cys (-1) and NAC (-1). These data are concordant with adduct formation observed by LC-MS/MS as reported above, where adduction products were detected in systems with cysteine-containing nucleophilic trapping agents (*i.e.*, NAC, GSH, AcPAACAA) but were not detected in samples containing other nucleophiles (*i.e.*, NAH, NAK). Morphine quinone methide's designation as a soft

electrophile with high preferential reactivity for biological thiols is consistent with descriptions of the unknown reactive morphine metabolite in earlier literature and explains the structure of the resultant adduction products.

Even though epoxides are classified as soft electrophiles and cocaine-3,4-epoxide is a softer electrophile than its progenitor, cocaine, it is evident from *in silico* calculations that cocaine-3,4-epoxide is a harder electrophile than either morphine biotransformation product. Reactivity indices for cocaine-3,4-epoxide demonstrated preferential interaction with soft cysteine thiolates Cys (-1) and NAC (-1), while displaying calculated reactivity data uncharacteristic of a soft electrophile when paired with harder nucleophiles (*i.e.*, His, Lys, NAH, NAK). While conventional analysis of nucleophile reactivity generally designates neutral basic amino acids as the more reactive species, reaction indices calculated for cocaine-3,4-epoxide showed the protonated basic amino acids (*i.e.*, His (+1), Lys (+1), NAH (+1), NAK (+1)) to be more likely to be adducted. Similarly, *in silico* calculations determined the thiol form of GSH to be more reactive with cocaine epoxide than the thiolate. Data from *in vitro* incubations of cocaine with nucleophilic trapping agents are concordant with the prediction that cysteine thiols have preferential reactivity with the cocaine epoxide intermediate, in that adduction products involving oxidation of the aryl moiety were only detected in thiol-containing systems (*i.e.*, NAC, GSH, AcPAACAA). However, predicted reactivity indices for the cocaine epoxide and GSH deviate from the accepted designation of deprotonated thiolates as preferential nucleophilic targets over protonated thiols. Even though the predicted electronic reactivity for the epoxide/GSH system deviates from generally accepted HSAB principles, compounding factors aside from those relying on electronic descriptors of molecular reactivity (*e.g.*, steric factors, influence of GST enzymes) offer a potential explanation for adduct formation between GSH and reactive cocaine epoxide intermediates in assay samples.

While the electronic potentials of each nucleophile are vital parameters in their respective reactivities, the distribution of charge states as a function of pH of the microenvironment directly controls the availability of electronically "active" forms of each nucleophile. Table 22 presents generally accepted $pK_a$ values for each nucleophile along with the percent existing in each of the ionization states at pH 7.4, based on Henderson-Hasselbalch calculations. With the exception of His and NAH, the more

electronically reactive form of the nucleophile is not prevalent at physiological pH, thus limiting the reservoir of reactive sites within biological media. However, occurrences of catalytic diads and other $pK_a$-modifying anomalies can shift ionization state distributions by depressing functional $pK_a$ values of specific nucleophiles, consequently increasing the availability of favorable reaction sites.[56,57]

**Table 22: Nucleophile ionization state distribution at physiological pH**

| Nucleophile | $pK_a$ | % at pH 7.4 |
|---|---|---|
| **Cys (0)**[a] | 8.15 | 85 |
| **Cys (-1)** | 8.15 | 15 |
| **His (+1)** | 6.04 | 4 |
| **His (0)** | 6.04 | 96 |
| **Lys (+1)** | 10.79 | 99.96 |
| **Lys (0)** | 10.79 | 0.04 |
| **NAC (0)** | 9.52 | 99.25 |
| **NAC (-1)** | 9.52 | 0.75 |
| **NAH (+1)** | 7.00 | 28 |
| **NAH (0)** | 7.00 | 72 |
| **NAK (+1)** | 15.9 | 100 |
| **NAK (0)** | 15.9 | ~0 |
| **GSH (0)** | 8.56 | 93.5 |
| **GSH (-1)** | 8.56 | 6.5 |

[a] Ionization state of molecule is presented in parentheses

## 5. SUMMARY AND PROSPECT

This study was successful in utilizing LC-MS/MS technologies in conjunction with *in vitro* metabolic assays to deliver a more complete understanding of the metabolic fate of cocaine, methamphetamine, and morphine in humans. Investigations of *in vitro* assay conditions demonstrated marked shifts in metabolic profiles obtained for these drugs that were directly mediated by additive supplementation and incubation time. In all cases, the *in vitro* assays systems tested were capable of metabolizing each drug of abuse to the anticipated major metabolic products based on literature reports of the enzymatic components present. Minor and trace biotransformation products were minimally detected by the methods utilized, most likely due to their optimization for rapid production of major metabolites. However, comparisons among the metabolic model systems examined did offer novel insight into regioselective hydroxylation events for cocaine, in addition to new data on the enzymatic contributions to *N*-demethylation of methamphetamine and glucuronidation of morphine. Results from these experiments not only lead to improvements in the efficacy of *in vitro* metabolic model systems for the controlled production of metabolic profiles for drugs of abuse, but also demonstrate their usefulness in examining specific routes of biotransformation and designation of the impact of enzyme class on individual metabolic transformations.

Utilizing rhCYP-based *in vitro* assay systems, biotransformation processes yielding the primary Phase I metabolic products for cocaine, methamphetamine, and morphine were phenotyped for each drug. Results of this study demonstrated CYP isoform specificity for substrate and metabolic process, designating the contributions of individual CYP isozymes for cocaine and methamphetamine not previously catalogued in existing literature. Particular attention was given to the aryl hydroxylation products of cocaine (2-, 3-, and 4-hydroxycocaine) and methamphetamine (2-, 3-, and 4-hydroxymethamphetamine), where it was found that formation of the 4-hydroxy isomers of both drugs is mediated by regioselective CYP activity. Conversely, the formation of 3-hydroxycocaine and 2- and 3-hydroxymethamphetamine could not be attributed to one of the CYP isoforms studied, suggesting contributions from either the FMO superfamily of enzymes or one of the CYP isoforms not examined in this study. *In vitro* phenotyping incubations did not demonstrate the formation of 2-hydroxycocaine or

ephedrine, supporting the conclusion that CYP-mediated oxidation does not result in the production of either metabolite in humans after exposure to cocaine or methamphetamine, respectively.

The main portion of this research examined the potential for cocaine, methamphetamine, and morphine to form irreversible adduction products with endogenous proteins, by means of biomolecular trapping agents added to the *in vitro* metabolic systems to model reactive protein nucleophilic sites. The analysis methods used were unable to demonstrated covalent adduction products from methamphetamine with and of the model nucleophiles tested, or from cocaine or morphine with model nucleophiles containing lysine or histidine. However, clear evidence for covalent adduction products with cocaine and morphine and free cysteine thiols was obtained. In addition, it was demonstrated that cocaine adduct formation is mediated by CYPs 2C19, 1A2, and 2D6, via a novel mechanism involving reactive aryl epoxide formation and subsequent nucleophilic attack by reactive sulfhydryl groups, resulting in a stable monohydroxylated cocaine adduction moiety.

Data from morphine investigations demonstrated two distinct pathways that result in covalent adduction products with cysteine thiols. The first pathways involves the bioactivation of morphine to the known reactive metabolite morphinone, forming 8-*S*-(cysteinyl)morphinone adducts by means of 1,4-Michael-type addition. This data corroborated existing knowledge of non-NADPH-mediated formation of morphinone by morphine-6-dehydrogenase with no significant influence from CYP-catalyzed oxidative activity. In addition, a second metabolic pathway was determined, involving production of a novel morphine metabolite, morphine quinone methide, and subsequent 1,6-Michael addition resulting in 10-*S*-(cysteinyl)morphine adduction products. Reaction phenotyping for the formation of morphine quinone methide adduction products confirmed a NADPH-mediated oxidative process almost exclusively catalyzed by CYP3A4. Data on the formation of reactive electrophilic morphine metabolites corroborate existing knowledge of morphine bioactivation and binding and provide novel insight into mechanisms responsible for the adduction process and structural characteristics associated with thiol-bound products.

Further probing of the mechanisms of covalent adduction by cocaine and morphine with biological thiols was performed via computational analysis of postulated reactive intermediates/metabolites in conjunction with model nucleophiles. Calculated reactive indices for electrophile− nucleophile interactions

were generally in good agreement with the *in vitro* data collected in the study, designating biological thiols as the preferential targets for adduct formation resulting from cocaine epoxide intermediates, morphinone, and morphine quinone methide. While focusing primarily on electronic factors involved in the adduction process, the results obtained further support the feasibility of putative mechanisms for irreversible protein binding by cocaine and morphine, including the participation of the novel morphine metabolite, morphine quinone methide.

The protein adduction processes described by this research represent novel routes for cocaine and morphine biotransformation with significant implications for the toxicology associated with each of these important and heavily abused drugs. In addition to providing medical professionals with a more complete understanding of possible mechanisms behind drug-induced toxicity, results of this research open the door for analytical and forensic scientists to develop methodologies for detecting cocaine- and morphine-derived conjugates that unequivocally confirm exposure to either drug of abuse. Likewise, detection of macromolecular protein targets for the covalent binding of cocaine and morphine would give insight into downstream toxicodynamics associated with each drug, but also could be utilized by forensic scientists to extend the timeline of detection for cocaine and morphine from days to months without having to rely on alternative (and potentially problematic) specimens such as hair. In summary, data collected in this project describe novel metabolic events for several important drugs of abuse, culminating in detection methods and mechanistic descriptors useful to both medical and forensic investigators when examining the toxicology associated with cocaine, methamphetamine, and morphine exposure in humans.

REFERENCES


1. Kerns, E. H.; Di, L. Metabolic Stability. In *Drug-like Properties: Concepts, Structure Design and Methods: from ADME to Toxicity Optimization*, Elsevier, Inc.: New York, 2008; pp 137-168.

2. Eddershaw, P.; Dickins, M. Phase I Metabolism. In *A Handbook of Bioanalysis and Drug Metabolism*, Evans, G., Ed.; CRC Press: Boca Raton, 2004; pp 208-221.

3. Testa, B. Drug Metabolism. In *Burger's Medicinal Chemistry and Drug Discovery: Volume 1: Principles and Practice*, 5th ed.; Wolff, M. E., Ed.; John Wiley & Sons, Inc.: New York, 1995; Vol. 1, pp 129-180.

4. Testa, B.; Krämer, S. D. The biochemistry of drug metabolism - An introduction Part 2. Redox reactions and their enzymes. *Chem. Biodiversity* **2007,** *4* (3), 257-405.

5. Newcomb, M.; Hollenberg, P. F.; Coon, M. J. Multiple mechanisms and multiple oxidants in P450-catalyzed hydroxylations. *Arch. Biochem. Biophys.* **2003,** *409* (1), 72-79.

6. Parkinson, A.; Ogilvie, B. W. Biotransformation of Xenobiotics. In *Casarett & Doull's Toxicology: The Basic Science of Poisons*, 7 ed.; Klaassen, C. D., Ed.; McGraw Hill Medical: New York, 2008; pp 161-304.

7. Zangar, R. C.; Davydov, D. R.; Verma, S. Mechanisms that regulate production of reactive oxygen species by cytochrome P450. *Toxicol. Appl. Pharmacol.* **2004,** *199* (3), 316-331.

8. Auclair, K.; Hu, Z. B.; Little, D. M.; de Montellano, P. R. O.; Groves, J. T. Revisiting the mechanism of P450 enzymes with the radical clocks norcarane and spiro[2,5]octane. *J. Am. Chem. Soc.* **2002,** *124* (21), 6020-6027.

9. Williams, J. A.; Hyland, R.; Jones, B. C.; Smith, D. A.; Hurst, S.; Goosen, T. C.; Peterkin, V.; Koup, J. R.; Ball, S. E. Drug-drug interactions for UDP-glucuronosyltransferase substrates: A pharmacokinetic explanation for typically observed low exposure (AUC(i)/AUC) ratios. *Drug Metab. Dispos.* **2004,** *32* (11), 1201-1208.

10. Guengerich, F. P. Oxidative, reductive, and hydrolytic metabolism of drugs. In *Drug Metabolism in Drug Design and Development: Basic Concepts and Practice*, Zhang, D., Zhu, M., Humphreys, W. G., Eds.; John Wiley & Sons, Inc.: Hoboken, 2008; pp 15-35.

11. Testa, B.; Krämer, S. D. The biochemistry of drug metabolism - An introduction Part 4. Reactions of conjugation and their enzymes. *Chem. Biodiversity* **2008,** *5* (11), 2171-2336.

12. Hirom, P. C.; Millburn, P.; Smith, R. L.; Williams, R. T. Species variation in the threshold molecular-weight factor for the biliary excretion of organic anions. *Biochem. J.* **1972,** *129*, 1071-1077.

13. Hirom, P. C.; Millburn, P.; Smith, R. L. Bile and urine as complementary pathways for the excretion of foreign organic compounds. *Xenobiotica* **1976,** *6* (1), 55-64.

14. Manchee, G.; Dickins, M.; Pickup, E. Phase II Enzymes. In *A Handbook of Bioanalysis and Drug Metabolism*, Evans, G., Ed.; CRC Press: Boca Raton, 2004; pp 222-243.

15. Boyland, E.; Chasseaud, L. F. The role of glutathione and glutathione S-transferases in mercapturic acid biosynthesis. In *Advances in Enzymology and Related Areas of*

*Molecular Biology*, Nord, F. F., Ed.; John Wiley & Sons, Inc.: Hoboken, NJ, 2006; Vol. 32.

16. Wang, W.; Ballatori, N. Endogenous glutathione conjugates: Occurrence and biological functions. *Pharmacol. Rev.* **1998,** *50* (3), 335-355.

17. Lemoine, A.; Gautier, J. C.; Azoulay, D.; Kiffel, L.; Belloc, C.; Guengerich, F. P.; Maurel, P.; Beaune, P.; Leroux, J. P. Major Pathway of Imipramine Metabolism Is Catalyzed by Cytochromes P-450 1A2 and P-450 3A4 in Human Liver. *Mol. Pharmacol.* **1993,** *43* (5), 827-832.

18. Granfors, M. T.; Backman, J. T.; Neuvonen, M.; Neuvonen, P. J. Ciprofloxacin greatly increases concentrations and hypotensive effect of tizanidine by inhibiting its cytochrome P450 1A2-mediated presystemic metabolism. *Clin. Pharmacol. Ther.* **2004,** *76* (6), 598-606.

19. DeCaprio, A. P. Biomarkers of exposure and susceptibility. In *General and Applied Toxicology, 2nd Edition*, Ballantyne, B., Marrs, T. C., Syversen, T., Eds.; Macmillan Reference Ltd.: London, 2000; pp 1875-1898.

20. Isenschmid, D. Cocaine. In *Principles of Forensic Toxicology*, 2nd ed. ed.; Levine, B., Ed.; AACC Press: Washington, DC, 2006; pp 239-260.

21. Moser, V. C.; Aschner, M.; Richardson, R. J.; Philbert, M. A. Toxic Responses of the nervous system. In *Casarett & Doull's Toxicology: The Basic Science of Poisons*, 7th ed.; Klaassen, C. D., Ed.; McGraw Hill Medical: New York, 2008; pp 631-664.

22. *Clarke's Analysis of Drugs and Poisons;* 3rd ed.; Pharmaceutical Press: Grayslake, 2004; Vol. 2.

23. Boelsterli, U. A.; Göldlin, C. Biomechanisms of cocaine-induced hepatocyte injury mediated by the formation of reactive metabolites. *Arch. Toxicol.* **1991,** *65* (5), 351-360.

24. Pindel, E. V.; Kedishvili, N. Y.; Abraham, T. L.; Brzezinski, M. R.; Zhang, J.; Dean, R. A.; Bosron, W. F. Purification and cloning of a broad substrate specificity human liver carboxylesterase that catalyzes the hydrolysis of cocaine and heroin. *J. Biol. Chem.* **1997,** *272* (23), 14769-14775.

25. Jindal, S. P.; Lutz, T. Ion Cluster Techniques in Drug-Metabolism - Use of A Mixture of Labeled and Unlabeled Cocaine to Facilitate Metabolite Identification. *J. Anal. Toxicol.* **1986,** *10* (4), 150-155.

26. Moore, K. Amphetamines/Sympathomimetic Amines. In *Principles of Forensic Toxicology*, 2 ed.; Levine, B., Ed.; AACC Press: Washington, DC, 2006; pp 277-296.

27. Shima, N.; Katagi, M.; Tsuchihashi, H. Direct analysis of conjugate metabolites of methamphetamine, 3,4-methylenedioxymethamphetamine, and their designer drugs in biological fluids. *J. Health Sci.* **2009,** *55* (4), 495-502.

28. Kerrigan, S.; Goldberger, B. A. Opiods. In *Principles of Forensic Toxicology*, 2nd ed.; Levine, B., Ed.; AACC Press: Washington, DC, 2006; pp 219-237.

29. Cho, A. K.; Narimatsu, S.; Kumagai, Y. Metabolism of drugs of abuse by cytochromes P450. *Addict. Biology* **1999,** *4* (3), 283-301.

30. Evans, D. C.; Watt, A. P.; Nicoll-Griffith, D. A.; Baillie, T. A. Drug-protein adducts: An industry perspective on minimizing the potential for drug bioactivation in drug discovery and development. *Chem. Res. Toxicol.* **2005,** *17* (1), 3-16.

31. Mitchell, M. D.; Elrick, M. M.; Walgren, J. L.; Mueller, R. A.; Morris, D. L.; Thompson, D. C. Peptide-based in vitro assay for the detection of reactive metabolites. *Chem. Res. Toxicol.* **2008,** *21* (4), 859-868.

32. Brandon, E. F. A.; Raap, C. D.; Meijerman, I.; Beijnen, J. H.; Schellens, J. H. M. An update on in vitro test methods in human hepatic drug biotransformation research: pros and cons. *Toxicol. Appl. Pharmacol.* **2003,** *189* (3), 233-246.

33. Kerns, E. H.; Di, L. Metabolic Stability Methods. In *Drug-like Properties: Concepts, Structure Design and Methods: from ADME to Toxicity Optimization*, Elsevier, Inc.: New York, 2008; pp 329-347.

34. Yamazaki, H.; Ueng, Y. F.; Shimada, T.; Guengerich, F. P. Roles of Divalent Metal-Ions in Oxidations Catalyzed by Recombinant Cytochrome-P450 3A4 and Replacement of Nadph-Cytochrome P450 Reductase with Other Flavoproteins, Ferredoxin, and Oxygen Surrogates. *Biochemistry* **1995,** *34* (26), 8380-8389.

35. Fisher, M. B.; Campanale, K.; Ackermann, B. L.; Vandenbranden, M.; Wrighton, S. A. In vitro glucuronidation using human liver microsomes and the pore-forming peptide alamethicin. *Drug Metab. Dispos.* **2000,** *28* (5), 560-566.

36. Meech, R.; MacKenzie, P. I. Structure and function of uridine diphosphate glucuronosyltransferases. *Clin. Exp. Pharmacol. Phisiol.* **1997,** *24* (12), 907-915.

37. Tieleman, D. P.; Berendsen, H. J. C.; Sansom, M. S. P. An alamethicin channel in a lipid bilayer: Molecular dynamics simulations. *Biophys. J.* **1999,** *76* (4), 1757-1769.

38. Reichman, M.; Gill, H. Automated Drug Screening for ADMET Properties. In *Drug Metabolism Handbook: Concepts and Applications*, Nassar, A. F., Hollenberg, P. F., Scatina, J., Eds.; John Wiley & Sons, Inc.: Hoboken, 2009; pp 129-166.

39. Argoti, D.; Liang, L.; Conteh, A.; Chen, L. F.; Bershas, D.; Yu, C. P.; Vouros, P.; Yang, E. Cyanide trapping of iminium ion reactive intermediates followed by detection and structure identification using liquid chromatography-tandem mass spectrometry (LC-MS/MS). *Chem. Res. Toxicol.* **2005,** *18* (10), 1537-1544.

40. Defoy, D.; Dansette, P. M.; Neugebauer, W.; Wagner, J. R.; Klarskov, K. Evaluation of Deuterium Labeled and Unlabeled Bis-methyl Glutathione Combined with Nano liquid Chromatography Mass Spectrometry to Screen and Characterize Reactive Drug Metabolites. *Chem. Res. Toxicol.* **2011,** *24* (3), 412-417.

41. Dieckhaus, C. M.; Fernandez-Metzler, C. L.; King, R.; Krolikowski, P. H.; Baillie, T. A. Negative ion tandem mass spectrometry for the detection of glutathione conjugates. *Chem. Res. Toxicol.* **2005,** *18* (4), 630-638.

42. Hoos, J. S.; Damsten, M. C.; de Vlieger, J. S. B.; Commandeur, J. N. M.; Vermeulen, N. P. E.; Niessen, W. M. A.; Henk, L.; Irth, H. Automated detection of covalent adducts to human serum albumin by immunoaffinity chromatography, on-line solution phase digestion and liquid chromatography - mass spectrometry. *J. Chromatogr. , B: Anal. Technol. Biomed. Life Sci.* **2007,** *859* (2), 147-156.

43. Jian, W. Y.; Yao, M.; Zhang, D. X.; Zhu, M. S. Rapid Detection and Characterization of in Vitro and Urinary N-Acetyl-L-cysteine Conjugates Using Quadrupole-Linear Ion Trap Mass Spectrometry and Polarity Switching. *Chem. Res. Toxicol.* **2009,** *22* (7), 1246-1255.

44. Li, F.; Lu, J.; Ma, X. C. Profiling the Reactive Metabolites of Xenobiotics Using Metabolomic Technologies. *Chem. Res. Toxicol.* **2011,** *24* (5), 744-751.

45. Meneses-Lorente, G.; Sakatis, M. Z.; Schulz-Utermoehl, T.; De Nardi, C.; Watt, A. P. A quantitative high-throughput trapping assay as a measurement of potential for bioactivation. *Anal. Biochem.* **2006,** *351* (2), 266-272.

46. Natsch, A.; Gfeller, H. LC-MS-based characterization of the peptide reactivity of chemicals to improve the *in vitro* prediction of the skin sensitization potential. *Toxicol. Sci.* **2008,** *106* (2), 464-478.

47. Prakash, C.; Sharma, R.; Gleave, M.; Nedderman, A. In Vitro Screening Techniques for Reactive Metabolites for Minimizing Bioactivation Potential in Drug Discovery. *Curr. Drug Metab.* **2008,** *9* (9), 952-964.

48. Yan, Z. Y.; Maher, N.; Torres, R.; Huebert, N. Use of a trapping agent for simultaneous capturing and high-throughput screening of both "soft" and "hard" reactive metabolites. *Anal. Chem.* **2007,** *79* (11), 4206-4214.

49. Hakkinen, M. R.; Laine, J. E.; Juvonen, R. O.; Auriola, S.; Hayrinen, J.; Pasanen, M. 2 '-Deoxyguanosine as a surrogate trapping agent for DNA reactive drug metabolites. *Toxicol. Lett.* **2011,** *207* (1), 34-41.

50. Wyatt, M. D.; Pittman, D. L. Methylating agents and DNA repair responses: Methylated bases and sources of strand breaks. *Chem. Res. Toxicol.* **2006,** *19* (12), 1580-1594.

51. Nexo, B. A.; Dybdahl, M.; Damgaard, J.; Olsen, L. S.; Moller, P.; Wassermann, K. Proficient deoxyribonucleic acid repair of methylation damage in hamster ERCC-gene mutants. *Mutat. Res.* **1998,** *407* (3), 261-268.

52. Pearson, R. G. Hard and soft acids and bases. *J. Am. Chem. Soc.* **1963,** *85* (22), 3533-3539.

53. Pearson, R. G. The HSAB principle - more quantitative aspects. *Inorg. Chim. Acta* **1995,** *240* (1-2), 93-98.

54. Srivastava, A.; Maggs, J. L.; Antoine, D. J.; Williams, D. P.; Smith, D. A.; Park, B. K. Role of reactive metabolites in drug-induced hepatotoxicity. In *Adverse Drug Reactions*, Uetrecht, J., Ed.; Springer: New York, 2010; pp 165-194.

55. Isom, D. G.; Castaneda, C. A.; Cannon, B. R.; Garcia-Moreno, B. E. Large shifts in pK(a) values of lysine residues buried inside a protein. *Proc. Natl. Acad. Sci. U. S. A.* **2011,** *108* (13), 5260-5265.

56. LoPachin, R. M.; Barber, D. S. Synaptic cysteine sulfhydryl groups as targets of electrophilic neurotoxicants. *Toxicol. Sci.* **2006,** *94* (2), 240-255.

57. Harris, T. K.; Turner, G. J. Structural basis of perturbed pK(a) values of catalytic groups in enzyme active sites. *IUBMB Life* **2002,** *53* (2), 85-98.

58. Smith, S. L.; Jennett, R. B.; Sorrell, M. F.; Tuma, D. J. Acetaldehyde Substoichiometrically Inhibits Bovine Neurotubulin Polymerization. *J. Clin. Invest.* **1989,** *84* (1), 337-341.

59. Mauch, T. J.; Tuma, D. J.; Sorrell, M. F. The Binding of Acetaldehyde to the Active-Site of Ribonuclease - Alterations in Catalytic Activity and Effects of Phosphate. *Alcohol Alcohol.* **1987,** *22* (2), 103-112.

60. Mauch, T. J.; Donohue, T. M.; Zetterman, R. K.; Sorrell, M. F.; Tuma, D. J. Covalent Binding of Acetaldehyde Selectively Inhibits the Catalytic Activity of Lysine-Dependent Enzymes. *Hepatology* **1986,** *6* (2), 263-269.

61. Viitala, K.; Israel, Y.; Blake, J. E.; Niemela, O. Serum IgA, IgG, and IgM antibodies directed against acetaldehyde-derived epitopes: Relationship to liver disease severity and alcohol consumption. *Hepatology* **1997,** *25* (6), 1418-1424.

62. Niemelä, O.; Parkkila, S.; Juvonen, R. O.; Viitala, K.; Gelboin, H. V.; Pasanen, M. Cytochromes P450 2A6 2E1, and 3A and production of protein-aldehyde adducts in the liver of patients with alcoholic and non-alcoholic liver diseases. *J. Hepatol.* **2000,** *33* (6), 893-901.

63. Rolla, R.; Vay, D.; Mottaran, E.; Parodi, M.; Traverso, N.; Arico, S.; Sartori, M.; Bellomo, G.; Klassen, L. W.; Thiele, G. M.; Tuma, D. J.; Albano, E. Detection of circulating antibodies against malondialdehyde-acetaldehyde adducts in patients with alcohol-induced liver disease. *Hepatology* **2000,** *31* (4), 878-884.

64. Nestmann, E. R.; Bryant, D. W.; Carr, C. J. Toxicological significance of DNA adducts: Summary of discussions with an Expert Panel. *Regul. Toxicol. Pharmacol.* **1996,** *24* (1), 9-18.

65. Schnell, F. C. Protein adduct-forming chemicals and molecular dosimetry: Potential for environmental and occupational biomarkers. *Rev. Environ. Toxicol.* **1993,** *5*, 51-160.

66. Wild, C. P.; Jiang, Y.-Z.; Sabbioni, G.; Chapot, B.; Montesano, R. Evaluation of methods for quantitation of aflatoxin-albumin adducts and their application to human exposure assessment. *Cancer Res.* **1990,** *50* (2), 245-251.

67. DeCaprio, A. P. Biomarkers: Coming of age for environmental health and risk assessment. *Environ. Sci. Technol.* **1997,** *31* (7), 1837-1848.

68. Koivisto, H.; Hietala, J.; Anttila, P.; Parkkila, S.; Niemela, O. Long-term ethanol consumption and macrocytosis: diagnostic and pathogenic implications. *J. Lab. Clin. Med.* **2006,** *147* (4), 191-196.

69. Erve, J. C. L. Chemical toxicology: reactive intermediates and their role in pharmacology and toxicology. *Expert Opin. Drug Metab. Toxicol.* **2006,** *2* (6), 923-946.

70. Niemela, O. Alcoholic macrocytosis - is there a role for acetaldehyde and adducts? *Addict. Biology* **2004,** *9* (1), 3-10.

71. Braun, K. P.; Cody, R. B.; Jones, D. R.; Peterson, C. M. A Structural Assignment for A Stable Acetaldehyde-Lysine Adduct. *J. Biol. Chem.* **1995,** *270* (19), 11263-11266.

72. Niemela, O.; Parkkila, S.; Pasanen, M.; Iimuro, Y.; Bradford, B.; Thurman, R. G. Early alcoholic liver injury: Formation of protein adducts with acetaldehyde and lipid peroxidation

products, and expression of CYP2E1 and CYP3A. *Alcohol. : Clin. Exp. Res.* **1998,** *22* (9), 2118-2124.

73. Braun, K. P.; Pavlovich, J. G.; Jones, D. R.; Peterson, C. M. Stable acetaldehyde adducts: Structural characterization of acetaldehyde adducts of human hemoglobin N-terminal β-globin chain peptides. *Alcohol. : Clin. Exp. Res.* **1997,** *21* (1), 40-43.

74. Tuma, D. J.; Thiele, G. M.; Xu, D. S.; Klassen, L. W.; Sorrell, M. F. Acetaldehyde and malondialdehyde react together to generate distinct protein adducts in the liver during long-term ethanol administration. *Hepatology* **1996,** *23* (4), 872-880.

75. Shebley, M.; Jushchyshyn, M. I.; Hollenberg, P. F. Selective pathways for the metabolism of phencyclidine by cytochrome P4502B enzymes: Identification of electrophilic metabolites, glutathione, and N-acetyl cysteine adducts. *Drug Metab. Dispos.* **2006,** *34* (3), 375-383.

76. Driscoll, J. P.; Kornecki, K.; Wolkwski, J. P.; Chupak, L.; Kalgutkar, A. S.; O'Donnell, J. P. Bioactivation of phencyclidine in rat and human liver Microsomes and recombinant p450 2B enzymes: Evidence for the formation of a novel quinone methide intermediate. *Chem. Res. Toxicol.* **2007,** *20* (10), 1488-1497.

77. Ward, D. P.; Trevor, A. J.; Kalir, A.; Adams, J. D.; Baillie, T. A.; Castagnoli, N. Metabolism of Phencyclidine - the Role of Iminium Ion Formation in Covalent Binding to Rabbit Microsomal Protein. *Drug Metab. Dispos.* **1982,** *10* (6), 690-695.

78. Jushchyshyn, M. I.; Wahlstrom, J. L.; Hollenberg, P. F.; Wienders, L. C. Mechanism of inactivation of human cytochrome p450 2B6 by phencyclidine. *Drug Metab. Dispos.* **2006,** *34* (9), 1523-1529.

79. Hoag, M. K. P.; Trevor, A. J.; Asscher, Y.; Weissman, J.; Castagnoli, N. Metabolism-Dependent Inactivation of Liver Microsomal-Enzymes by Phencyclidine. *Drug Metab. Dispos.* **1984,** *12* (3), 371-375.

80. Kumagai, Y.; Todaka, T.; Toki, S. A New Metabolic Pathway of Morphine - Invivo and Invitro Formation of Morphinone and Morphinone-Glutathione Adduct in Guinea-Pig. *J. Pharmacol. Exp. Ther.* **1990,** *255* (2), 504-510.

81. Yamano, S.; Takahashi, A.; Todaka, T.; Toki, S. In vivo and in vitro formation of morphinone from morphine in rat. *Xenobiotica* **1997,** *27* (7), 645-656.

82. Todaka, T.; Ishida, T.; Kita, H.; Narimatsu, S.; Yamano, S. Bioactivation of morphine in human liver: Isolation and identification of morphinone, a toxic metabolite. *Biol. Pharm. Bull.* **2005,** *28* (7), 1275-1280.

83. Toki, S.; Yamano, S. Production of morphinone as a metabolite of morphine and its physiological role. *Yakugaku Zasshi* **1999,** *119* (4), 249-267.

84. Kumagai, Y.; Ikeda, Y.; Toki, S. Hydroxyl Radical-Mediated Conversion of Morphine to Morphinone. *Xenobiotica* **1992,** *22* (5), 507-513.

85. Ishida, T.; Kumagai, Y.; Ikeda, Y.; Ito, K.; Yano, M.; Toki, S.; Mihashi, K.; Fujioka, T.; Iwase, Y.; Hachiyama, S. (8S)-(Glutathion-S-Yl)Dihydromorphinone, A Novel Metabolite of Morphine from Guinea-Pig Bile. *Drug Metab. Dispos.* **1989,** *17* (1), 77-81.

86. Nagamatsu, K.; Kido, Y.; Terao, T.; Ishida, T.; Toki, S. Studies on the Mechanism of Covalent Binding of Morphine Metabolites to Proteins in Mouse. *Drug Metab. Dispos.* **1983,** *11* (3), 190-194.

87. Nagamatsu, K.; Ohno, Y.; Ikebuchi, H.; Takahashi, A.; Terao, T.; Takanaka, A. Morphine-Metabolism in Isolated Rat Hepatocytes and Its Implications for Hepatotoxicity. *Biochem. Pharmacol.* **1986,** *35* (20), 3543-3548.

88. Correia, M. A.; Krowech, G.; Caldera-Munoz, P.; Yee, S. L.; Straub, K.; Castagnoli, N. Morphine metabolism revisited. II. Isolation and chemical characterization of a glutathionylmorphine adduct from rat-liver microsomal preparations. *Chem. -Biol. Interact.* **1984,** *51* (1), 13-24.

89. Correia, M. A.; Wong, J. S.; Soliven, E. Morphine-Metabolism Revisited .1. Metabolic-Activation of Morphine to A Reactive Species in Rats. *Chem. -Biol. Interact.* **1984,** *49* (3), 255-268.

90. Krowech, G.; Calderamunoz, P. S.; Straub, K.; Castagnoli, N.; Correia, M. A. Morphine-Metabolism Revisited .3. Confirmation of A Novel Metabolic Pathway. *Chem. -Biol. Interact.* **1986,** *58* (1), 29-40.

91. Kovacic, P. Role of oxidative metabolites of cocaine in toxicity and addiction: oxidative stress and electron transfer. *Med. Hypotheses* **2005,** *64* (2), 350-356.

92. Göldlin, C.; Boelsterli, U. A. Dissociation of covalent protein adduct formation from oxidative injury in cultured hepatocytes exposed to cocaine. *Xenobiotica* **1994,** *24* (3), 251-264.

93. Bouis, P.; Boelsterli, U. A. Modulation of cocaine metabolism in primary rat hepatocyte cultures: Effects on irreversible binding and protein-biosynthesis. *Toxicol. Appl. Pharmacol.* **1990,** *104* (3), 429-439.

94. Boelsterli, U. A.; Atanasoski, S.; Göldlin, C. Ethanol-induced enhancement of cocaine bioactivation and irreversible protein-binding: Evidence against a role of cytochrome P-450IIE1. *Alcohol. : Clin. Exp. Res.* **1991,** *15* (5), 779-784.

95. Ndikum-Moffor, F. M.; Roberts, S. M. Cocaine-protein targets in mouse liver. *Biochem. Pharmacol.* **2003,** *66* (1), 105-113.

96. Ndikum-Moffor, F. M.; Munson, J. W.; Bokinkere, N. K.; Brown, J. L.; Richards, N.; Roberts, S. M. Immunochemical detection of hepatic cocaine-protein adducts in mice. *Chem. Res. Toxicol.* **1998,** *11* (3), 185-192.

97. Charkoudian, J. C.; Shuster, L. Electrochemistry of norcocaine nitroxide and related compounds: Implications for cocaine hepatotoxicity. *Biochem. Biophys. Res. Comm.* **1985,** *130* (3), 1044-1051.

98. Deng, S. X.; Bharat, N.; Fischman, M. C.; Landry, D. W. Covalent modification of proteins by cocaine. *Proc. Nat. Acad. Sci. USA* **2002,** *99* (6), 3412-3416.

99. Myers, A. L. Glutathione conjugation of a cocaine pyrolysis product AEME and related compounds. Ph.D. Dissertation, West Virginia University, 2005.

100. Claffey, D. J.; Ruth, J. A. Amphetamine adducts of melanin intermediates demonstrated by matrix-assisted laser desorption/ionization time-of-flight mass spectrometry. *Chem. Res. Toxicol.* **2001,** *14* (9), 1339-1344.

101. Capela, J. P.; Macedo, C.; Branco, P. S.; Ferreira, L. M.; Lobo, A. M.; Fernandes, E.; Remião, F.; Bastos, M. L.; Dirnagl, U.; Meisel, A.; Carvalho, F. Neurotoxicity mechanisms of thioether ecstasy metabolites. *Neuroscience* **2007,** *146* (4), 1743-1757.

102. Capela, J. P.; Carmo, H.; Remiao, F.; Bastos, M. L.; Meisel, A.; Carvalho, F. Molecular and Cellular Mechanisms of Ecstasy-Induced Neurotoxicity: An Overview. *Mol. Neurobiol.* **2009,** *39* (3), 210-271.

103. Neises, B.; Steglich, W. Einfaches Verfahren zur Veresterung von Carbonsäuren. *Angew. Chem.* **1978,** *90* (7), 556-557.

104. Zhang, J. Y.; Foltz, R. L. Cocaine metabolism in man: Identification of four previously unreported cocaine metabolites in human urine. *J. Anal. Toxicol.* **1990,** *14* (4), 201-205.

105. Tolonen, A.; Petsalo, A.; Turpeinen, M.; Uusitalo, J.; Pelkonen, O. In vitro interaction cocktail assay for nine major cytochrome P450 enzymes with 13 probe reactions and a single LC/MSMS run: analytical validation and testing with monoclonal anti-CYP antibodies. *J. Mass Spectrom.* **2007,** *42*, 960-966.

106. Stormer, E.; von Moltke, L. L.; Greenblatt, D. J. Scaling drug biotransformation data from cDNA-expressed cytochrome P-450 to human liver: A comparison of relative activity factors and human liver abundance in studies of mirtazapine metabolism. *J. Pharmacol. Exp. Ther.* **2000,** *295* (2), 793-801.

107. Kalgutkar, A. S.; Gardner, I.; Obach, R. S.; Shaffer, C. L.; Callegari, E.; Henne, K. R.; Mutlib, A. E.; Dalvie, D. K.; Lee, J. S.; Nakai, Y.; O'Donnell, J. P.; Boer, J.; Harriman, S. P. A comprehensive listing of bioactivation pathways of organic functional groups. *Curr. Drug Metab.* **2005,** *6* (3), 161-225.

108. Gaussian 03, Revision B.03, Frisch, M. J., Trucks, G. W., Schlegel, H. B., Scuseria, G. E., Robb, M. A., Cheeseman, J. R., Montgomery Jr, J. A., Vreven, T., Kudin, K. N., Burant, J. C., Millam, J. M., Iyengar, S. S., Tomasi, J., Barone, V., Mennucci, B., Cossi, M., Scalmani, G., Rega, N., Petersson, G. A., Nakatsuji, H., Hada, M., Ehara, M., Toyota, K., Fukuda, R., Hasegawa, J., Ishida, M., Nakajima, T., Honda, Y., Kitao, O., Nakai, H., Klene, M., Li, X., Knox, J. E., Hratchian, H. P., Cross, J. B., Bakken, V., Adamo, C., Jaramillo, J., Gomperts, R., Stratmann, R. E., Yazyev, O., Austin, A. J., Cammi, R., Pomelli, C., Ochterski, J. W., Ayala, P. Y., Morokuma, K., Voth, G. A., Salvador, P., Dannenberg, J. J., Zakrzewski, V. G., Dapprich, S., Daniels, A. D., Strain, M. C., Farkas, O., Malick, D. K., Rabuck, A. D., Raghavachari, K., Foresman, J. B., Ortiz, J. V., Cui, Q., Baboul, A. G., Clifford, S., Cioslowski, J., Stefanov, B. B., Liu, G., Liashenko, A., Piskorz, P., Komaromi, I., Martin, R. L., Fox, D. J., Keith, T., Al-Laham, M. A., Peng, C. Y., Nanayakkara, A., Challacombe, M., Gill, P. M. W., Johnson, B., Chen, W., Wong, M. W., Gonzalez, C., and Pople, J. A.; Gaussian, Inc., Wallingford CT, 2004.

109. Ge, L. Y.; Yong, J. W. H.; Tan, S. N.; Yang, X. H.; Ong, E. S. Analysis of positional isomers of hydroxylated aromatic cytokinins by micellar electrokinetic chromatography. *Electrophoresis* **2005,** *26* (9), 1768-1777.

110. Jagerdeo, E.; Montgomery, M. A.; Lebeau, M. A.; Sibum, M. An automated SPE/LC/MS/MS method for the analysis of cocaine and metabolites in whole blood. *J. Chromatogr. B* **2008,** *874* (1-2), 15-20.

111. Wang, P. P.; Bartlett, M. G. Collision-induced dissociation mass spectra of cocaine, and its metabolites and pyrolysis products. *J. Mass Spectrom.* **1998,** *33* (10), 961-967.

112. von Moltke, L. L.; Greenblatt, D. J.; Granda, B. W.; Duan, S. X.; Grassi, J. M.; Venkatakrishnan, K.; Harmatz, J. S.; Shader, R. I. Zolpidem metabolism in vitro: responsible cytochromes, chemical inhibitors, and in vivo correlations. *Br. J. Clin. Pharmacol.* **1999,** *48* (1), 89-97.

113. Guo, J.; Zhou, D. S.; Grimm, S. W. Liquid chromatography-tandem mass spectrometry method for measurement of nicotine N-glucuronide: A marker for human UGT2B10 inhibition. *J. Pharm. Biomed. Anal.* **2011,** *55* (5), 964-971.

114. Greene, N.; Naven, R. Early toxicity screening strategies. *Curr. Opin. Drug Disc.* **2009,** *12* (1), 90-97.

115. Yamazaki, H.; Ueng, Y. F.; Shimada, T.; Guengerich, F. P. Roles of divalent metal ions in oxidations catalyzed by recombinant cytochrome-P450 3A4 and replacement of NADPH-cytochrome P450 reductase with other flavoproteins, ferredoxin, and oxygen surrogates. *Biochemistry* **1995,** *34* (26), 8380-8389.

116. Peters, F. T.; Meyer, M. R. In vitro approaches to studying the metabolism of new psychoactive compounds. *Drug Test. Anal.* **2011,** *3* (7-8), 483-495.

117. Kanamori, T.; Kuwayama, K.; Tsujikawa, K.; Miyaguchi, H.; Togawa-Iwata, Y.; Inoue, H. A model system for prediction of the in vivo metabolism of designer drugs using three-dimensional culture of rat and human hepatocytes. *Forensic Toxicol.* **2011,** *29* (2), 142-151.

118. Isenschmid, D. S.; Levine, B. S.; Caplan, Y. H. A comprehensive study of the stability of cocaine and its metabolites. *J. Anal. Toxicol.* **1989,** *13* (5), 250-256.

119. Smirnow, D.; Logan, B. K. Analysis of ecgonine and other cocaine biotransformation products in postmortem whole blood by protein precipitation-extractive alkylation and GC-MS. *J. Anal. Toxicol.* **1996,** *20* (6), 463-467.

120. Isenschmid, D. S.; Fischman, M. W.; Foltin, R. W.; Caplan, Y. H. Concentration of cocaine and metabolites in plasma of humans following intravenous administration and smoking of cocaine. *J. Anal. Toxicol.* **1992,** *16* (5), 311-314.

121. Laizure, S. C.; Mandrell, T.; Gades, N. M.; Parker, R. B. Cocaethylene metabolism and interaction with cocaine and ethanol: Role of carboxylesterases. *Drug Metab. Dispos.* **2003,** *31* (1), 16-20.

122. Li, P.; Zhao, K.; Deng, S. X.; Landry, D. W. Nonenzymatic hydrolysis of cocaine via intramolecular acid catalysis. *Helv. Chim. Acta* **1999,** *82* (1), 85-89.

123. Kaminsky, L. S.; Zhang, Z. Y. Human P450 metabolism of warfarin. *Pharmacol. Ther.* **1997,** *73* (1), 67-74.

124. Porter, W. R. Warfarin: history, tautomerism and activity. *J. Comput. Aided Mol. Des.* **2010,** *24* (6-7), 553-573.

125. Troutman, J. A.; Foertsch, L. M.; Kern, P. S.; Dai, H. J.; Quijano, M.; Dobson, R. L. M.; Lalko, J. F.; Lepoittevin, J. P.; Gerberick, G. F. The incorporation of lysine into the peroxidase peptide reactivity assay for skin sensitization assessments. *Toxicol. Sci.* **2011,** *122* (2), 422-436.

126. Park, B. K.; Kitteringham, N. R.; Maggs, J. L.; Pirmohamed, M.; Williams, D. P. The role of metabolic activation in drug-induced hepatotoxicity. *Annu. Rev. Pharmacol. Toxicol.* **2005,** 177-202.

127. Walgren, J. L.; Mitchell, M. D.; Thompson, D. C. Role of metabolism in drug-induced idiosyncratic hepatotoxicity. *Crit. Rev. Toxicol.* **2005,** *35* (4), 325-361.

128. Fandino, A. S.; Toennes, S. W.; Kauert, G. F. Studies on hydrolytic and oxidative metabolic pathways of anhydroecgonine methyl ester (methylecgonidine) using microsomal preparations from rat organs. *Chem. Res. Toxicol.* **2002,** *15* (12), 1543-1548.

129. Toennes, S. W.; Thiel, M.; Walther, M.; Kauert, G. F. Studies on metabolic pathways of cocaine and its metabolites using microsome preparations from rat organs. *Chem. Res. Toxicol.* **2003,** *16* (3), 375-381.

130. Roberts, S. M.; Harbison, R. D.; James, R. C. Human microsomal N-oxidative metabolism of cocaine. *Drug Metab. Dispos.* **1991,** *19* (6), 1046-1051.

131. Lin, L. Y.; DiStefano, E. W.; Schmitz, D. A.; Hsu, L.; Ellis, S. W.; Lennard, M. S.; Tucker, G. T.; Cho, A. K. Oxidation of methamphetamine and methylenedioxymethamphetamine by CYP2D6. *Drug Metab. Dispos.* **1997,** *25* (9), 1059-1064.

132. Projean, D.; Morin, P. E.; Tu, T. M.; Ducharme, J. Identification of CYP3A4 and CYP2C8 as the major cytochrome P450 s responsible for morphine N-demethylation in human liver microsomes. *Xenobiotica* **2003,** *33* (8), 841-854.

133. LoPachin, R. M.; Gavin, T.; Geohagan, B. C.; Das, S. Neurotoxic mechanisms of electrophilic type-2 alkenes: Soft-soft interactions described by quantum mechanical parameters. *Toxicol. Sci.* **2007,** *98* (2), 561-570.

134. LoPachin, R. M.; Barber, D. S.; Gavin, T. Molecular mechanisms of the conjugated α,β-unsaturated carbonyl derivatives: Relevance to neurotoxicity and neurodegenerative diseases. *Toxicol. Sci.* **2008,** *104* (2), 235-249.

135. Leduc, B. W.; Sinclair, P. R.; Shuster, L.; Sinclair, J. F.; Evans, J. E.; Greenblatt, D. J. Norcocaine and N-Hydroxynorcocaine Formation in Human Liver-Microsomes - Role of Cytochrome-P-450-3A4. *Pharmacology* **1993,** *46* (5), 294-300.

136. Yamazaki, H.; Shimada, T. Human liver cytochrome P450 enzymes involved in the 7-hydroxylation of R- and S-warfarin enantiomers. *Biochem. Pharmacol.* **1997,** *54* (11), 1195-1203.

137. Schep, L. J.; Slaughter, R. J.; Beasley, D. M. G. The clinical toxicology of metamfetamine. *Clin. Toxicol.* **2010,** *48* (7), 675-694.

138. Caldwell, J.; Dring, L. G.; Williams, R. T. Metabolism of [C-14]methamphetamine in man, the guinea pig and the rat. *Biochem. J.* **1972,** *129*, 11-22.

139. Baumann, P.; Hiemke, C.; Ulrich, S.; Eckermann, G.; Gaertner, I.; Gerlach, M.; Kuss, H.-J.; Laux, G.; Muller-Oerlinghausen, B.; Rao, M. L.; Riederer, P.; Zernig, G. The AGNP-TDM expert group consensus guidelines: Therapeutic drug monitoring in psychiatry. *Pharmacopsychiatry* **2004,** *37*, 243-265.

140. Kuhar, M. J.; Ritz, M. C.; Boja, J. W. The Dopamine Hypothesis of the Reinforcing Properties of Cocaine. *Trends Neurosci.* **1991,** *14* (7), 299-302.

141. Logan, J.; Volkow, N. D.; Fowler, J. S.; Wang, G. J.; Fischman, M. W.; Foltin, R. W.; Abumrad, N. N.; Vitkun, S.; Gatley, S. J.; Pappas, N.; Hitzemann, R.; Shea, C. E. Concentration and occupancy of dopamine transporters in cocaine abusers with [C-11]cocaine and PET. *Synapse* **1997,** *27* (4), 347-356.

142. Volkow, N. D.; Wang, G. J.; Fischman, M. W.; Foltin, R. W.; Fowler, J. S.; Abumrad, N. N.; Vitkun, S.; Logan, J.; Gatley, S. J.; Pappas, N.; Hitzemann, R.; Shea, C. E. Relationship between subjective effects of cocaine and dopamine transporter occupancy. *Nature* **1997,** *386* (6627), 827-830.

143. Singh, S.; Basmadjian, G. P.; Avor, K. S.; Pouw, B.; Seale, T. W. Synthesis and ligand binding studies of 4'-iodobenzoyl esters of tropanes and piperidines at the dopamine transporter. *J. Med. Chem.* **1997,** *40*, 2474-2481.

144. Aleksic, M.; Thain, E.; Roger, D.; Saib, O.; Davies, M.; Li, J.; Aptula, A.; Zazzeroni, R. Reactivity profiling: Covalent modification of single nucleophile peptides for skin sensitisation risk assessment. *Toxicol. Sci.* **2009,** *108* (2), 401-411.

145. Zhu, X. C.; Kalyanaraman, N.; Subramanian, R. Enhanced Screening of Glutathione-Trapped Reactive Metabolites by In-Source Collision-Induced Dissociation and Extraction of Product Ion Using UHPLC-High Resolution Mass Spectrometry. *Anal. Chem.* **2011,** *83* (24), 9516-9523.

146. Boelsterli, U. A. Specific targets of covalent drug-protein interactions in hepatocytes and their toxicological significance in drug-induced liver-injury. *Drug Metab. Rev.* **1993,** *25* (4), 395-451.

147. LoPachin, R. M.; DeCaprio, A. P. Protein adduct formation as a molecular mechanism in neurotoxicity. *Toxicol. Sci.* **2005,** *86* (2), 214-225.

148. Atici, S.; Cinel, I.; Cinel, L.; Doruk, N.; Eskandari, G.; Oral, U. Liver and kidney toxicity in chronic use of opioids: An experimental long term treatment model. *J. Biosci.* **2005,** *30* (2), 245-252.

149. Cagen, L. M.; Fales, H. M.; Pisano, J. J. Formation of glutathione cojugates of prostaglandin A1 in human red blood cells. *J. Biol. Chem.* **1976,** *251* (21), 6550-6554.

150. Yamazaki, H.; Suemizu, H.; Igaya, S.; Shimizu, M.; Shibata, N.; Nakamura, M.; Chowdhury, G.; Guengerich, F. P. In Vivo Formation of a Glutathione Conjugate Derived from Thalidomide in Humanized uPA-NOG Mice. *Chem. Res. Toxicol.* **2011,** *24* (3), 287-289.

151. Noort, D.; Fidder, A.; Hulst, A. G.; de Jong, L. P. A.; Benschop, H. P. Diagnosis and dosimetry of exposure to sulfur mustard: Development of a standard operating procedure for mass spectrometric analysis of haemoglobin adducts: Exploratory research on albumin and keratin adducts. *J. Appl. Toxicol.* **2000,** *20(Suppl 1)*, S187-S192.

152. Rappaport, S. M.; Li, H.; Grigoryan, H.; Funk, W. E.; Williams, E. R. Adductomics: Characterizing exposures to reactive electrophiles. *Toxicol. Lett.* **2012,** *213* (1), 83-90.

153. Paul, B. D.; Lalani, S.; Bosy, T.; Jacobs, A. J.; Huestis, M. A. Concentration profiles of cocaine, pyrolytic methyl ecgonidine and thirteen metabolites in human blood and urine:

determination by gas chromatography-mass spectrometry. *Biomed. Chromatogr.* **2005,** *19* (9), 677-688.

154. Kolbrich, E. A.; Barnes, A. J.; Gorelick, D. A.; Boyd, S. J.; Cone, E. J.; Huestis, M. A. Major and minor metabolites of cocaine in human plasma following controlled subcutaneous cocaine administration. *J. Anal. Toxicol.* **2006,** *30* (8), 501-510.

155. Srinivasan, K.; Wang, P.; Eley, A. T.; White, C. A.; Bartlett, M. G. Liquid chromatography-tandem mass spectrometry analysis of cocaine and its metabolites from blood, amniotic fluid, placental and fetal tissues: study of the metabolism and distribution of cocaine in pregnant rats. *J. Chromatogr. , B: Anal. Technol. Biomed. Life Sci.* **2000,** *745* (2), 287-303.

156. Kanel, G. C.; Cassidy, W.; Shuster, L.; Reynolds, T. B. Cocaine-Induced Liver-Cell Injury - Comparison of Morphological Features in Man and in Experimental-Models. *Hepatology* **1990,** *11* (4), 646-651.

157. Cone, E. J.; Heit, H. A.; Caplan, Y. H.; Gourlay, D. Evidence of morphine metabolism to hydromorphone in pain patients chronically treated with morphine. *J. Anal. Toxicol.* **2006,** *30* (1), 1-5.

158. Zheng, M.; McErlane, K. M.; Ong, M. C. Identification and synthesis of norhydromorphone, and determination of antinociceptive activities in the rat formalin test. *Life Sci.* **2004,** *75* (26), 3129-3146.

159. Zheng, M.; McErlane, K. M.; Ong, M. C. Hydromorphone metabolites: isolation and identification from pooled urine samples of a cancer patient. *Xenobiotica* **2002,** *32* (5), 427-439.

160. Goumon, Y.; Laux, A.; Muller, A.; Aunis, D. Central and peripheral endogenous morphine. *An. Real Acad. Nac. F.* **2009,** *75* (3), 389-418.

APPENDICES

Appendix 1: Biotransformation of cocaine

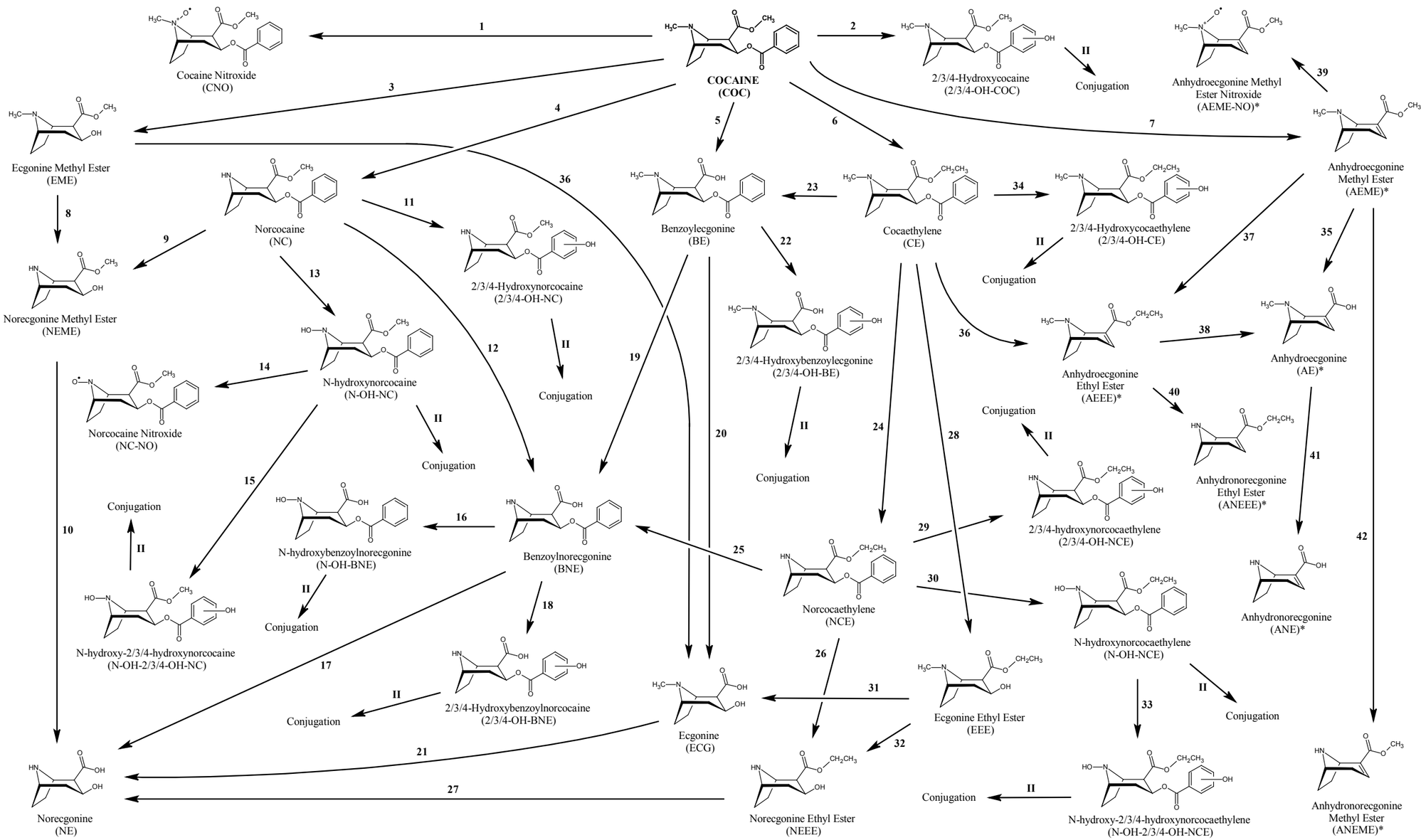

Cocaine Biotransformation Pathway Enzymes/Mechanisms

| # | Process | Enzyme/Mechanism | Source # |
|---|---|---|---|
| **1** | *N*-Oxidation | FMO | 29 |
| **2** | Aromatic oxidation | Enzymatic oxidation | 129 |
| **3** | Ester hydrolysis | hCE-2, serum cholinesterase, minor non-enzymatic hydrolysis | 24, 29, 122 |
| **4** | *N*-Dealkylation | CYP (CYP3A4) | 29, 135 |
| **5** | Ester hydrolysis | Non-enzymatic hydrolysis, hCE-1 | 122, 24 |
| **6** | Transesterification | hCE-1 in presence of ethanol, FAES in presence of ethanol | 29, 24, 20 |
| **7** | Pyrolysis | Pyrolytic decomposition | 20 |
| **8** | *N*-Dealkylation | Enzymatic oxidation | 129 |
| **9** | Ester hydrolysis | hCE-2 | 129 |
| **10** | Ester hydrolysis | Postulated | - |
| **11** | Aromatic oxidation | Enzymatic oxidation | 129 |
| **12** | Ester hydrolysis | hCE-1 | 129 |
| **13** | *N*-Oxidation | FMO, CYP | 23, 156 |
| **14** | *N*-Oxidation | CYP | 130, 23, 156 |
| **15** | Aromatic oxidation | Postulated enzymatic oxidation | 129 |
| **16** | *N*-Oxidation | Postulated | - |
| **17** | Ester hydrolysis | Not available in literature | 20 |
| **18** | Aromatic oxidation | Postulated | - |
| **19** | *N*-Dealkylation | CYP | 129 |
| **20** | Ester hydrolysis | hCE-2, serum cholinesterase | 156 |
| **21** | *N*-Dealkylation | Postulated | - |
| **22** | Aromatic oxidation | Enzymatic oxidation | 129 |
| **23** | Ester hydrolysis | Non-enzymatic hydrolysis, hCE-1 | 20, 24, 121 |
| **24** | *N*-Dealkylation | Enzymatic oxidation | 129 |
| **25** | Ester hydrolysis | hCE-1 | 129 |
| **26** | Ester hydrolysis | hCE-2 | 129 |
| **27** | Ester hydrolysis | Postulated | - |
| **28** | Ester hydrolysis | hCE-2 | 129, 121 |
| **29** | Aromatic oxidation | Postulated | - |
| **30** | *N*-Oxidation | Postulated | - |
| **31** | Ester hydrolysis | Not available in literature | 20 |
| **32** | *N*-Dealkylation | Postulated | - |
| **33** | Aromatic oxidation | Postulated | - |
| **34** | Aromatic oxidation | Enzymatic oxidation | 129 |
| **35** | Ester hydrolysis | Not available in literature | 20 |
| **36** | Pyrolysis | Pyrolytic decomposition | 20 |
| **37** | Transesterification | Not available in literature | 128 |
| **38** | Ester hydrolysis | Not available in literature | 128 |
| **39** | *N*-Oxidation | Not available in literature | 128 |
| **40** | *N*-Dealkylation | Not available in literature | 128 |
| **41** | *N*-Dealkylation | Postulated | - |
| **42** | *N*-Dealkylation | Not available in literature | 128 |
| **II** | Phase II conjugation | Indirect evidence of UGT and SULT | 104 |
| * | Protein adduction | 1,4-Michael addition on α,β-unsaturated carbonyl | 99 |

Appendix 2: Biotransformation of methamphetamine

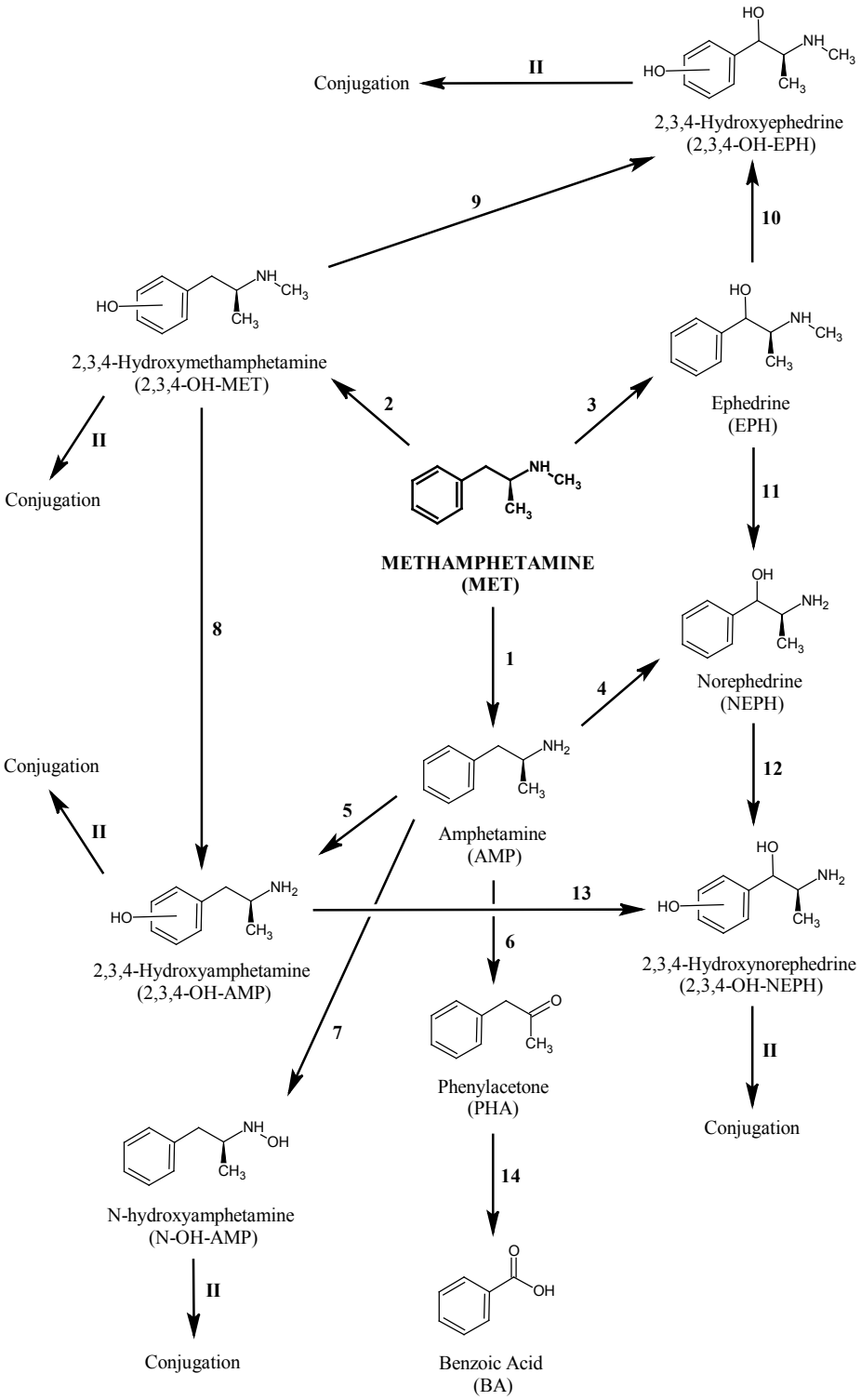

Methamphetamine Biotransformation Pathway Enzymes/Mechanisms

| # | Process | Enzyme/Mechanism | Source # |
|---|---|---|---|
| **1** | *N*-Dealkylation | CYP (CYP2D6), FMO | 131 |
| **2** | Aromatic oxidation | CYP (CYP2D6) | 131 |
| **3** | Aliphatic oxidation | Postulated | - |
| **4** | Aliphatic oxidation | Not available in literature | 26, 138, 137 |
| **5** | Aromatic oxidation | CYP (CYP2D6) | 131 |
| **6** | Oxidative deamination | Not available in literature | 26, 138, 137 |
| **7** | *N*-Oxidation | Postulated | - |
| **8** | *N*-Dealkylation | Not available in literature | 138, 137 |
| **9** | Aliphatic oxidation | Postulated | - |
| **10** | Aromatic oxidation | Postulated | - |
| **11** | *N*-Dealkylation | Postulated | - |
| **12** | Aromatic oxidation | Not available in literature | 26, 138, 137 |
| **13** | Aliphatic oxidation | Not available in literature | 26, 138, 137 |
| **14** | Side chain oxidation | Not available in literature | 26, 138, 137 |
| **II** | Phase II conjugation | UGT, SULT | 27 |

Appendix 3: Biotransformation of morphine

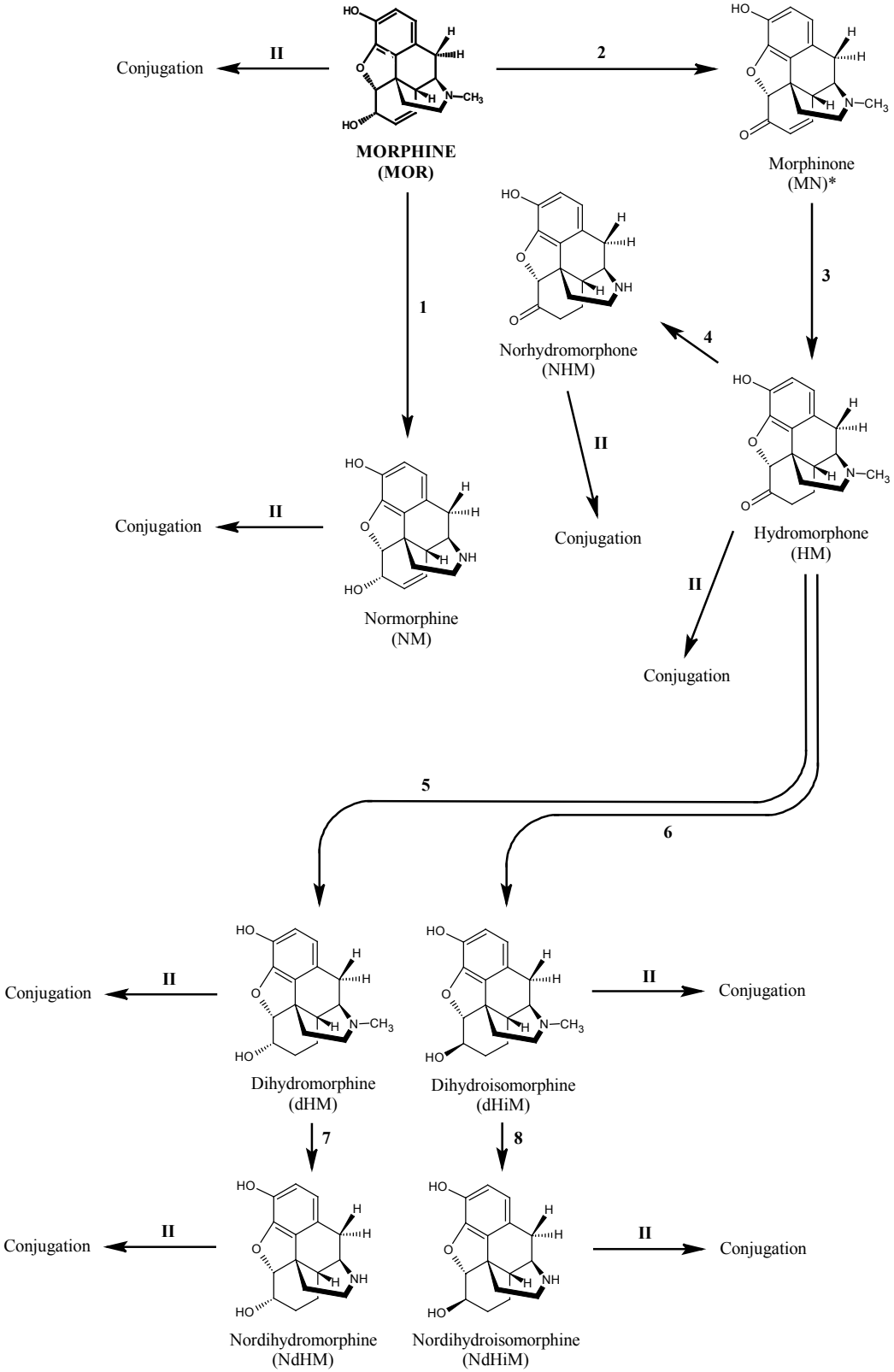

Morphine Biotransformation Pathway Enzymes/Mechanisms

| # | Process | Enzyme/Mechanism | Source # |
|---|---|---|---|
| **1** | *N*-Dealkylation | CYP (CYPs 3A4, 2C8) | 132 |
| **2** | Alcohol oxidation | Morphine-6-dehydrogenase, OH radicals | 82, 83, 84 |
| **3** | Alkene reduction | Morphinone reductase | 157 |
| **4** | *N*-Dealkylation | Not available in literature | 158 |
| **5** | Ketone reduction | Not available in literature | 159 |
| **6** | Ketone reduction | Not available in literature | 159 |
| **7** | *N*-Dealkylation | Not available in literature | 159 |
| **8** | *N*-Dealkylation | Not available in literature | 159 |
| **II** | Phase II conjugation | UGT (UGT2B7), SULT | 159, 160 |
| * | Protein adduction | 1,4-Michael addition on α,β-unsaturated carbonyl | 80, 83 |

Appendix 4: Steglich esterification mechanism

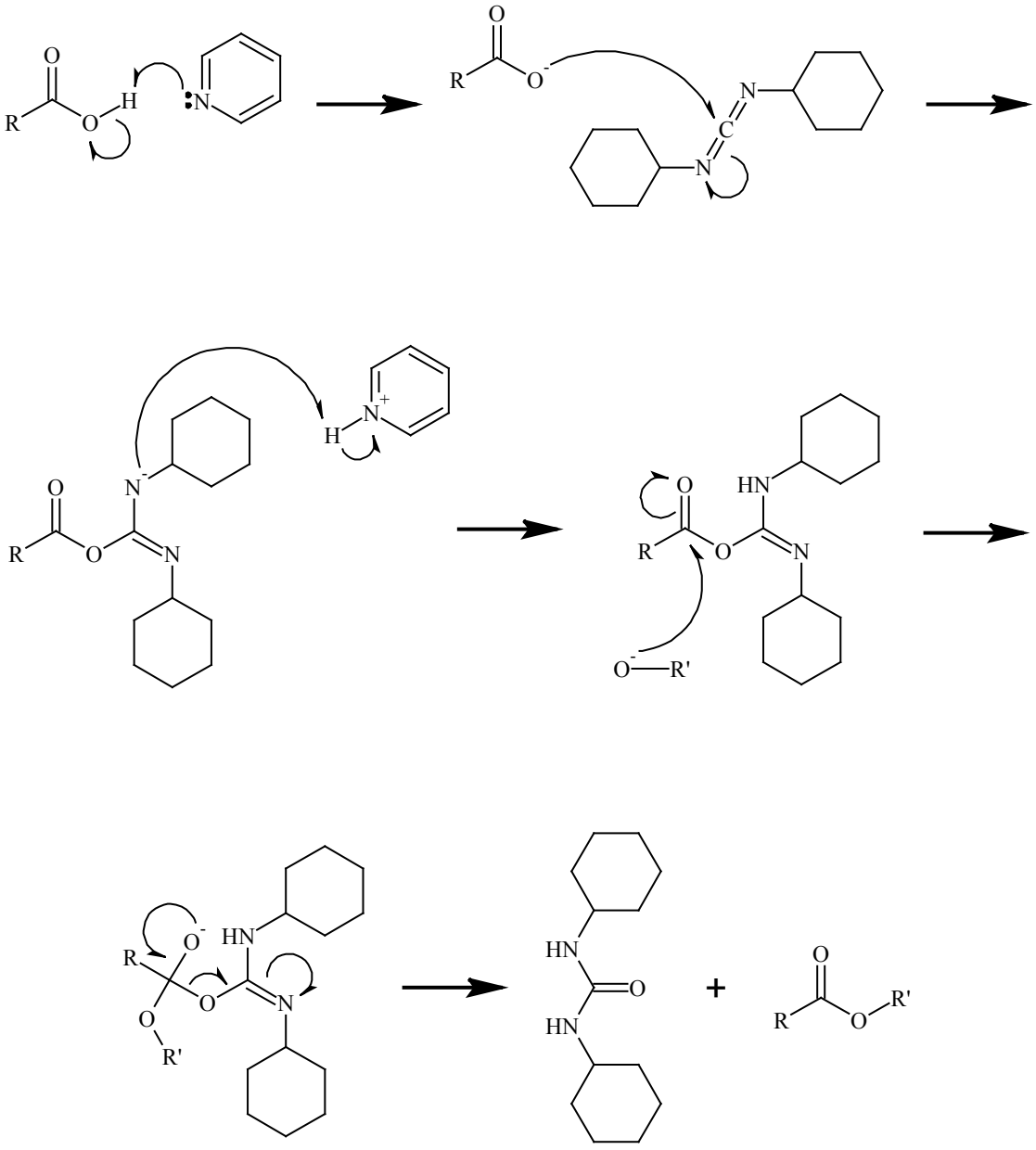

Appendix 5: Cocaine metabolism MRM ionization and dissociation parameters

| Compound (Abbreviation) | $[M+H]^+$ | Fragmentor (V) | Transitions[a] | Collision Energy (V) | RT (min)[b,c] |
|---|---|---|---|---|---|
| norecgonine* (NE) | 172.1 | 110 | **172.1 → 154**<br>172.1 → 68 | 18<br>26 | N.D. |
| ecgonine (ECG) | 186.1 | 110 | **186.1 → 168**<br>186.1 → 82 | 18<br>26 | 0.295 ± 0.002 |
| norecgonine methyl ester* (NEME) | 186.1 | 105 | **186.1 → 168**<br>186.1 → 68 | 14<br>26 | N.D. |
| ecgonine methyl ester (EME) | 200.1 | 105 | **200.1 → 182**<br>200.1 → 82 | 14<br>26 | 0.288 ± 0.000 |
| norecgonine ethyl ester* (NEEE) | 200.1 | 115 | **200.1 → 182**<br>200.1 → 68 | 14<br>26 | N.D. |
| ecgonine ethyl ester (EEE) | 214.1 | 115 | **214.1 → 196**<br>214.1 → 82 | 14<br>26 | 0.389 ± 0.001 |
| benzoylnorecgonine* (BNE) | 276.1 | 120 | **276.1 → 154**<br>276.1 → 68 | 14<br>30 | 3.005 ± 0.003 |
| benzoylecgonine (BE) | 290.1 | 120 | **290.1 → 168**<br>290.1 → 105 | 14<br>30 | 2.940 ± 0.001 |
| norcocaine (NC) | 290.1 | 110 | **290.1 → 168**<br>290.1 → 136 | 10<br>22 | 4.454 ± 0.002 |
| 2-hydroxybenzoylnorecgonine* (2-OH-BNE) | 292.1 | 120 | **292.1 → 172**<br>292.1 → 154 | 14<br>30 | N.D. |
| 3-hydroxybenzoylnorecgonine* (3-OH-BNE) | 292.1 | 120 | **292.1 → 154**<br>292.1 → 68 | 14<br>30 | N.D. |
| 4-hydroxybenzoylnorecgonine* (4-OH-BNE) | 292.1 | 120 | **292.1 → 154**<br>292.1 → 68 | 14<br>30 | N.D. |
| *N*-hydroxybenzoylnorecgonine* (N-OH-BNE) | 292.1 | 120 | **292.1 → 170**<br>292.1 → 84 | 14<br>30 | N.D. |
| cocaine (COC) | 304.2 | 120 | **304.2 → 182**<br>304.2 → 82 | 14<br>30 | 4.164 ± 0.003 |
| norcocaethylene (NCE) | 304.2 | 125 | **304.2 → 182**<br>304.2 → 68 | 18<br>30 | 5.550 ± 0.007 |

| Compound (Abbreviation) | $[M+H]^+$ | Fragmentor (V) | Transitions[a] | Collision Energy (V) | RT (min)[b,c] |
|---|---|---|---|---|---|
| norcocaine nitroxide*<br>(NC-NO) | 305.1 | 110 | **305.1 → 169**<br>305.1 → 151 | 10<br>22 | N.D. |
| 2-hydroxybenzoylecgonine<br>(2-OH-BE) | 306.1 | 115 | **306.1 → 186**<br>306.1 → 168 | 14<br>30 | 3.199 ± 0.003 |
| 2-hydroxynorcocaine*<br>(2-OH-NC) | 306.1 | 110 | **306.1 → 186**<br>306.1 → 168 | 10<br>22 | 4.613 ± 0.005 |
| 3-hydroxybenzoylecgonine<br>(3-OH-BE) | 306.1 | 120 | **306.1 → 168**<br>306.1 → 121 | 18<br>26 | 2.322 ± 0.002 |
| 3-hydroxynorcocaine*<br>(3-OH-NC) | 306.1 | 110 | **306.1 → 168**<br>306.1 → 150 | 10<br>22 | 3.014 ± 0.000 |
| 4-hydroxybenzoylecgonine<br>(4-OH-BE) | 306.1 | 120 | **306.1 → 168**<br>306.1 → 121 | 15<br>35 | 2.030 ± 0.003 |
| 4-hydroxynorcocaine*<br>(4-OH-NC) | 306.1 | 110 | **306.1 → 168**<br>306.1 → 150 | 10<br>22 | 2.639 ± 0.003 |
| *N*-hydroxynorcocaine*<br>(N-OH-NC) | 306.1 | 110 | **306.1 → 168**<br>306.1 → 150 | 10<br>22 | N.D. |
| cocaethylene<br>(CE) | 318.2 | 130 | **318.2 → 196**<br>318.2 → 82 | 18<br>30 | 5.284 ± 0.002 |
| 2-hydroxycocaine<br>(2-OH-COC) | 320.1 | 115 | **320.1 → 200**<br>320.1 → 182 | 18<br>30 | 4.302 ± 0.005 |
| 2-hydroxynorcocaethylene*<br>(2-OH-NCE) | 320.1 | 125 | **320.1 → 200**<br>320.1 → 182 | 18<br>30 | N.D. |
| 3-hydroxycocaine<br>(3-OH-COC) | 320.1 | 135 | **320.1 → 182**<br>320.1 → 82 | 18<br>40 | 2.813 ± 0.003 |
| 3-hydroxynorcocaethylene*<br>(3-OH-NCE) | 320.1 | 125 | **320.1 → 182**<br>320.1 → 68 | 18<br>30 | N.D. |
| 4-hydroxycocaine<br>(4-OH-COC) | 320.1 | 135 | **320.1 → 182**<br>320.1 → 121 | 18<br>34 | 2.466 ± 0.000 |
| 4-hydroxynorcocaethylene*<br>(4-OH-NCE) | 320.1 | 125 | **320.1 → 182**<br>320.1 → 68 | 18<br>30 | N.D. |
| cocaine nitroxide*<br>(CNO) | 320.1 | 120 | **320.1 → 198**<br>320.1 → 82 | 14<br>30 | N.D. |

| Compound (Abbreviation) | $[M+H]^+$ | Fragmentor (V) | Transitions[a] | Collision Energy (V) | RT (min)[b,c] |
|---|---|---|---|---|---|
| *N*-hydroxynorcocaethylene* (N-OH-NCE) | 320.1 | 125 | **320.1 → 198**<br>320.1 → 84 | 18<br>30 | N.D. |
| *N*-hydroxy-2-hydroxynorcocaine* (N-OH-2-HO-NC) | 322.1 | 110 | **322.1 → 202**<br>322.1 → 184 | 10<br>22 | N.D. |
| *N*-hydroxy-3-hydroxynorcocaine* (N-OH-3-HO-NC) | 322.1 | 110 | **322.1 → 184**<br>322.1 → 152 | 10<br>22 | N.D. |
| *N*-hydroxy-4-hydroxynorcocaine* (N-OH-4-HO-NC) | 322.1 | 110 | **322.1 → 184**<br>322.1 → 152 | 10<br>22 | N.D. |
| 2-hydroxycocaethylene (2-OH-CE) | 334.2 | 130 | **334.2 → 214**<br>334.2 → 196 | 14<br>30 | 5.424 ± 0.003 |
| 3-hydroxycocaethylene (3-OH-CE) | 334.2 | 130 | **334.2 → 196**<br>334.2 → 82 | 18<br>34 | 3.658 ± 0.002 |
| 4-hydroxycocaethylene (4-OH-CE) | 334.2 | 130 | **334.2 → 196**<br>334.2 → 82 | 18<br>34 | 3.214 ± 0.002 |
| dihydroxycocaine (isomers)* (dOH-COC) | 336.1 | 120 | **336.1 → 182**<br>336.1 → 82 | 14<br>30 | 0.625 ± 0.013<br>1.788 ± 0.004<br>2.937 ± 0.003 |
| *N*-hydroxy-2-hydroxynorcocaethylene* (N-OH-2-OH-NCE) | 336.1 | 125 | **336.1 → 216**<br>336.1 → 198 | 18<br>30 | N.D. |
| *N*-hydroxy-3-hydroxynorcocaethylene* (N-OH-3-OH-NCE) | 336.1 | 125 | **336.1 → 198**<br>336.1 → 84 | 18<br>30 | N.D. |
| *N*-hydroxy-4-hydroxynorcocaethylene* (N-OH-4-OH-NCE) | 336.1 | 125 | **336.1 → 198**<br>336.1 → 84 | 18<br>30 | N.D. |
| dihydroxycocaethylene (isomers)* (dOH-CE) | 350.2 | 130 | **350.2 → 196**<br>350.2 → 82 | 18<br>30 | 1.125 ± 0.012<br>2.402 ± 0.007<br>3.758 ± 0.004 |
| hydroxybenzoylnorecgonine glucuronide* (OH-BNE-G) | 468.1 | 120 | **468.1 → 292**<br>468.1 → 154 | 14<br>30 | N.D. |
| hydroxybenzoylecgonine glucuronide* (OH-BE-G) | 482.1 | 120 | **482.1 → 306**<br>482.1 → 168 | 14<br>30 | N.D. |
| hydroxynorcocaine glucuronide* (OH-NC-G) | 482.1 | 110 | **482.1 → 306**<br>482.1 → 168 | 10<br>22 | N.D. |

| Compound (Abbreviation) | $[M+H]^+$ | Fragmentor (V) | Transitions[a] | Collision Energy (V) | RT (min)[b,c] |
|---|---|---|---|---|---|
| hydroxycocaine glucuronide* (OH-COC-G) | 496.1 | 120 | **496.1 → 320**<br>496.1 → 182 | 14<br>30 | N.D. |
| hydroxynorcocaethylene glucuronide* (OH-NCE-G) | 496.1 | 125 | **496.1 → 320**<br>496.1 → 182 | 18<br>30 | N.D. |
| hydroxycocaethylene glucuronide* (OH-CE-G) | 510.2 | 130 | **510.2 → 334**<br>510.2 → 196 | 18<br>30 | N.D. |
| dihydroxynorcocaine diglucuronide* (dOH-NC-dG) | 674.1 | 110 | **674.1 → 498**<br>674.1 → 322 | 10<br>22 | N.D. |
| dihydroxynorcocaethylene diglucuronide* (dOH-NCE-dG) | 688.1 | 125 | **688.1 → 512**<br>688.1 → 336 | 18<br>30 | N.D. |
| benzoylecgonine-$D_3$ (IS) (BE-D3) | 293.2 | 120 | **293.2 → 171**<br>293.2 → 105 | 14<br>30 | 2.934 ± 0.002 |

* parameters determined theoretically, not by direct optimization

[a] **bold = quantifier**; plain text = qualifier

[b] N.D. = not detected and no standard

[c] n=10

Appendix 6: Methamphetamine metabolism MRM ionization and dissociation parameters

| Compound (Abbreviation) | $[M+H]^+$ | Fragmentor (V) | Transitions[a] | Collision Energy (V) | RT (min)[b,c] |
|---|---|---|---|---|---|
| phenylacetone*<br>(PHA) | 135.1 | 75 | **135.1 → 91**<br>135.1 → 119 | 16<br>4 | 0.987 ± 0.010 |
| amphetamine<br>(AMP) | 136.1 | 75 | **136.1 → 91**<br>136.1 → 119 | 16<br>4 | 2.043 ± 0.003 |
| methampethamine<br>(MET) | 150.1 | 80 | **150.1 → 91**<br>150.1 → 119 | 16<br>4 | 2.684 ± 0.005 |
| 2-hydroxyamphetamine*<br>(2-OH-AMP) | 152.1 | 75 | **152.1 → 107**<br>152.1 → 135 | 16<br>4 | 1.381 ± 0.002 |
| 3-hydroxyamphetamine*<br>(3-OH-AMP) | 152.1 | 75 | **152.1 → 107**<br>152.1 → 135 | 16<br>4 | 0.876 ± 0.002 |
| 4-hydroxyamphetamine*<br>(4-OH-AMP) | 152.1 | 75 | **152.1 → 107**<br>152.1 → 135 | 16<br>4 | 0.690 ± 0.002 |
| *N*-hydroxyamphetamine*<br>(N-OH-AMP) | 152.1 | 75 | **152.1 → 91**<br>152.1 → 119 | 16<br>4 | N.D. |
| norephedrine<br>(NEPH) | 152.1 | 75 | **152.1 → 134**<br>152.1 → 117 | 5<br>17 | 0.975 ± 0.002 |
| 2-hydroxymethamphetamine*<br>(2-OH-MET) | 166.1 | 80 | **166.1 → 107**<br>166.1 → 135 | 16<br>4 | 1.824 ± 0.002 |
| 3-hydroxymethamphetamine*<br>(3-OH-MET) | 166.1 | 80 | **166.1 → 107**<br>166.1 → 135 | 16<br>4 | 1.053 ± 0.003 |
| 4-hydroxymethamphetamine*<br>(4-OH-MET) | 166.1 | 80 | **166.1 → 107**<br>166.1 → 135 | 16<br>4 | 0.788 ± 0.002 |
| ephedrine<br>(EPH) | 166.1 | 80 | **166.1 → 148**<br>166.1 → 117 | 9<br>17 | 1.425 ± 0.003 |
| 2-hydroxynorephedrine*<br>(2-OH-NEPH) | 168.1 | 75 | **168.1 → 150**<br>168.1 → 133 | 5<br>17 | 0.803 ± 0.002 |
| 3-hydroxynorephedrine*<br>(3-OH-NEPH) | 168.1 | 75 | **168.1 → 150**<br>168.1 → 133 | 5<br>17 | 0.470 ± 0.001 |
| 4-hydroxynorephedrine*<br>(4-OH-NEPH) | 168.1 | 75 | **168.1 → 150**<br>168.1 → 133 | 5<br>17 | 0.378 ± 0.000 |

| Compound (Abbreviation) | [M+H]$^+$ | Fragmentor (V) | Transitions[a] | Collision Energy (V) | RT (min)[b,c] |
|---|---|---|---|---|---|
| dihydroxyamphetamine*<br>(di-OH-AMP) [major isomer] | 168.1 | 75 | **168.1 → 123**<br>168.1 → 151 | 16<br>4 | 0.459 ± 0.004 |
| 2-hydroxyephedrine*<br>(2-OH-EPH) | 182.1 | 80 | **182.1 → 164**<br>182.1 → 133 | 9<br>17 | 1.120 ± 0.003 |
| 3-hydroxyephedrine*<br>(3-OH-EPH) | 182.1 | 80 | **182.1 → 164**<br>182.1 → 133 | 9<br>17 | 0.586 ± 0.001 |
| 4-hydroxyephedrine*<br>(4-OH-EPH) | 182.1 | 80 | **182.1 → 164**<br>182.1 → 133 | 9<br>17 | 0.426 ± 0.001 |
| dihydroxymethamphetamine*<br>(di-OH-MET) [major isomer] | 182.1 | 80 | **182.1 → 123**<br>182.1 → 151 | 16<br>4 | 0.508 ± 0.002 |
| dihydroxynorephedrine*<br>(di-OH-NEPH) [major isomer] | 184.1 | 75 | **184.1 → 166**<br>184.1 → 149 | 5<br>17 | 0.375 ± 0.003 |
| dihydroxyephedrine*<br>(di-OH-EPH) [major isomer] | 198.1 | 80 | **198.1 → 180**<br>198.1 → 149 | 9<br>17 | 0.394 ± 0.005 |
| hydroxyamphetamine-β-D-glucuronide*<br>(OH-AMP-G) | 328.1 | 75 | **328.1 → 152**<br>328.1 → 107 | 4<br>16 | N.D. |
| *N*-hydroxyamphetamine-β-D-glucuronide*<br>(N-OH-AMP-G) | 328.1 | 75 | **328.1 → 152**<br>328.1 → 91 | 4<br>16 | N.D. |
| hydroxymethamphetamine-β-D-glucuronide*<br>(OH-MET-G) | 342.2 | 80 | **342.2 → 166**<br>342.2 → 107 | 4<br>16 | N.D. |
| hydroxynorephedrine-β-D-glucuronide*<br>(OH-NEPH-G) | 344.1 | 75 | **344.1 → 168**<br>344.1 → 150 | 5<br>17 | N.D. |
| hydroxyephedrine-β-D-glucuronide*<br>(OH-EPH-G) | 358.2 | 80 | **358.2 → 182**<br>358.2 → 164 | 9<br>17 | N.D. |
| methamphetamine-$D_5$ (IS)<br>(MET-D5) | 155.2 | 85 | **155.2 → 92**<br>155.2 → 121 | 17<br>5 | 2.721 ± 0.004 |

* parameters determined theoretically, not by direct optimization

[a] **bold = quantifier**; plain text = qualifier

[b] N.D. = not detected and no standard

[c] n=10

Appendix 7: Morphine metabolism MRM ionization and dissociation parameters

| Compound (Abbreviation) | $[M+H]^+$ | Fragmentor (V) | Transitions[a] | Collision Energy (V) | RT (min)[b,c] |
|---|---|---|---|---|---|
| normorphine (NM) | 272.1 | 140 | **272.1 → 165**<br>272.1 → 181 | 38<br>38 | 0.511 ± 0.001 |
| norhydromorphone (NHM) | 272.1 | 130 | **272.1 → 185**<br>272.1 → 157 | 27<br>50 | 0.821 ± 0.003 |
| nordihydroisomorphine* (NdHiM) | 274.1 | 130 | **274.1 → 185**<br>274.1 → 157 | 27<br>50 | N.D. |
| nordihydromorphine* (NdHM) | 274.1 | 130 | **274.1 → 185**<br>274.1 → 157 | 27<br>50 | N.D. |
| morphinone* (MN) | 284.1 | 160 | **284.1 → 185**<br>284.1 → 227 | 38<br>38 | 0.799 ± 0.005 |
| hydromorphone (HM) | 286.1 | 160 | **286.1 → 185**<br>286.1 → 157 | 33<br>45 | 0.942 ± 0.003 |
| morphine (MOR) | 286.1 | 150 | **286.1 → 165**<br>286.1 → 157 | 45<br>41 | 0.601 ± 0.002 |
| dihydroisomorphine* (dHiM) | 288.2 | 160 | **288.2 → 185**<br>288.2 → 157 | 33<br>45 | N.D. |
| dihydromorphine* (dHM) | 288.2 | 160 | **288.2 → 185**<br>288.2 → 157 | 33<br>45 | N.D. |
| norhydromorphone-3-β-D-glucuronide* (NHM3G) | 448.2 | 165 | **448.2 → 272**<br>448.2 → 185 | 33<br>50 | N.D. |
| normorphine-3-β-D-glucuronide* (NM3G) | 448.2 | 145 | **448.2 → 272**<br>448.2 → 165 | 33<br>50 | N.D. |
| normorphine-6-β-D-glucuronide* (NM6G) | 448.2 | 145 | **448.2 → 272**<br>448.2 → 165 | 33<br>50 | N.D. |
| nordihydroisomorphine-3-β-D-glucuronide* (NdHiM3G) | 450.2 | 145 | **450.2 → 274**<br>450.2 → 185 | 33<br>50 | N.D. |
| nordihydromorphine-3-β-D-glucuronide* (NdHM3G) | 450.2 | 145 | **450.2 → 274**<br>450.2 → 185 | 33<br>50 | N.D. |
| hydromorphone-3-β-D-glucuronide (HM3G) | 462.2 | 165 | **462.2 → 286**<br>462.2 → 185 | 33<br>50 | 0.464 ± 0.003 |

| Compound (Abbreviation) | $[M+H]^+$ | Fragmentor (V) | Transitions[a] | Collision Energy (V) | RT (min)[b,c] |
|---|---|---|---|---|---|
| morphine-3-β-D-glucuronide (M3G) | 462.2 | 145 | **462.2 → 286**<br>462.2 → 201 | 33<br>50 | 0.398 ± 0.002 |
| morphine-6-β-D-glucuronide (M6G) | 462.2 | 145 | **462.2 → 286**<br>462.2 → 201 | 33<br>50 | 0.553 ± 0.005 |
| dihydroisomorphine-3-β-D-glucuronide* (dHiM3G) | 464.2 | 145 | **464.2 → 288**<br>464.2 → 185 | 33<br>50 | N.D. |
| dihydromorphine-3-β-D-glucuronide* (dHM3G) | 464.2 | 145 | **464.2 → 288**<br>464.2 → 185 | 33<br>50 | N.D. |
| dihydroisomorphine-6-β-D-glucuronide* (dHiM6G) | 464.2 | 145 | **464.2 → 288**<br>464.2 → 185 | 33<br>50 | N.D. |
| dihydromorphine-6-β-D-glucuronide* (dHM6G) | 464.2 | 145 | **464.2 → 288**<br>464.2 → 185 | 33<br>50 | N.D. |
| normorphine-3,6-di-β-D-glucuronide* (NM36dG) | 624.2 | 145 | **624.2 → 448**<br>624.2 → 272 | 33<br>50 | N.D. |
| morphine-3,6-di-β-D-glucuronide* (M36dG) | 638.2 | 145 | **638.2 → 462**<br>638.2 → 286 | 33<br>50 | N.D. |
| dihydroisomorphine-3,6-di-β-D-glucuronide* (dHiM36dG) | 640.3 | 145 | **640.3 → 464**<br>640.3 → 288 | 33<br>50 | N.D. |
| dihydromorphine-3,6-di-β-D-glucuronide* (dHM36dG) | 640.3 | 145 | **640.3 → 464**<br>640.3 → 288 | 33<br>50 | N.D. |
| morphine-$D_3$ (IS) (MOR-D3) | 289.2 | 155 | **289.2 → 165**<br>289.2 → 157 | 50<br>45 | 0.600 ± 0.002 |

* parameters determined theoretically, not by direct optimization

[a] **bold = quantifier**; plain text = qualifier

[b] N.D. = not detected and no standard

[c] n=10

Appendix 8: LC-MS/MS Methods

Cocaine metabolism

| Time (min) | % B |
|---|---|
| **0.0** | 5 |
| **7.0** | 30 |
| **8.0** | 95 |
| **9.0** | 95 |

Run Time: 12.5 min

A: 2 mM ammonium formate and 0.1% formic acid in $H_2O$

B: 90/10/0.1 acetonitrile:$H_2O$:formic acid

Flow Rate: 0.5 mL/min Injection Volume: 1 µL

Post-run Equlibration: 3.5 min at 5% B

MS Mode: QQQ; Dynamic MRM

MS Parameters: See Appendix 5

Methamphetamine metabolism

| Time (min) | % B |
|---|---|
| **0.0** | 5 |
| **3.5** | 5 |
| **4.5** | 95 |
| **5.5** | 95 |

Run Time: 9.0 min

A: 2 mM ammonium formate and 0.1% formic acid in $H_2O$

B: 90/10/0.1 acetonitrile:$H_2O$:formic acid

Flow Rate: 0.5 mL/min Injection Volume: 5 µL

Post-run Equlibration: 3.5 min at 5% B

MS Mode: QQQ; Dynamic MRM

MS Parameters: See Appendix 6

Morphine metabolism

| Time (min) | % B |
|---|---|
| **0.0** | 5 |
| **3.5** | 5 |
| **4.5** | 95 |
| **5.5** | 95 |

Run Time: 9.0 min

A: 2 mM ammonium formate and 0.1% formic acid in $H_2O$

B: 90/10/0.1 acetonitrile:$H_2O$:formic acid

Flow Rate: 0.5 mL/min Injection Volume: 5 µL

Post-run Equlibration: 3.5 min at 5% B

MS Mode: QQQ; Dynamic MRM

MS Parameters: See Appendix 7

rhCYP bactosome isoform viability cocktail

| Time (min) | % B |
|---|---|
| **0.0** | 5 |
| **5.0** | 65 |
| **6.0** | 95 |
| **7.0** | 95 |

Run Time: 10.5 min

A: 2 mM ammonium formate and 0.1% formic acid in $H_2O$

B: 90/10/0.1 acetonitrile:$H_2O$:formic acid

Flow Rate: 0.5 mL/min Injection Volume: 5 µL

Post-run Equlibration: 3.5 min at 5% B

MS Mode: QQQ; Dynamic MRM

MS Parameters: See Table 7

General adduct screening

| Time (min) | % B |
|---|---|
| **0.0** | 4 |
| **0.5** | 4 |
| **20.0** | 90 |
| **22.0** | 90 |

Run Time: 28.0 min

A: 10 mM ammonium acetate (pH 4.0)

B: Methanol

Flow Rate: 0.3 mL/min Injection Volume: 10 µL

Post-run Equlibration: 6.0 min at 4% B

MS Mode: QQQ; SIM of theoretical *m/z* values & Product Ion of suspected adduction products

MS Parameters: Frag 120 V (COC), 90 V (MET), 160 V (MOR); CE 10, 20, 30, 40 V

Cocaine–*N*-acetylcysteine adduct

| Time (min) | % B |
|---|---|
| **0.0** | 4 |
| **0.5** | 4 |
| **10.0** | 15 |
| **11.0** | 90 |
| **13.0** | 90 |

Run Time: 19.0 min

A: 10 mM ammonium acetate (pH 4.0)

B: Methanol

Flow Rate: 0.3 mL/min Injection Volume: 10 µL

Post-run Equlibration: 6.0 min at 4% B

MS Mode: QTOF; Targeted MS/MS of *m/z* 483.18

MS Parameters: Frag 120 V; CE 10, 20, 30, 40 V

Cocaine– glutathione adduct

| Time (min) | % B |
|---|---|
| **0.0** | 4 |
| **0.5** | 4 |
| **5.0** | 26 |
| **6.0** | 90 |
| **8.0** | 90 |

Run Time: 14.0 min

A: 10 mM ammonium acetate (pH 4.0)

B: Methanol

Flow Rate: 0.3 mL/min Injection Volume: 10 µL

Post-run Equlibration: 6.0 min at 4% B

MS Mode: QQQ; SIM & Product Ion of *m/z* 627

MS Parameters: Frag 150 V; CE 10, 20, 30, 40, 50 V

Cocaine– AcPAACAA adduct

| Time (min) | % B |
|---|---|
| **0.0** | 4 |
| **0.5** | 4 |
| **11.0** | 50 |
| **12.0** | 90 |
| **14.0** | 90 |

Run Time: 20.0 min

A: 10 mM ammonium acetate (pH 4.0)

B: Methanol

Flow Rate: 0.3 mL/min Injection Volume: 10 µL

Post-run Equlibration: 6.0 min at 4% B

MS Mode: QQQ; SIM & Product Ion of *m/z* 864

MS Parameters: Frag 140 V; CE 20, 30, 40, 50 V

Morphine– *N*-acetylcysteine adduct

| Time (min) | % B |
|---|---|
| **0.0** | 4 |
| **0.5** | 4 |
| **7.0** | 7.5 |
| **8.0** | 90 |
| **10.0** | 90 |

Run Time: 16.0 min

A: 10 mM ammonium acetate (pH 4.0)

B: Methanol

Flow Rate: 0.3 mL/min Injection Volume: 10 µL

Post-run Equlibration: 6.0 min at 4% B

MS Mode: QTOF; Targeted MS/MS of *m/z* 447.16 & 449.17

MS Parameters: Frag 160 V; CE 10, 20, 30, 40, 50 V

Morphine– glutathione adduct

| Time (min) | % B |
|---|---|
| **0.0** | 4 |
| **5** | 4 |
| **6.0** | 90 |
| **8.0** | 90 |

Run Time: 14.0 min

A: 10 mM ammonium acetate (pH 4.0)

B: Methanol

Flow Rate: 0.3 mL/min Injection Volume: 10 µL

Post-run Equlibration: 6.0 min at 4% B

MS Mode: QQQ; SIM & Product Ion of *m/z* 591

MS Parameters: Frag 160 V; CE 10, 20, 30, 40, 50 V

Morphine– AcPAACAA adduct

| Time (min) | % B |
|---|---|
| **0.0** | 4 |
| **0.5** | 4 |
| **11.0** | 50 |
| **12.0** | 90 |
| **14.0** | 90 |

Run Time: 20.0 min

A: 10 mM ammonium acetate (pH 4.0)

B: Methanol

Flow Rate: 0.3 mL/min Injection Volume: 10 µL

Post-run Equlibration: 6.0 min at 4% B

MS Mode: QQQ; SIM & Product Ion of *m/z* 823

MS Parameters: Frag 160 V; CE 10, 20, 30, 40, 50 V

Appendix 9: MS/MS fragmentation of native peptides (a) GSH and (b) AcPAACAA

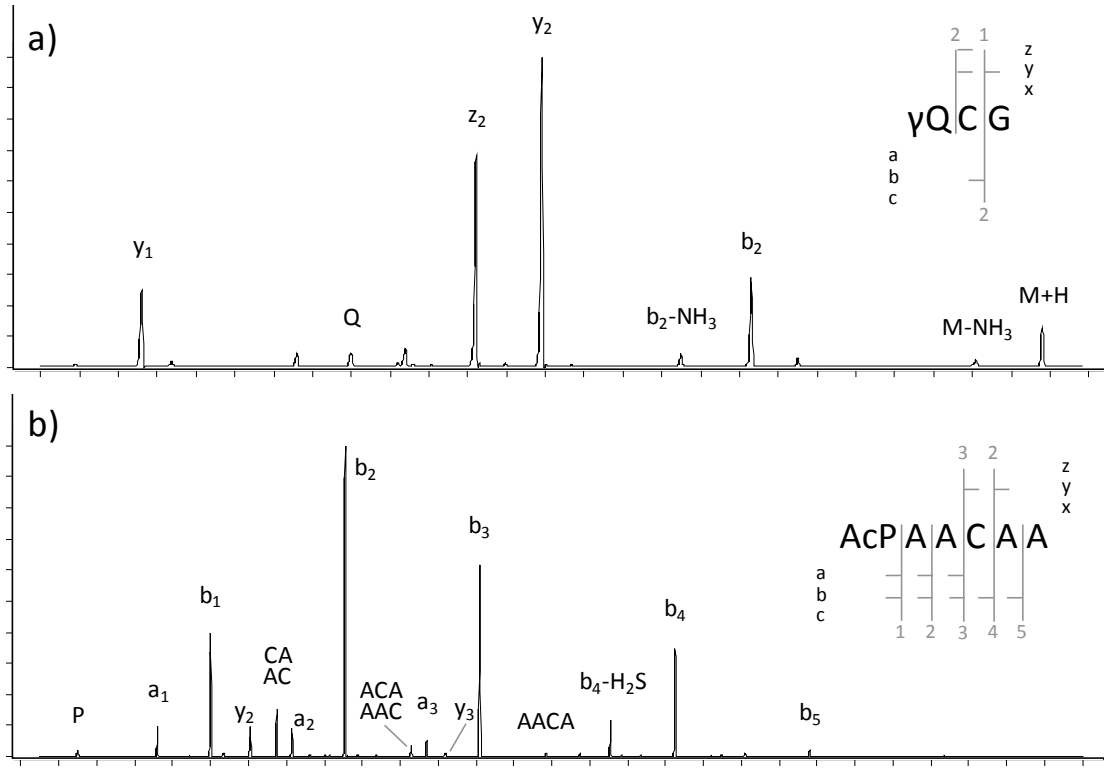

# VITA

## KEVIN J. SCHNEIDER

| | |
|---|---|
| 2004-2008 | B.S., Biochemistry & Applied Forensic Sciences, *summa cum laude*, honors<br>B.A., Religious Studies, *summa cum laude*, honors<br>Mercyhurst University<br>Erie, Pennsylvania |
| 2008 -2013 | Doctoral Candidate, Chemistry<br>Florida International University<br>Miami, Florida |

PUBLICATIONS AND PRESENTATIONS

Schneider, K.J. and Williams, J.D. Sodium sulfide catalyzed isomerization of itaconic anhydride to citraconic anhydride. *Current Organic Chemistry* **2011,** *15* (16), 2893-2896.

Schneider, K.J. and DeCaprio, A.P. Evaluation of in vitro metabolic assay systems for common drugs of abuse. Presented at the 2011 Joint Meeting of the Society of Forensic Toxicologists & The International Association of Forensic Toxicologists, San Francisco, California USA, September 25-30, 2011.

Schneider, K.J. and DeCaprio, A.P. Identification of specific cytochrome P450 isozymes mediating biotransformation of three common drugs of abuse. Presented at the 2012 Meeting of the Society of Forensic Toxicologists, Boston, Massachusetts USA, July 1-6, 2012.

Schneider, K.J. and DeCaprio, A.P. Covalent thiol adducts arising from cocaine and morphine biotransformation. Presented at the 2013 Meeting of the Society of Toxicology, San Antonio, Texas USA, March 10-14, 2013.

Schneider, K.J. and DeCaprio, A.P. Evaluation of in vitro metabolic assay systems for common drugs of abuse. 1. Cocaine. (In Preparation)

Schneider, K.J. and DeCaprio, A.P. Evaluation of in vitro metabolic assay systems for common drugs of abuse. 2. Methamphetamine and morphine. (In Preparation)

Schneider, K.J. and DeCaprio, A.P. Identification of specific cytochrome P450 isozymes mediating biotransformation of cocaine and methamphetamine. (In Preparation)

Schneider, K.J. and DeCaprio, A.P. Reactive metabolites and macromolecular protein binding of morphine. (In Preparation)

Schneider, K.J. and DeCaprio, A.P. Covalent thiol adducts arising from reactive intermediates of cocaine biotransformation. (In Preparation)